Studies on angiogenesis and lymphangiogenesis

in the metastasis of canine mammary gland tumor

（犬の乳腺腫瘍の転移における血管新生およびリンパ管新生に関する研究）

李秀貞

I

Studies on angiogenesis and lymphangiogenesis

in the metastasis of canine mammary gland tumor

（犬の乳腺腫瘍の転移における血管新生およびリンパ管新生に関する研究）

Laboratory of Veterinary Surgery
Department of Veterinary Medical Sciences
Graduate School of Agricultural and Life Sciences
The University of Tokyo

東京大学大学院農学生命科学研究科
獣医学専攻博士課程　獣医外科学研究科室

平成 18 年度入学

Soojung Lee
李秀貞

Contents

Preface

Preface

Metastasis, the spread of tumor cells from the primary lesion to lymph nodes and distant organs, is the most malignant aspect of cancers. Various pathways with a large number of molecules may contribute to the dissemination of primary malignant cancer cells (Tobler and Detmar, 2006). Primary tumor cells locally invade into the surrounding tissue, enter the systemic circulation, translocate through the vasculature, arrest in distant capillaries, extravasate into the surrounding tissues and finally proliferate from initial microscopic growth into macroscopic secondary tumors (Tang and Honn, 1994).

On the step of entering the systemic circulation, angiogenic metastasis via tumor-associated blood vessels to distant organs such as the lung, liver, brain and bone, and lymphangiogenic metastasis via tumor-associated lymphatic vessels to draining sentinel lymph nodes, distal lymph nodes and finally distant organs are proceeding coinstantaneously (Tobler and Detmar, 2006). Folkman reported that angiogenesis was crucial for the growth and metastasis of breast cancers and several other solid tumors in human, which provided a considerable number of therapeutic targets (Folkman, 1971; Folkman, 1995). Additionally, Achen and Stacker have shown that lymphangiogenic growth factors secreted from primary tumor cells can induce lymphangiogenesis in nearby lymph nodes, which may facilitate further metastasis and potentially other changes to the morphology and function of various vessel types in the lymph node, providing a site for rearrangement of the vessel structures and abnormal connections between the vascular and lymphatic networks (Figure 1) (Achen and Stacker, 2008). Lymph node lymphangiogenesis and increased lymph flow through the tumor-draining lymph nodes may actively promote metastasis via the lymphatics (Harrell *et al*, 2007). The mechanisms by which malignant tumors leave the primary tumor site, invade lymphatics, and

metastasize to regional lymph nodes and distant organs are complex and interrelated.

Through *in vitro* and *in vivo* studies on various cancers, many factors have been found to be related to the biological behavior of tumors, such as promotion of tumor cell growth, survival, angiogenesis, lymphangiogenesis, invasion and metastasis. The most important factors for the angiogenesis and lymphangiogenesis network are vascular endothelial growth factors (VEGFs) and their VEGF receptors (VEGFRs), one of the ligands and recepter tyrosine kinases (RTKs). They are essential for their processes during embryonic development as well as during processes such as wound healing, muscle growth or the estrous cycle in adult organisms, and also play central roles in pathological angiogenesis and lymphangiogenesis, for example, in cancers and various inflammatory diseases (Lohela *et al*, 2009).

The VEGF family includes 6 members in mammals: VEGF-A (or VEGF), VEGF-B, VEGF-C, VEGF-D, VEGF-E and placenta growth factor (PlGF-1 and -2). The VEGF homologues produced by Orf viruses are collectively termed VEGF-E, and a homologue isolated from snake venom is called VEGF-F. The VEGF ligands bind with differing specificities to three mostly endothelial transmembrane RTKs, VEGFR-1/fms-like tyrosine kinase 1 (Flt1), VEGFR-2/human kinase insert domain receptor (KDR)/mouse fetal liver kinase 1 (Flk1) and VEGFR-3/fms-like tyrosine kinase 4 (Flt4) and two nonkinase receptors, neuropilin-1 and -2 (Figure 2) (Karamysheva, 2008; Shibuya, 2009).

VEGF-A signaling is the major pathway that activates angiogenesis by inducing the proliferation, survival, sprouting and migration of endothelial cells (ECs), and also by increasing endothelial permeability (Shibuya and Claesson-Welsh, 2006). Studies over the past twenty years have generated direct evidence for the role played by VEGF-A in embryonic vasculogenesis and angiogenesis: the inactivation of a single VEGF-A allele results in embryonic lethality at embryonic day (E) of 11-12. In the mutant embryos, blood islands, ECs

and major vessel tubes fail to develop, and reduced numbers of red blood cells are found (Carmeliet *et al*, 1996; Ferrara, 1996). VEGF-A gene expression is up-regulated in hypoxia via the oxygen sensor hypoxia-inducible factor (HIF)-1α (Pugh and Ratcliffe, 2003). Furthermore, several growth factors, inflammatory cytokines, oncogenes and hormones have also been reported to induce VEGF-A (Ferrara, 2004). VEGF-A activity causes vessel hyperpermeability that leads to leakage of plasma proteins into the tumor stroma, stimulating angiogenesis and increasing the interstitial pressure (Dvorak *et al*, 1987). VEGF-A secreted by the tumor cells also induces the expression of plasminogen activators and matrix metalloproteinases (MMPs), contributing to the degradation of basement membranes (Egeblad and Werb, 2002). Interestingly, 50% of embryos that lack both the tyrosine kinase and transmembrane domains die at E 8.5-9 due to vascular malformations, indicating that membrane anchorage is important for the role of VEGFR-1 in vascular development, but the remaining 50% of the mice are viable (Hiratsuka *et al*, 2005). On the other hand, decreased expression of VEGFR-1, disturbing the balance of VEGF-A/VEGFR-2 signaling, seems to be the mechanism behind the formation of hemangiomas, benign but disfiguring vascular tumors that are relatively common in infant (Jinnin *et al*, 2008).

Meanwhile, VEGF-C expression during embryonic development is observed where the first lymph sacs develop and in regions where the lymph vessel sprouts. VEGF-C is an essential chemotactic and survival factor during embryonic lymphangiogenesis (Karkkainen *et al*, 2004; Alitalo *et al*, 2005). In the study using a mouse model of lymph node removal, VEGF-C therapy was shown to regenerate mature, functional collecting lymph vessels that could fuse to transplanted lymph nodes and regenerate the immunological barrier against metastasizing tumor cells (Baldwin *et al*, 2001). The binding affinities of VEGF-C for their receptors are regulated by proteolytic processing of the propeptides, with their affinity for VEGFR-3 increasing with

processing, and only the mature forms binding VEGFR-2 (Joukov *et al*, 1997). The VEGF-C/VEGFR-3 axis plays a critical role in cancer progression by inducing lymphangiogenesis and facilitating the mobility of several types of cancer cells (Alitalo *et al*, 2005; Su *et al*, 2007). The VEGF-C/VEGFR-3 axis may affect cancer development or progression by directly affecting tumor cells. Unlike the well-characterized axis of VEGF-A and VEGFR-2, there may be many undefined functions and molecular mechanisms involved in the tumor progression mediated by the VEGF-C/VEGFR-3 axis; thus, further study of the axis is needed. VEGFR-3 is initially expressed widely in ECs during murine embryogenesis, but later in development its expression becomes largely restricted to the lymphatic endothelium (Kaipainen *et al*, 1995; Dumont *et al*, 1998). In adult human tissues, VEGFR-3 is specific to the lymphatic endothelium, with the exception of some fenestrated and discontinuous blood capillary buds (Partanen *et al*, 2000).

Proteolytically processed VEGF-C activates VEGFR-2 and can induce blood vessel growth (Joukov *et al*, 1997). Conversely, VEGF-A, which binds to VEGFR-2, can induce lymphatic hyperplasia but cannot substitute for VEGF-C in lymphatic development (Cursiefen *et al*, 2004; Baluk *et al*, 2005; Wirzenius *et al*, 2007). By contrast, in a mouse insulinoma tumor model, VEGF-A stimulates only angiogenesis (Gannon *et al*, 2002). At least some of the effects of VEGF-A on lymphatic vessels may be secondary to the induction of vascular hyperpermeability and to the recruitment of the inflammatory cells that produce VEGF-C (Cursiefen *et al*, 2004). Angiogenesis and lymphagiogenesis of VEGF-A and VEGF-C to the metastasis on the microenvironment of cancer are still controversial and the mechanism of metastasis remains unclear.

VEGF-A signaling through VEGFR-2 is the major angiogenic pathway, and blockage of VEGF-A/VEGFR-2 signaling is the first antiangiogenic strategy for cancer therapy (Folkman,

1971; Lohela *et al*, 2009). In 2004, the monoclonal anti-VEGF antibody, bevacizumab, used in combination with traditional chemotherapy, became the first approved anti-angiogenic therapy for several solid tumors, including human breast cancer (Hurwitz *et al*, 2004). Its use in combination with either paclitaxel or docetaxel has prolonged progression-free survival and increased response rates in the first-line treatment of patients with metastatic breast cancers (Goldfarb *et al*, 2010). In addition to direct anti-angiogenic effects, VEGF-A/VEGFR-2 inhibitors are thought to function by causing 'vascular normalization', where pruning of excess branches, increased vessel stability and reduction of leakage lead to improved perfusion and access for chemotherapeutic agents to the tumor (Jain, 2005). However, VEGF-A/VEGFR-2 inhibitors are not effective in all tumors, and the benefit even for responding patients is usually modest, indicating that mechanisms of intrinsic and evasive resistance to anti-VEGF therapy exist (Bergers and Hanahan, 2008). In addition to the VEGF-C trap and blocking of VEGFR-3 activation with the antagonistic antibody could be used for the inhibition of tumor metastasis. Tyrosine kinase inhibitors that block all three VEGFRs are already used in the clinical practice, and at least in pre-clinical models, also blocked the tumor lymphangiogenesis and even metastasis (Roberts *et al*, 2006; Heckman *et al*, 2008; Matsui *et al*, 2008).

Targeting anti-angiogenesis and -lymphangiogenesis to prevent tumor metastasis may be useful. Three scenarios are shown: first, during preoperative chemotherapy; second, as a part of postoperative adjuvant therapy for patients with high risk for subsequent recurrence; and third, during palliative systemic therapy of advanced tumors. In all phases, it is envisaged that the anti-angiogenic and anti-lymphangiogenic agent would most likely be effective in combination with cytotoxic chemotherapy and/or metronomic chemotherapy (Achen *et al*, 2006; Pasquier *et al*, 2010).

Although impressive knowledge about the role of blood vessels and lymphatic vessels in

cancer progression has been acquired over the last few years, there still remain unanswered questions to be solved: What are the molecular mechanisms that control the interaction of cancer cells with blood vessel and lymphatic vessel endothelium? Are there organ-specific differences between tumor angiogenesis and lymphangiogenesis? What is the meaning of the differences in peritumoral and intratumoral angiogenesis and lymphangiogenesis? Are there molecules that are specifically expressed by tumor-activated lymphatic endothelial cells and that might promote lymphatic metastasis? Can we identify additional molecules not related to the VEGF / VEGFR system, which mediate blood vessel and lymphatic vessel development and function, and if so, could these serve as targets for the development of novel, anticancer treatment strategies? How do we define the relationship of other factors as immune cells and microenvironment of the tumor with the VEGFs/VEGFRs system? Is it safe with anti-VEGFs/VEGFRs therapy on normal blood vessels and lymphatic vessels?

Canine mammary gland tumor (CMGT) is the most common type of tumors in female dogs. It is reported that CMGT comprised 13.4% of all tumors in dogs and 41.7% of all tumors in intact female dogs (Sorenmo, 2003). Histological evidence of malignancy does not invariably imply a malignant clinical course. Also, marked variation in histological appearance can occur within the same tumor patients (Withrow and Vail, 2007). There have been some reports on CMGT-xenografted animal models for the evaluation of drug and therapy (Yamashita *et al*, 2001) and a few studies to investigate on the molecular mechanism of CMGT metastasis have been reported (Dore *et al*, 2003; Sarli *et al*, 2004).

Induction of VEGF-A, thought to be involved in human breast carcinogenesis, also has been evaluated in CMGT. Kato et al. measured the plasma and serum VEGF-A level using an ELISA assay, and they found that circulating VEGF-A level was expected to be clinically available for the determination of prognosis in CMGT(Kato *et al*, 2007). Another study on

VEGF-A/VEGFR2 system determined the role of promoting tumor proliferation and "angiogenic shift" in canine mammary carcinomas (Millanta *et al*, 2006).

Nevertheless, in the veterinary medicine, there have been a few studies on an inhibitor of VEGFRs, most of which are related to block Kit phophorylation, toceranib phosphate (London *et al*, 2009). Moreover, studies on the relationship between VEGF-C and angiogenesis/lymphangiogenesis are not sufficient to understand angiogenic and lymohangiogenic metastasis in CMGT. Based on these backgrounds, a series of experiments was carried out in this thesis to investigate the role of VEGF-A and VEGF-C in angiogenic and lymphangiogenic metastasis of CMGT.

In Chapter 1, I examined the expression of VEGF-A and VEGF-C on the primary lesion excised from spontaneous CMGT patients and evaluated the correlation with proliferation index (PI), macrophages and their clinicopathological features. In Chapter 2, I used cloned cell lines established from a CMGT patient. I investigated the expression levels of VEGF-A and VEGF-C on these cell lines. Then using a nude mouse model transplanted with these cell lines, expression of VEGF-A and -C on tissues developed in xenografted nude mice was measured and the relationship between these expressions and angiogenesis or lymphangiogenesis in the tissues was analyzed.
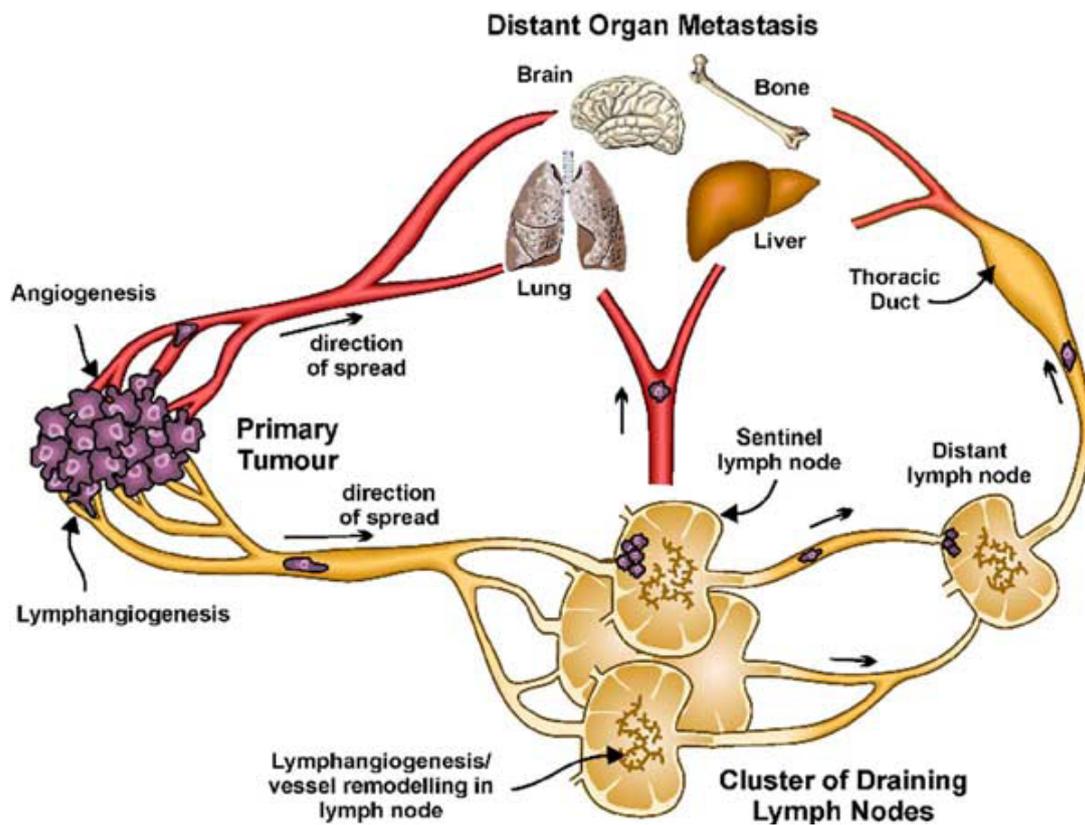
Figure 1. Schematic representation of potential routes of metastasis via the blood vessels (red) and lymphatic vasculature (yellow). The presence of tumor cells can induce angiogenesis and lymphangiogenesis stimulated by such growth factors as VEGF-A and VEGF-C. Tumor cells could spread directly from the primary tumor to distant organs, such as the lungs, liver, brain, or bone, via blood vessels, a process that may be facilitated by tumor angiogenesis. Alternatively, tumor cells could also spread from lymph nodes, providing a site for rearrangement of the vessel structures and abnormal connections between the vascular and lymphatic networks to distant organs via blood vessels associated with the nodes or by entering the venous system via the major lymphatic ducts and then spreading via blood vessels, a process that may be facilitated by tumor lymphangiogenesis. (Achen and Stacker, 2008).
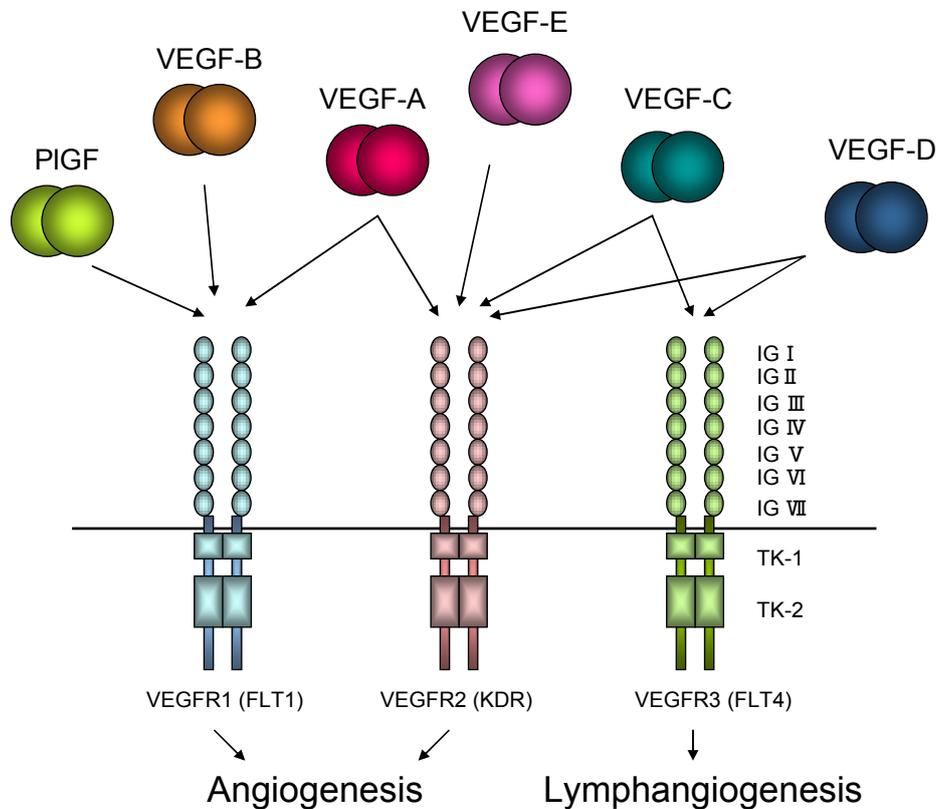
Figure 2. Interaction of growth factors of VEGF family with their own VEGF receptors. VEGF, other closely related factors were later detected, which formed a family that now consists of growth factors VEGF-A (VEGF), VEGF-B, VEGF-C, VEGF-D, VEGF-E, and placental growth factor (PlGF). Growth factors of the VEGF family exert their biological effect via interaction with receptors located on endothelial cell and/or lymphatic endothelial cell membranes. Three receptors have been identified that bind different VEGF growth factors: VEGFR1 (FLT1), VEGFR2 (Flk1/KDR), and VEGFR3 (FLT4). These receptors belong to the superfamily of receptor tyrosine kinases (RTKs) and, based on their structural peculiarities, they comprise a special class within it. Like all RTKs, the VEGF receptors are transmembrane proteins with a single transmembrane domain. The extracellular region of VEGFR is formed by seven immunoglobulin-like domains (IG I~VII), whereas the intracellular part exhibits tyrosine kinase activity, and the tyrosine kinase domain in these receptors is separated to two fragments (TK-1 and TK-2) by an inter-kinase insert. Signalings by VEGFR1 and 2 regulate angiogenesis and signaling by VEGFR3 regulates lymphangiogenesis (Karamysheva, 2008; Shibuya, 2009).

Chapter 1

VEGF-A and VEGF-C expression on the tissue of canine patients

with MGT

Introduction

Misdorp et al. classified the mammary tumor of the dog into 3 histological categories; mammary hyperplasia, benign tumors and malignant tumors. Most of the malignant CMGTs are the epithelial tumors or carcinomas. Benign tumors include simple adenoma and benign mixed tumor which are composed of benign cells morphologically resembling epithelial components (luminal and/or myoepithelial) and mesenchymal cells that have produced cartilage and/or bone and/or fat eventually in combination with fibrous tissues. Most epithelial proliferations probably begin in the terminal ducts and manifest themselves as hyperplastic changes of ductal hyperplasia and/or lobular hyperplasia (Misdorp *et al*, 1999).

Based on several studies, the following factors have been determined to be prognostic factors: tumor size, histological type, malignancy grade, degree of nuclear differentiation, index of proliferation, evidence of lymphoid cellular reactivity in the tumor vicinity, degree of invasion, intravascular growth, estrogen/progesterone receptors activity, lymph node metastasis, and distant metastasis (Withrow and Vail, 2007). However to obtain more reliable prediction of the prognosis or to define potential targets for therapeutic strategies, more information on other molecular markers relating to progression of CMGT might be needed.

The ability of tumors to induce new blood vessel formation has been a major focus of cancer research over the past few decades, and VEGF (refers VEGF-A) is now known to play the central role of this process (Ferrara, 2002). VEGF-A is produced and secreted by a number of normal cell types and its expression is markedly increased in tumor cells as wells as in the immediate tumor stroma (Cuevas and Boudreau, 2009). Studies on human breast cancer reported a significant relationship between high expression of VEGF-A and tumors with higher proliferation rate and poor prognosis (Mohammed *et al*, 2007).

VEGF-C is produced as pro-prepeptide dimers that undergo proteolysis in the extracellular matrix to a mature form that has much higher affinity to VEGFR-3. Proteolytically processed form of VEGF-C can also bind with VEGFR-2, inducing angiogenesis. Overexpression of VEGF-C on invasive breast carcinomas was found to be an independent indicator of patient's poor prognosis, though it was not related to lymph node metastasis (Mylona *et al*, 2007).

Ki-67 is a marker of cell proliferation that is expressed in all active phases of the cell cycle except for G_0 phase. Several studies have evaluated Ki-67 as a proliferation index (PI) in human and veterinary literatures (Nishimura *et al*, 2010; van Rijn *et al*, 2010). In addition, strong angiogenetic recruitment from rapid tumor growth was indicated by Ki-67 expression, followed by high expression of VEGF (Hattori *et al*, 2005).

Recent studies have highlighted a link between high levels of macrophages, one of the inflammatory cells that exist in cancer microenvironment play an indispensable role in tumor progression, as called tumor-associated macrophages (TAMs) on tumor, and the process of metastasis, but not always, correlated with worse prognosis (Pollard, 2008). Accumulating evidences have shown that TAMs influence diverse processes such as angiogenesis, lymphangiogenesis, tumor growth and progression (Zhang *et al*, 2010). Macrophages and related myeloid cells may also reorganize tumor vasculature after treatment with inhibitors of VEGF signaling (Solinas *et al*, 2009). Interestingly, VEGF-C-producing TAMs were found to participate in lymphangiogenesis in two different ways, either by transdifferentiating and directly incorporating into the endothelial layer or by stimulating division of preexistent local lymphatic endothelial cells (Kerjaschki, 2005).

In this chapter, I investigated the expression of VEGF-A, VEGF-C, Ki-67 and macrophages on the CMGT tissues surgically removed from the spontaneous patients and the

correlation between their expression and clinical features and survival of these patients.

Materials and Methods

Tissue samples

Forty-nine primary CMGT tissues of the primary lesions were obtained from 25 dogs underwent surgical resection at Veterinary Medical Center, the University of Tokyo, between April 2006 and March 2008. Normal canine mammary gland (NCMG) tissues were obtained from 5 healthy beagle dogs without bearing any tumors, which were used in the other experiment and euthanized. The medical records of these CMGT patients were reviewed. The age, breed, body weight, history of spaying before the first estrus, number of tumor masses, tumor size, regional lymph node metastasis, distant metastasis, tumor recurrence, survival time and prognostic outcome were obtained from the medical records or telephone interviews to the owner and referred practitioners. Tumor size was calculated as the maximum diameter of the largest mass of the patients. The regional lymph node involvement was noticed by palpation and confirmed by histopathological examination and the distant metastasis was confirmed by thoracic radiography or histopathological examination after the autopsy. The WHO clinical staging system (Table 1.1.) was used for classification of CMGT patients. Survival time was defined as the time from the day of diagnosis to death.

Histopathology

The primary lesions of CMGT were fixed in 10% neutral buffered formalin and embedded in paraffin. A series of 4 μm-thick sections were stained with hematoxylin and eosin (HE) for histopathology. The tissues were histologically classified into the following 4 types, hyperplasia (HP), adenoma (AD), benign mixed tumor (BMT) and adenocarcinoma (AC) (Misdorp *et al*, 1999).

Immunohistochemistry

The expression of VEGF-A, VEGF-C and Ki-67 in the primary lesions of CMGT was analyzed by EnVision immunohistochemical procedures (DAKO EnVision+ kit/HRP, Diagnostics Japan, Inc., Kyoto, Japan).

Formalin-fixed paraffin-embedded sections were deparaffinized in xylene and rehydrated through graded ethanol, followed by distilled water. Antigen epitope retrieval was done by boiling the slides in autoclave at 121℃ for 10 minutes in citrate buffer (pH 6.0). Endogenous peroxidase activity was quenched in 0.03% hydrogen peroxide with the light interception condition for 10 minutes. Nonspecific protein binding was saturated using 5% normal goat serum (G9023; Sigma-Aldrich, Inc., MO, USA) in tris-buffered saline (TBS) for one hour at room temperature, except when staining for VEGF-A, where 5% normal rabbit serum (G9133; Sigma-Aldrich) was used. Then samples were reacted with the primary antibodies at 4℃ for overnight in a humid chamber and washed 3 times with TBS. Primary antibodies consisted of the following: polyclonal goat anti-canine VEGF-A, 1/50 (AF1603; R&D System, Inc., MN, USA); polyclonal rabbit anti-human VEGF-C, 1/200 (H-48; Santa Cruz Biotechnology, CA, USA); monoclonal mouse anti-human Ki-67, 1/100 (M7240; DAKO, Denmark); and rabbit anti-human Iba1, 1/250 (019-19741; Wako, Japan).

After being washed, samples were treated with polymer solution containing HRP-conjugated antibody against goat Ig (No. 414351; Nichirei bioscience, Tokyo, Japan) for VEGF-A, rabbit Ig (K4003; EnVision™-HRP labeled polymer, DAKO North America, Inc., CA, USA) for VEGF-C and Iba1, and mouse Ig (K4001; EnVision™-HRP labeled polymer, DAKO) for Ki-67, respectively, at room temperature for 30 minutes. Sections were visualized with liquid 3, 3'-diaminobenzidine (DAB)/hydrogen peroxide solution (K3468; DAKO North America, Inc.) and then counterstained with hematoxylin. Appropriate positive controls were

used to assess the specificity of the reactions. Negative controls were included where the primary antibody was replaced by TBS.

Evaluation of VEGF-A/-C expression, PI and Macrophages

For each sample, five high-power fields (×400) were randomly selected. Expression of VEGF-A and -C was assessed by the method of Mohammed et al.(Mohammed *et al*, 2007) using a semiquantitative immunohistochemical score (H score). Staining intensity was given four grades: (0) none, (1) weak, (2) moderate and (3) strong. The percentage of positive VEGF-A and VEGF-C expression cells were scored using ImageJ (NIH, USA). The score was calculated by multiplying the percentage of positive neoplastic cells by the staining intensity.

For assessment of PI, 5 high-power fields (×400) were randomly selected and 1,000 cells were counted in each CMGT section and the ratio of positive cell with of Ki-67 expression was calculated.

Iba1 positive cells, as considered macrophages, was observed and counted in the enriched field of view area under a light microscope at ×400 magnification for each CMGT section (Sasaki *et al*, 2001; Schoppmann *et al*, 2002). Iba1 positive cells of all tumors were evaluated by the author (SJL) and one student of Laboratory of Veterinary Pathology (ESP) and any discordant numbers led to re-evaluation to achieve a consensus.

The median values for VEGF-A, VEGF-C, PI and Iba1 positive cells of the whole specimens were used as cutoff points. This method in selecting an appropriate cutoff level was used in previous studies (Yang *et al*, 2002; Mohammed *et al*, 2007). Expression equal to or higher than the cutoff value was regarded as 'high' and expression below the cutoff value was regarded as 'low'.

Statistical analysis

For evaluation of VEGF-A/-C expression, the median values of samples were calculated. Statistical analyses for the degree of VEGF-A/-C expression among the histopathological types were made by Kruskal-Wallis test. If the statistical difference was observed, the difference between the two groups was determined by Mann-Whitney U-test with Bonferroni correction.

For evaluation of PI and Iba1 values, the mean ± SD values of samples were calculated. Comparison of the number of Ki-67 and Iba1 positive cells among the histopathological types was made by ANOVA, and the difference between the two groups was determined by the Bonferroni correction.

Spearman's rank correlation analysis was used to evaluate the relationship between the VEGF-A/-C expression, PI and Iba1 values of the tissue specimens. The relationship between expressions of VEGF-A, VEGF-C, PI and Iba1 values among 5 NCMG and 49 CMGT tissues was evaluated using an m×n square table and X^2 test. The relationship between expressions of these and clinicopathological characteristics in CMGT patients was evaluated in univariate analysis using a 2×2 table and X^2 test.

Survival curves of CMGT patients depending on the level of expression in VEGF-A, VEGF-C, PI and Iba1 values were obtained by Kaplan-Meier method and compared by the log-rank test. Statistical significance was evaluated by Statview ver. 5.0 (USA).

A probability of less than 5% ($P < 0.05$) was considered significant in all analyses.

Results

Clinical features and histological classification of CMGT patients

Clinical features of 25 CMGT patients are shown in Table 1.2. All the patients were female with a mean age of 10.7 years old (range: 5.8-15.2 years) and a mean body weight of 8.2 kg. Three dogs had history of spaying before the diagnosis of CMGT, but that was after the first estrus. Fifteen patients had multiple masses and 10 had solitary masses. Two patients with adenocarcinoma had both lymph node and lung metastasis at the time of diagnosis. Among the patients, 13 were classified into stage Ⅰ, 6 into stage Ⅱ, 4 into stage Ⅲ and 2 into stage Ⅴ, respectively. Mean and median survival times of patients were 596.9 days and 697 days, respectively (range: 1-1190 days). The breed distribution was as follows: 5 miniature Dachshunds, 3 maltases, 3 Yorkshire terriers, 2 Italian greyhounds, 2 Shetland sheepdogs, 2 Siberian huskies, 2 mixed breed dogs, 1 Cavalier King Charles spaniel, 1 miniature schnauzer, 1 papillon, 1 shih tzu, 1 toy poodle and 1 Welsh corgi.

Total CMGT tissue specimens were 49 from 25 patients, and their histopathological types are shown in Table 1.3. Among 49 primary tumor tissues, 11 were HP, 10 were AD, 10 were BMT and 18 were AC, respectively.

Expression of VEGF-A

The expression of VEGF-A was observed on all the tissues of various histological types (Figure 1.1). In NCMG tissues, VEGF-A was positively expressed homogeneously on intralobular duct epithelial cells. Expression patterns of VEGF-A were diffuse and/or granular on the cytoplasm of stromal cells, such as macrophages, fibroblasts, smooth muscle and endothelial cells with positivity. In HP tissues, VEGF-A was positively expressed

heterogeneously distributed and focused on some epithelial cells. The expression level was weak and/or moderate in benign tumor tissues, and moderate to strong localized expression was observed in malignant tumor cells. In some specimens, the staining intensity was heterogeneous among the areas on BMT and AC tissues.

Figure 1.2 shows the VEGF-A expression scores in tissues of NCMG and MGTs of each histopathological type. The median score of VEGF-A expression was 112.0 in NCMG, 126.0 in HP, 168.0 in AD, 210.0 in BMT and 259.0 in AC, respectively. VEGF-A expression scores tended to be higher according to the malignancy of CMGT tissues. The VEGF-A score of AC tissues was significantly higher than those of NCMG and HP tissues ($P = 0.0257$ and $P = 0.0108$, respectively).

Expression of VEGF-C

VEGF-C was expressed on the cytoplasm of both grandular and ductal epithelial cells in all of normal mammary gland and tumor tissues (Figure 1.3). Occasionally, myoepithelial cells and stromal cells of interlobular and intralobular connective tissues were stained positive for VEGF-C.

Figure 1.4 shows the VEGF-C expression scores on tissues of NCMG and MGT tissues. Although the VEGF-C expression score of AD was lower than those of other groups, there was no significant difference in VEGF-C expression among histological types including NCMG.

Expression of Ki-67 and PI

Nuclear expression of Ki-67 varied in percentage in all tissues (Figure 1.5). The percentage of Ki-67 positive cells (PI values) was calculated according to each histopthological type is shown in Figure 1.6. The mean ± SD percentage of PI was 5.22 ± 5.64 in NCMG, 14.60 ± 9.73 in HP, 17.93 ± 13.44 in AD, 4.88 ± 8.05 in BMT and 31.35 ± 15.21 in AC, respectively.

PI tended to be higher according to increase in the malignancy of CMGT except BMT. PI of AC was significantly higher than NCMG, HP, AD and BMT ($P = 0.0003$, $P = 0.0018$, $P = 0.0216$ and $P = 0.0001$, respectively).

Macrophage count

Figure 1.7 shows Iba1 positive cells in the tissues of healthy mammary gland and CMGT tissues. Iba1 antibody could detect macrophages. Most of macrophages were located at the intralobular and interlobular connective tissues near cancer cells, inflammatory cells and blood vessles.

Figure 1.8 shows the number of Iba1 positive cells in tissues of NCMG and MGTs of each histopathological type. The mean ± SD number of Iba1 positive cells was 16.60 ± 12.82 in NCMG, 15.55 ± 14.01 in HP, 52.30 ± 36.10 in AD, 89.70 ± 46.51 in BMT and 70.56 ± 51.94 in AC, respectively. Number of Iba1 positive cells was significantly higher in BMT than those of NCMG and HP ($P = 0.0176$ and $P = 0.0011$, respectively), and that of AC was significantly higher than that of HP ($P = 0.0083$).

Correlation among VEGF-A , VEGF-C, PI and Iba1 values

Figure 1.9 shows correlation between VEGF-A expression and Ki-67, and between VEGF-A expression and Iba1 positive cells in all tissues samples. Spearman's rank correlation analysis demonstrated significant correlation between VEGF-A expression and Ki-67 positive cells (%) (correlation coefficient $r = 0.4417$, $P = 0.0010$) and between VEGF-A expression and Iba1 positive cells (correlation coefficient $r = 0.4833$, $P = 0.0002$). However, no statistically significant correlation was found between the expression of VEGF-A and VEGF-C, and between VEGF-C expression and PI or Iba1 positive cells (data not shown).

***Relationship between the values of VEGF-A, VEGF-C, PI and Iba1 and
histopathological classification***

As previously defined in Materials and Methods, all these values were divided into the
low and high groups. Then, the correlation between low or high of VEGF-A/-C, PI and Iba1
values and each histopathological classification was examined (Table 1.4).

All of the NCMG, HP, AD tissues showed low expression of VEGF-A, while 13 of AC
tissues (72%) showed high expression. There was a significant difference in expression of
VEGF-A among the tissues of histopathological types ($P = 0.0003$). As for the expression level
of VEGF-C, most of AD tissues were classified as the low group and a half of AC tissues were
classified as the high group, however there was no significant difference in VEGF-C expression
among the histopathological types ($P = 0.0683$). Five of NCMG (100%), 9 of HP (82%), 6 of
AD (60%) and 9 of BMT (90%) tissues were classified into the low PI group, while 14 AC
tissues (78%) were classified into the high PI group. There was a significant difference in PI
value among the histopathological types ($P = 0.0041$). All of NCMG and HP tissues showed
low Iba1 counts and 6 of AD (60%), 7 of BMT (70%) and a half of AC tissues showed high
Iba1 coounts. There was a significant difference in Iba1 value among the histopathological types
($P = 0.0213$).

***Relationship between the values of VEGF-A, VEGF-C, PI and Iba1 and
clinical features of the CMGT patients***

In the following evaluation for the relationship between the values of VEGF-A, VEGF-C,
PI and Iba1 and clinicopathological characteristics of CMGT patients and analyses of the
survival rates, the worst histological diagnosis was used in each patient with multiple masses.

Table 1.5 shows the correlation between low or high of VEGF-A/-C, PI and Iba1 values

and clinicopathological features of CMGT patients.

VEGF-A expression was found to have no correlation with any clinicopathological features except the cytological atypia of CMGT. The high VEGF-A expression was recorded significantly more in tumor tissues with high cytological atypia compared with those with low VEGF-A expression ($P = 0.0048$). On the other hand, VEGF-C expression was correlated with the tumor size of CMGT. The high VEGF-C expression was recorded significantly more in tumor tissues with the size of smaller than 3cm compared with those with low VEGF-C expression ($P = 0.0472$), however there were no correlation with other clinicopathological features. Significant correlation were found between the PI value and lymphatic invasion ($P = 0.0149$) and cytological atypia ($P = 0.0048$). The all tissues with lymphatic invasion had high PI values. Iba1 positive cells were also not correlated with clinicopathological features, except for the age of the patients. Dogs with the high Iba1 value were significantly older (over 10 years) than those with low Iba1 values ($P = 0.0154$).

Prognostic significance of VEGF-A, VEGF-C, PI and Iba1 values

Kaplan-Meier analysis for survival rates was conducted to investigate whether expression of VEGF-A, VEGF-C, PI and Iba1 values had any prognostic significance. The mean and median survival of 25 patients were 596.9 ± 340.9 and 697 days (range: 1-1190 days), respectively. The overall 1-year survival rate was 68% and 2-year survival rate was 40% in 25 CMGT patients.

The survival rate of 13 dogs of the high VEGF-A expression group was significantly worse than that of 12 dogs with the low VEGF-A expression group ($P = 0.0447$) (Figure 1.10.A). On the other hand, the survival rate of 11 dogs of the low VEGF-C expression group was almost similar to that of 14 dogs of the high VEGF-C expression group ($P = 0.4239$)

(Figure 1.10.B). The survival rate of 13 dogs of the high PI group tended to be worse than that of 12 dogs with the low PI group ($P = 0.0563$) (Figure 1.10.C). The survival rate of 13 dogs of the high Iba1 (macrophages) group was almost similar to that of 12 dogs of the low Iba1 values group ($P = 0.7257$) (Figure 1.10.D).

On the other hand, Kaplan-Meier survival cure of 14 AC patients grouped according to the low and high VEGF-A, VEGF-C, PI and Iba1 values had no significant difference (data not shown).

Discussion

In this chapter, I studied on the expression of VEGF-A and VEGF-C in canine mammary gland tumor tissues from spontaneous patients and their correlations with the proliferation index, number of macrophages in tissues and clinical features.

Among the VEGF family members, VEGF-A is a specific ligand for the blood vessel endothelial tyrosine kinase VEGFR2 and VEGF-C is for lymphatic endothelial tyrosine kinase VEGFR3 (Lohela *et al*, 2009). Tyrosine phosphorylation is one of the key mechanisms which switch on signal transduction by regulating other proteins, such as VEGF-A/-C that concern with cancer progress by direct stimulation of enzymatic activity, re-localization within the cytoplasm, and enhancement of tyrosine phosphorylation (Kinoshita *et al*, 2001). However, detailed mechanisms of VEGF-A and VEGF-C signal transduction have not been clarified in the veterinary oncology.

In this present study, VEGF-A protein was immunodetected in the cytoplasm of the CMGT cells, similar to the previous reports (Van der Auwera *et al*, 2004; Kamath *et al*, 2009). In addition, the expression was also observed at the stromal compartment of the tumor tissues, as reported by Millanta et al. (Millanta *et al*, 2006). VEGF-A was reported to be detected not only on the tumor tissues but on the normal dog tissues (Uchida *et al*, 2008; Santos *et al*, 2010). Obermair et al. demonstrated that VEGF concentrations were significantly higher in the breast cancer tissue than in the normal epithelial tissue of the breast (Obermair *et al*, 1997). In this study, VEGF-A was stained on NCMG tissues with weaker levels than CMGT tissues. This may indicate that VEGF-A has both physiological and pathological roles in mammary glands of dogs. Since VEGF-A expression levels showed significantly higher in AC than NCMG and HP and, not significantly, than AD and BMT, it may suggest the potential involvement of VEGF-A

in the later stages of tumor development. Moreover, 72% of AC tissues were classified into the high VEGF-A expression group. In a recent study, VEGF-A immunoreactive tumor cells was significantly higher in canine inflammatory mammary carcinoma (IMC) than in non-IMC, that suggests VEGF-A may contribute to the high angiogenic phenotype of canine IMC (Millanta *et al*, 2010). The high VEGF-A expression was recorded significantly more in tumor tissues with high cytological atypia compared with those with low VEGF-A expression. This finding permits us to conclude the positive correlation between CMGT malignancy and VEGF-A expression.

Two patients with high VEGF-A expression were found to be positive with lymph node and distant metastasis, though the number of patients bearing metastasis was not enough to detect any correlation between VEGF-A expression and lymph node and distant metastasis. The high VEGF-A expression was recorded significantly more in tumor tissues with high cytological atypia compared with those with low VEGF-A expression. Furthermore, the survival rate showed a significant difference between groups of low and high VEGF-A expression, suggesting VEGF-A may be a prognostic factor in CMGT. This result also supports the previous study, in which tumors with higher VEGF-A expression behaved more aggressively and were significantly associated with the presence of lymph node metastasis, distant metastasis and poorer survival in human breast cancer, CMGT and other tumor types (Toi *et al*, 1995; O-charoenrat *et al*, 2001; Qiu *et al*, 2008).

In this study, VEGF-C was immunodetected predominantly in the cytoplasm of the malignant cells and the stromal fibroblasts, in which the localization was similar to that in human breast cancer (Nakamura *et al*, 2003; Mylona *et al*, 2007). To my best knowledge, this is the first study on VEGF-C expression on immunohistochemistry in CMGT. VEGF-C expression at the site of tumor invasion has been reported to be an important predictor of a higher malignancy potential and poorer prognosis of colorectal carcinoma, closely relating to

angiogenesis (Furudoi *et al*, 2002). Moreover, it was demonstrated that the coexistent overexpression of both VEGF-A and VEGF-C in gastric cancer patients, but not the overexpression of each of them, is responsible for lymph node metastasis (Kondo *et al*, 2007). However, in this study, VEGF-C expression on CMGT tissues was not significantly different among the histological types. Normal tissues also showed positive expression with the similar level. In the report by Qiu et al., VEGF-C mRNA expression levels of both normal mammary and benign MGT tissues in the dog were low, but in the malignant CMGT tissues with lymph node metastasis, VEGF-C expression was much higher than in other mammary tumor tissues (Qiu *et al*, 2008). RT-PCR assay could not reveal the protein level of VEGF-C expression correctly if microdissection was not performed. Further study should be needed to elucidate the reason why VEGF-C expression was low in adenoma tissues, which was the stage of the start point of tumorigenesis from hyperplasia of the mammary gland (Benjamin *et al*, 1999).

VEGF-C plays an important role in lymphangiogenesis, leading to a poor prognosis in aggressive human breast carcinoma (Gu *et al*, 2008). CMGT is one of the most well known tumors with lymph node metastasis. Lymphangiogenesis may serve as a predictor of lymph node metastasis and a prognostic factor in CMGT. However, in this study, VEGF-C expression was not related to the clinicopathological parameters, especially lymph node metastasis. The two-year survival rate was not related to low and high expression of VEGF-C. But, interestingly, 10 of 12 (83%) patients with smaller-size masses showed high VEGF-C expression compared with those with the mass larger than 3cm in diameter. This lack of correlation was also reported in some studies (Kinoshita *et al*, 2001), where there was a correlation between VEGF-C expression and lymphatic vessel invasion, but not between its expression and lymph node metastasis. One possible explanation is that VEGF-C might be responsible for very early events of lymphatic spread before the primary mass being bigger, prior to the lymph node metastasis,

such as report of Mylona *et al.(Mylona et al, 2007)*. On the other hand, this discrepancy may be reflected by the different antibody used in this study and probably due to a small number of patients. The correlation between VEGF-C expression and malignancy and/or survival of not only the breast cancer patients but the other tumors patients is still controversial (Straume *et al*, 2003; Stacker *et al*, 2004). Further studies should be needed to elucidate the role of VEGF-C in CMGT.

Ki-67 is a nuclear protein strictly associated with cell proliferation. Ki-67 protein is expressed during all active phases of the interphase in the cell cycle (G_1, S, G_2, and mitosis) (Scholzen and Gerdes, 2000). Ki-67 protein has been used in the assessment of cell proliferation, particularly in the assessment of the prognosis for human neoplasms and canine tumors (Endl and Gerdes, 2000; Ishikawa *et al*, 2006). In this study, Ki-67 expression was a good parameter of malignant tumor, because AC showed a significantly higher expression among other CMGT tissue types. Interestingly, BMT, characterized by the abundant myofibroblasts and stromal cells, showed the lowest Ki-67 expression level among all the histological types of CMGT.

On the other hand, Iba1 positive cells of BMT were significantly higher than those of NCMG and HP. Also, Iba1 positive cells of AC were significantly higher than that of HP. Iba1 (ionized calcium binding adaptor molecule 1) is a macrophage/microglia-specific calcium-binding protein. Iba1 has the actin-bundling activity and participates in membrane ruffling and phagocytosis in activated macrophages (Ohsawa *et al*, 2004). High levels of macrophages in BMT may be associated with cancer microenvironments. It is not clear whether BMT arises through an intermediate stage consisting of a complex adenoma, or BMT arises directly from lobular hyperplasia, or both (Benjamin *et al*, 1999). Generally, macrophages are a smaller proportion of the tumor tissue and are found in particular niches; the stroma surrounding the tumor, the invasive front, necrotic areas of advanced tumors and the abluminal side of the

vessels (Pollard, 2008). Pollard proposed that the macrophages in the tumor were educated by the local environment to perform tasks similar to the trophic, nonimmune roles that they perform to promote epithelial outgrowth and invasion during development. Further research should be needed to assess the character and malignancy of BMT in CMGT.

In this study, there was a significant positive correlation between the expression of VEGF-A and PI and between the expression of VEGF-A and macrophages, all of which showed high expressions depending on the level of malignancy of CMGT tissues. These findings may suggest the reciprocity with VEGF-A expression and tumor growth which may play a crucial role in angiogenic metastasis of CMGT. Although the effect of VEGF-A expression can be mediated by an increased vascular network, it should be noted that VEGF-A has also been shown to increase breast cancer cell survival through direct action on phosphorylation of VEGFR-2 that has been found to be expressed on the surface of the breast cancer cells. VEGF-A production by VEGFR-2 activation indicates the presence of a distinct autocrine signaling loop that enables breast cancer cells to promote their own growth and survival (Weigand *et al*, 2005).

Macrophages produce VEGF-A in human breast cancers (Leek *et al*, 2000). Thus at least one of the functions of macrophages in tumors is to deliver VEGF-A temporarily and spatially to constitutively promote angiogenesis. Furthermore, the localization of macrophages at the area with marked angiogenesis suggests that functions of macrophages would further promote tumor cell dissemination via the formation of more vessels that would be targets for tumor cell intravasation (Pollard, 2008). VEGF-A was reported to be linked to the hypoxic condition in the necrotic compartments (Shweiki *et al*, 1992). The hypoxic response could act synergistically with other tumor-related cytokines produced by macrophages and other inflammatory cells, and up-regulated VEGF-A cascade in neoplasms. In this regard, macrophages could play an

important role in VEGF-A-mediated angiogenesis (Leek *et al*, 2000; Tsutsui *et al*, 2005).

Macrophages were also strongly involved in lymphangiogenesis, a process mediated by a number of factors including VEGF-C and VEGF-D via VEGFR3. Lymphatic endothelial growth factors secreted by macrophages are related to peritumoral lymphangiogenesis (Schoppmann *et al*, 2002; Ji, 2006). However, in this study, there was no significant correlation between VEGF-C and macrophages. In addition, the survival rate showed no significant difference between low and high macrophages groups. In human medicine, macrophages were suggested to be an attractive target of novel biological therapies of tumors (Solinas *et al*, 2009). Further researches should be needed to clarify the relationship between macrophages and VEGF-A/-C in CMGT.

To the best of our knowledge, this study is the first report on investigating VEGF-A expression on hyperplastic tissues of CMGT. The median score of VEGF-A expression on hyperplastic tissues was higher than NCMG but significantly lower than that of AC. Bluff et al. showed that a significant increase in VEGF-A expression with increasing severity of human breast cancer lesions, which suggested that the angiogenic switch occurs at the onset of hyperplasia in the mammary duct before any morphological evidence of atypia (Pavlakis *et al*, 2008; Bluff *et al*, 2009). Probably, the pre-malignant conditions like hyperplasia of mammary gland, an early event during tumorigenesis, may play an important role in malignancy related with VEGF-A and angiogenesis although it is not yet clear (Raica *et al*, 2009). Further research should be needed to clarify the role of VEGF-A and tumor angiogenesis in hyperplasia of CMGT.

In this study, there were a few limitations. The number of CMGT cases investigated was small. In addition, some cases were lost during the follow up. Furthermore, the information was obtained by telephone interview to owners, thus accurate information such as latent lymphatic

invasion and metastasis could not be obtained. In the present study, I investigated only the primary lesion of CMGT for the purpose of evaluating the efficacy of VEGF-A, VEGF-C, PI and macrophages as a diagnostic tool. Evaluating its expression on the metastatic lesion of CMGT may clarify the relationship to distant metastasis, though tissue specimens of metastatic lesions such as lymph node and lung metastasis were difficult to obtain.

Further clinical studies of CMGT would be needed focusing on the relationship between angiogenesis and lymphangiogenesis with the metastasis from the point of prognostic parameter. It is required in order to clarify the role of VEGF-A/-C in CMGT with a valuation of angiogenesis and lymphangiogenesis potential as well as their possible prognostic value and usefulness as a novel target in CMGT. I tried to look for the marker of vascular and lymphatic endothelial cells and preliminarily tested with some of canine tissue samples, however, I could not find the adequate marker for lymphatic endothelial cells. Therefore, in the next chapter, I used a nude mouse model xenografted with CMGT cell lines.

Summary

In this chapter, I examined the expression of VEGF-A, VEGF-C, Ki-67 and Iba1 (macrophages) on the CMGT tissues of spontaneous patients and mammary tissues of healthy dogs and compared their expression levels. Then I investigated the relationship between their expressions and histological types, clinical features and prognostic outcome.

VEGF-A/-C were expressed in both normal canine mammary gland tissues and all CMGT. The scores of VEGF-A expression were higher in adenocarcinoma than those in normal mammary tissues benign and CMGT. VEGF-A expression was positively correlated with PI and Iba1 values in the primary, suggesting that VEGF-A may play an important role in the progression of mammary cancers and be a significant factor on patient prognosis.

On the other hand, VEGF-C expression seemed no correlation with malignancy and prognosis of CMGT. However VEGF-C might be responsible for very early stages of the primary mass proliferation.

Modified system			

T (Primary tumor)

T1	< 3 cm maximum diameter
T2	3-5 cm maximum diameter
T3	> 5 cm maximum diameter

N (Regional lymph nodes)

N0	Histologic or cytologic - No metastasis
N1	Histologic or cytologic - Metastasis present

M (Distant metastasis)

M0	No distant metastasis detected
M1	Distant metastasis detected

Stages	T	N	M
I	T1	N0	M0
II	T2	No	M0
III	T3	N0	M0
IV	Any T	N1	M0
V	Any T	Any N	M1

Table 1.1. Clinical staging of canine mammary gland tumors modified from Owen LN (Classification of tumors in domestic animals, Geneva: World Health Organization, 1980)

Clinical features	Value
No. of patients	25
Age(year)	
Mean ±SD	10.7 ± 2.5
(Range)	(5.8 - 15.2)
Weight(kg)	
Mean ±SD	8.2 ± 7.2
(Range)	(1.5 - 34.0)
Ovarian state	
Spayed	3 (12%)
Intact	22 (88%)
Number of tumors	
Solitary	10 (40%)
Multiple	15 (60%)
Tumor diameter(cm)	
Mean ±SD	3.3 ± 2.7
(Range)	(0.5 - 13.0)
<3	13 (52%)
3~5	8 (32%)
>5	4 (16%)
Lymph node metastasis	
Negative	23 (92%)
Positive	2 (8%)
Distant metastasis	
Negative	23 (92%)
Positive	2 (8%)
Clinical stage	
I	13 (52%)
II	6 (24%)
III	4 (16%)
IV	0 (0%)
V	2 (8%)
Tumor recurrence	
No	17 (68%)
Yes	8 (32%)
Survival time (days)	
Mean ±SD	596.9 ± 340.9
Median	697
(Range)	(1- 1190)

Table 1.2. Clinical features of CMGT patients.

Histopathological diagnosis	No. of tissue samples	Total
Hyperplasia (HP)	11	11
Adenoma (AD)		10
Complex adenoma	3	
Adenoma	7	
Benign mixed tumor (BMT)	10	10
Adenocarcinoma (AC)		18
Complex carcinoma	3	
Adenocarcinoma	12	
Solid carcinoma	3	
Total		49

Table 1.3. Histopathological diagnosis of CMGT tissues

Histopathological classification	No. of tissue samples	No. (%) of VEGF-A expressing specimens			No. (%) of VEGF-C expressing specimens			No. (%) of Ki-67 positive expressing specimens			No. (%) of Iba1 positive expressing specimens		
		Low	High	*P*	Low	High	*P*	Low	High	*P*	Low	High	*P*
NCMG	5	5 (100)	0 (0)	0.0003**	1 (20)	4 (80)	0.0683	5 (100)	0 (0)	0.0041**	5 (100)	0 (0)	0.0213*
HP	11	11 (100)	0 (0)		4 (36)	7(64)		9 (82)	2 (18)		11 (100)	0 (0)	
AD	10	10 (100)	0 (0)		9 (90)	1 (10)		6 (60)	4 (40)		4 (40)	6 (60)	
BMT	10	7 (70)	3 (30)		2 (20)	8 (80)		9 (90)	1 (10)		3 (30)	7 (70)	
AC	18	5 (28)	13 (72)		8 (44)	10 (56)		4 (22)	14 (78)		9 (50)	9 (50)	

Table 1.4. Correlation between low or high VEGF-A, VEGF-C, Ki-67 and Iba1 values and NCMG and CMGT tissues.

*, **: Significant difference between the groups (*: *P*<0.05, **: *P*<0.01)

		No. of VEGF-A expressing patients			No. of VEGF-C expressing patients			No. of Ki-67 positive expressing patients			No. of Iba1 positive expressing patients		
Variable	No.	Low	High	P	Low	High	P	Low	High	P	Low	High	P
No.	25	12	13		11	14		12	13		12	13	
Age(year)				0.8063			0.4139			0.5673			0.0154*
＜ 10	10	5	5		3	7		6	4		8	2	
≧ 10	15	7	8		8	7		6	9		4	11	
Weight(kg)				0.5930			0.2878			0.0957			0.3217
＜ 12	21	11	10		8	13		12	9		9	12	
≧ 12	4	1	3		3	1		0	4		3	1	
Ovarian state				0.5930			1.0000			1.0000			0.5930
Intact	22	10	12		10	12		11	11		10	12	
Spayed	3	2	1		1	2		1	2		2	1	
Number of tumor				0.5673			0.0992			0.8063			0.8063
Solitary	10	6	4		2	8		4	6		5	5	
Multiple	15	6	9		9	6		8	7		7	8	
Tumor diameter(cm)				0.8350			0.0472*			0.3127			0.3127
＜ 3	13	7	6		3	10		8	5		8	5	
≧ 3	12	5	7		8	4		4	8		4	8	
Cytological atypia				0.0048**			0.3252			0.0048**			0.8350
Low~Moderate	13	10	3		4	9		10	3		6	7	
High	12	2	10		7	5		2	10		6	6	
Vascular invasion				0.4800			0.1833			0.4800			0.4800
Negative	23	12	11		9	14		12	11		12	11	
Positive	2	0	2		2	0		0	2		0	2	
Lymphatic invasion				0.0593			0.1333			0.0149*			0.6447
Negative	20	12	8		7	13		12	8		9	11	
Positive	5	0	5		4	1		0	5		3	2	
Lymph node metastasis				0.4800			0.1833			1.0000			0.4800
Negative	23	12	11		9	14		11	12		12	11	
Positive	2	0	2		2	0		1	1		0	2	
Distant metastasis				0.4800			0.1833			1.0000			0.4800
Negative	23	12	11		9	14		11	12		12	11	
Positive	2	0	2		2	0		1	1		0	2	
Clinical stage				0.1620			0.3500			0.6447			1.0000
Ⅰ～Ⅱ	19	10	9		7	12		10	9		9	10	
Ⅲ～Ⅴ	6	2	4		4	2		2	4		3	3	
Tumor recurrence				0.6728			0.2337			0.2016			0.4110
No	17	9	8		9	8		10	7		7	10	
Yes	8	3	5		2	6		2	6		5	3	

Table 1.5. Correlation between VEGF-A, VEGF-C, PI and Iba1 values and clinicopathological features of CMGT patients.

*, **: Significant difference between the groups (*: *P*<0.05, **: *P*<0.01)
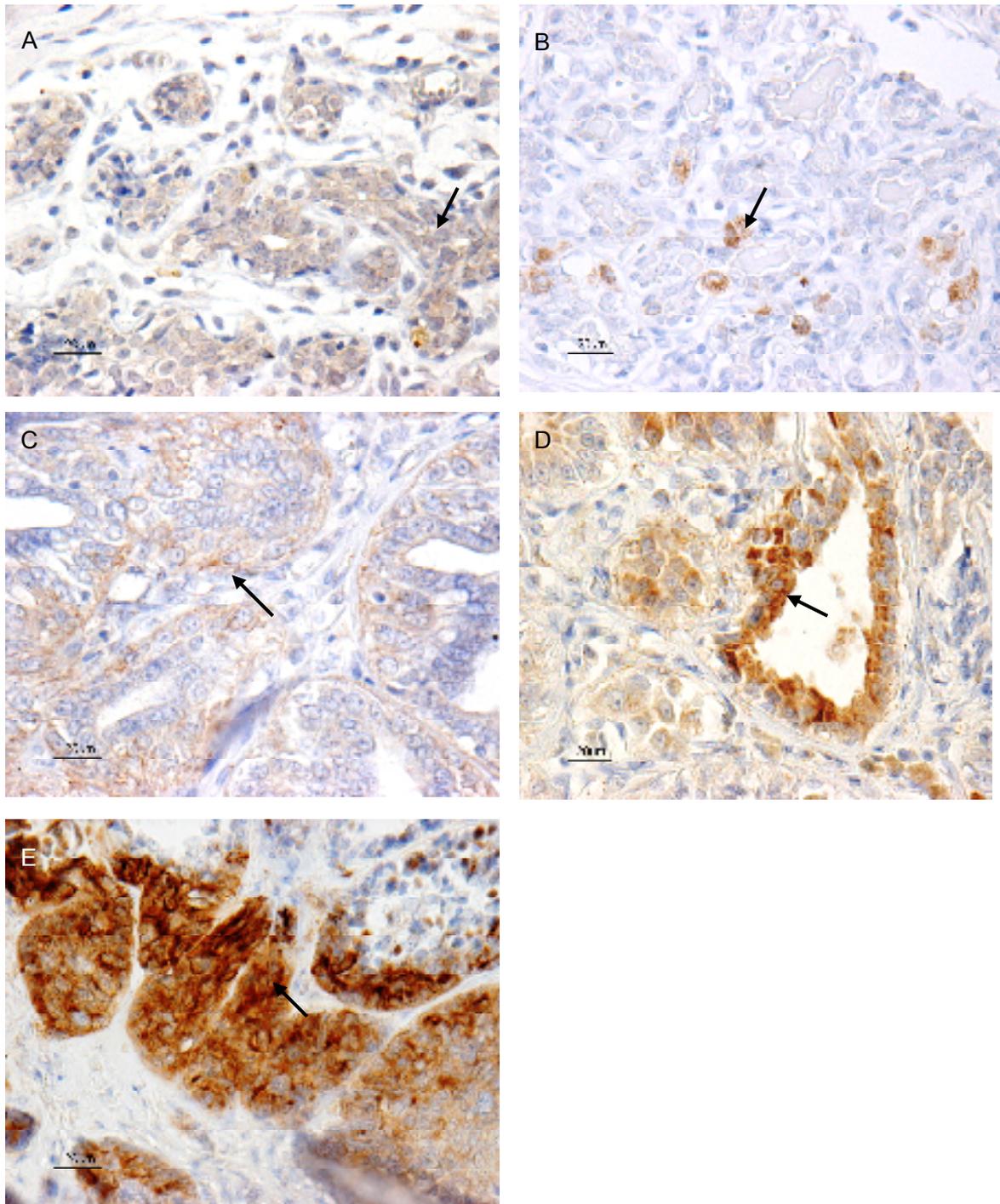
Figure 1.1. Immunohistochemical staining of VEGF-A on NCMG (A) and CMGT primary lesions; HP (B), AD (C), BMT (D) and AC (E). Arrows indicate the positive cells.

(Magnification ×400)
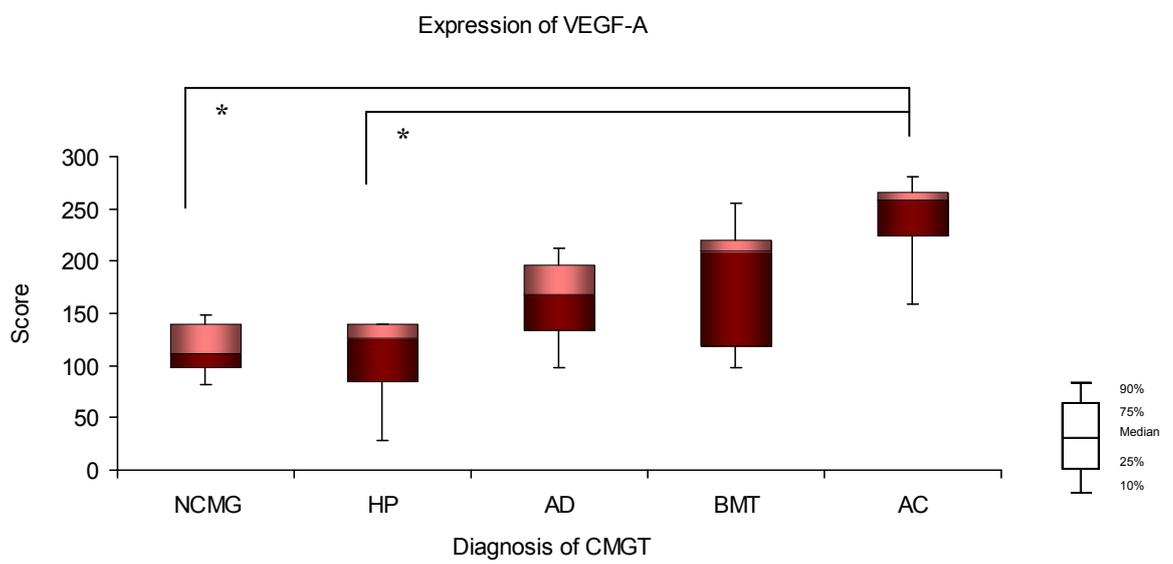
**Figure 1.2.** VEGF-A scores on NCMG and CMGT tissues.

*: Significant difference between the groups (*P*<0.05)
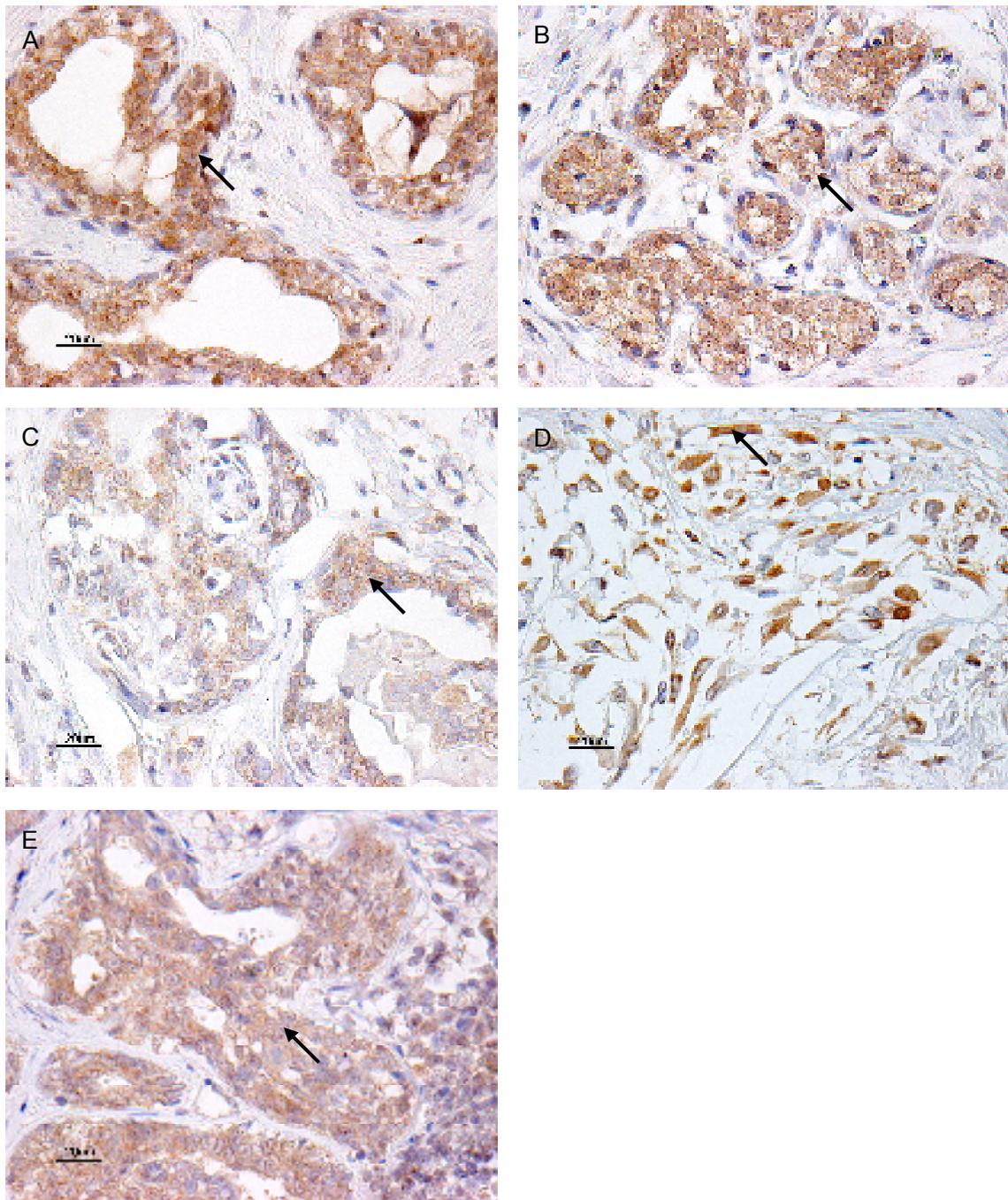
Figure 1.3. Immunohistochemical staining of VEGF-C on NCMG (A) and CMGT primary lesions; HP (B), AD (C), BMT (D) and AC (E). Arrows indicate the positive cells. (Magnification ×400)
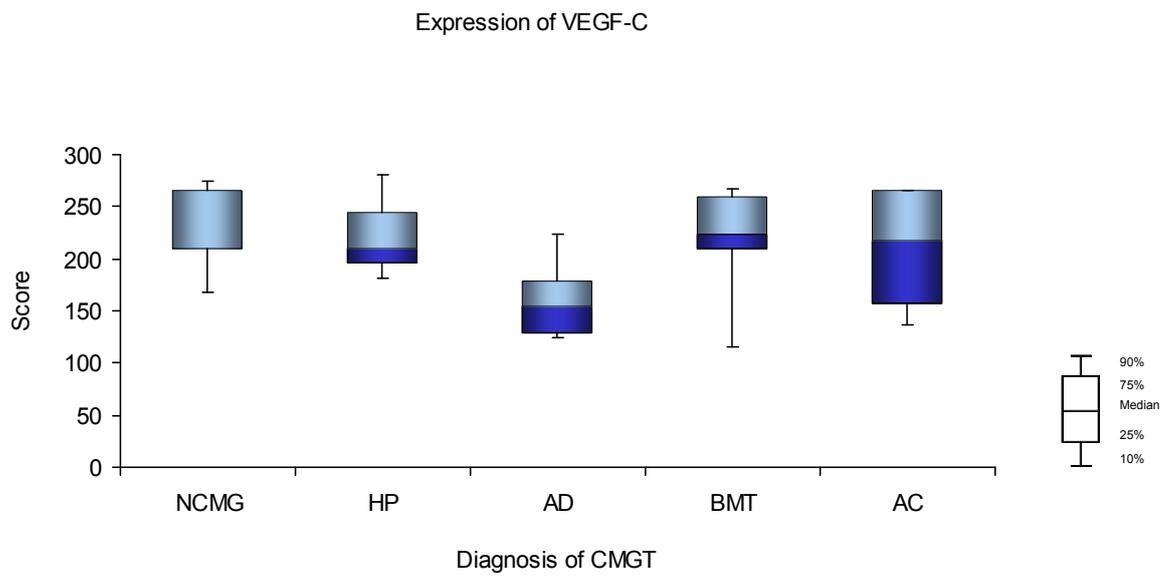
Figure 1.4. VEGF-C score on NCMG and CMGT tissues.

There was no significant difference between the groups.
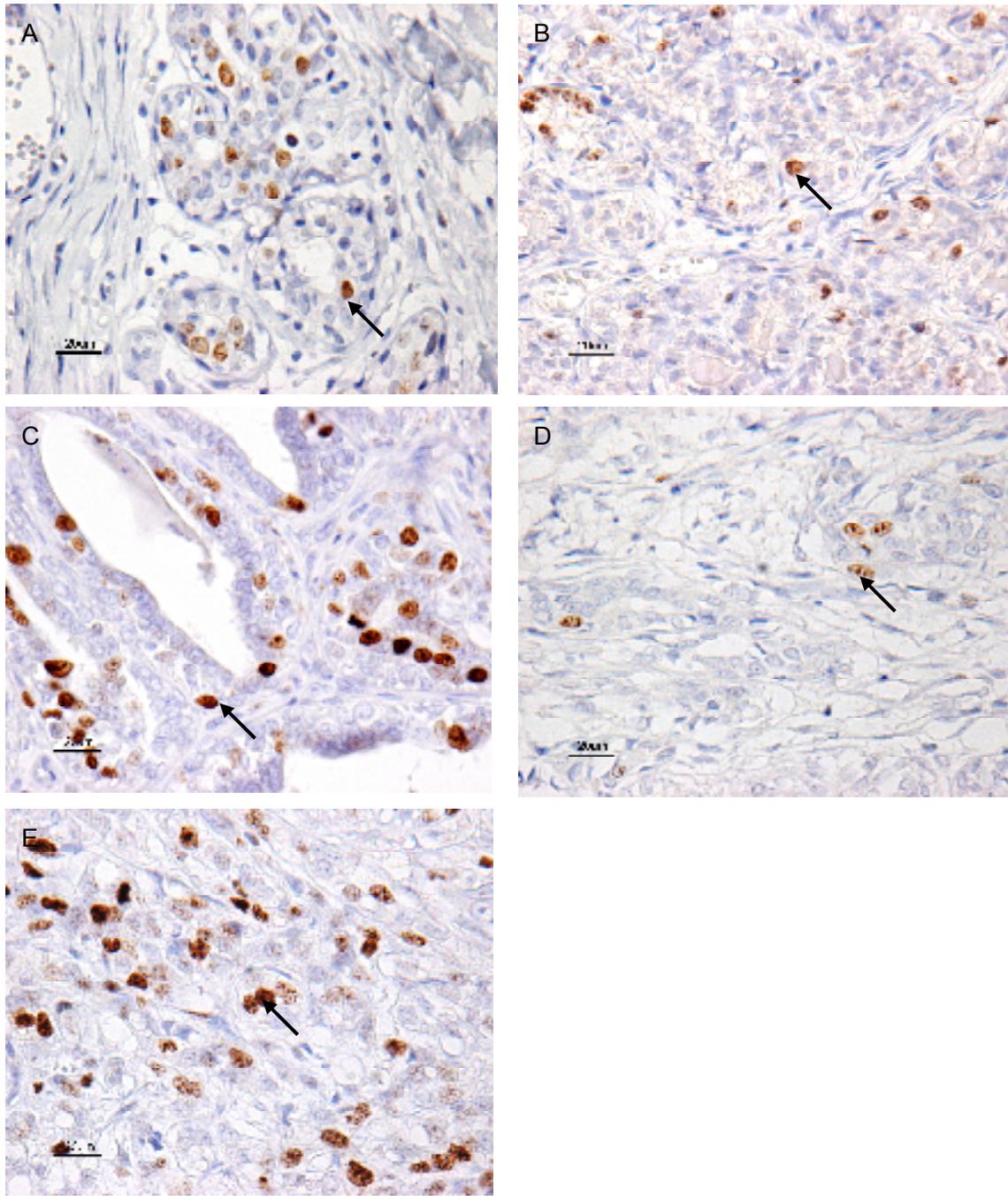
Figure 1.5. Immunohistochemical staining of Ki-67 on NCMG (A) and CMGT primary lesions; HP (B), AD (C), BMT (D) and AC (E). Arrows indicate the positive cells. (Magnification ×400)
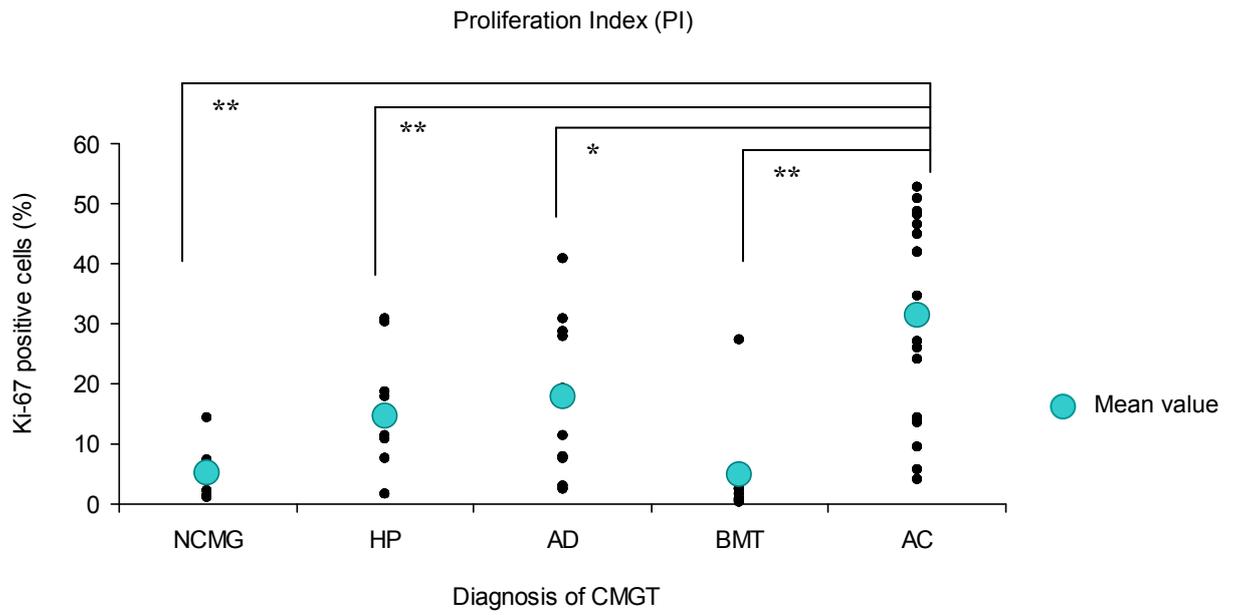
Figure 1.6. PI values in NCMG and CMGT tissues.

*, **: Significant difference between the groups (*: $P<0.05$, **: $P<0.01$)
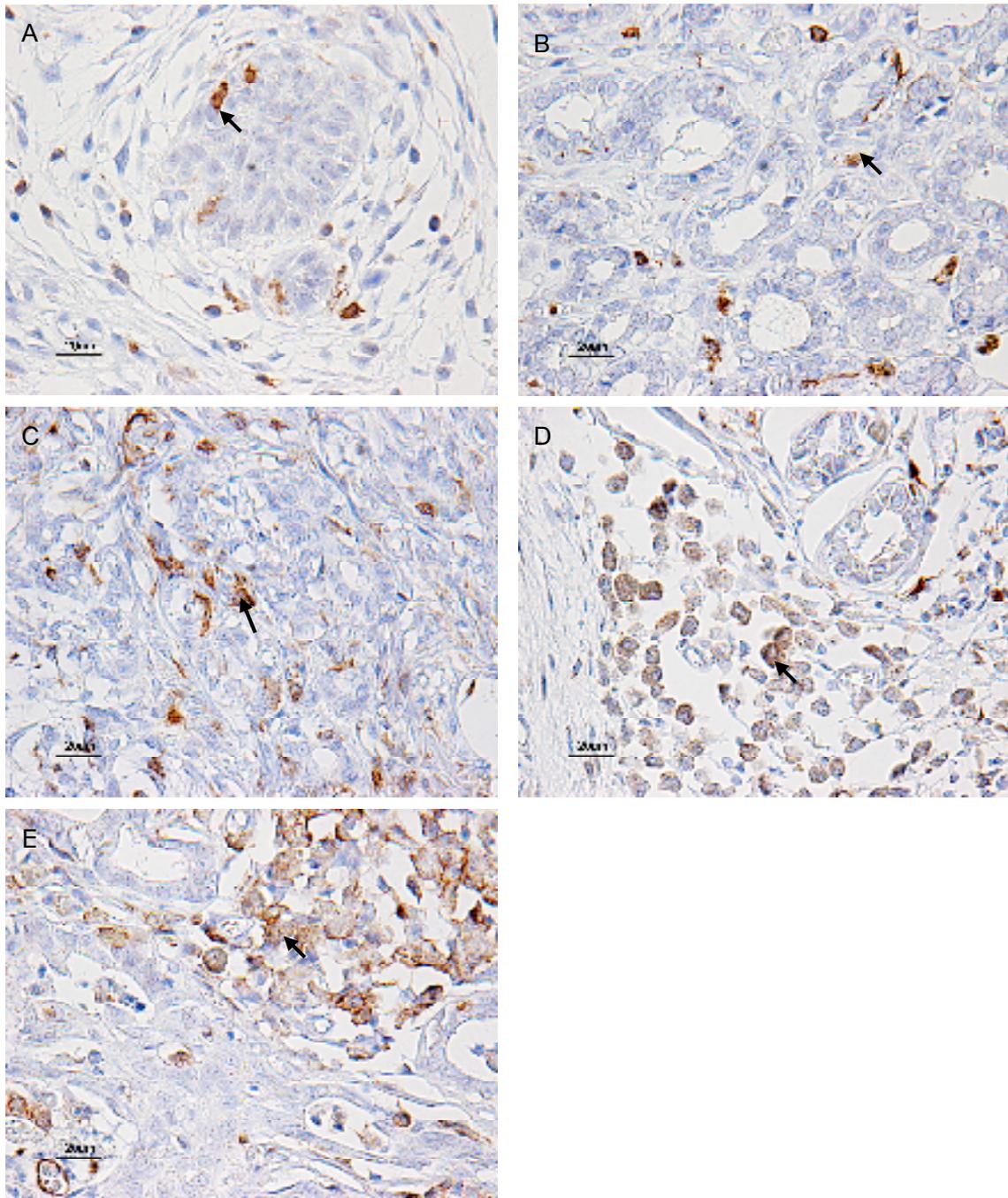
Figure 1.7. Iba1-positive cell counting for evaluation of macrophages in NCMG (A) and CMGT primary lesions; HP (B), AD (C), BMT (D) and AC (E). Arrows indicate the positive cells. (Magnification ×400)
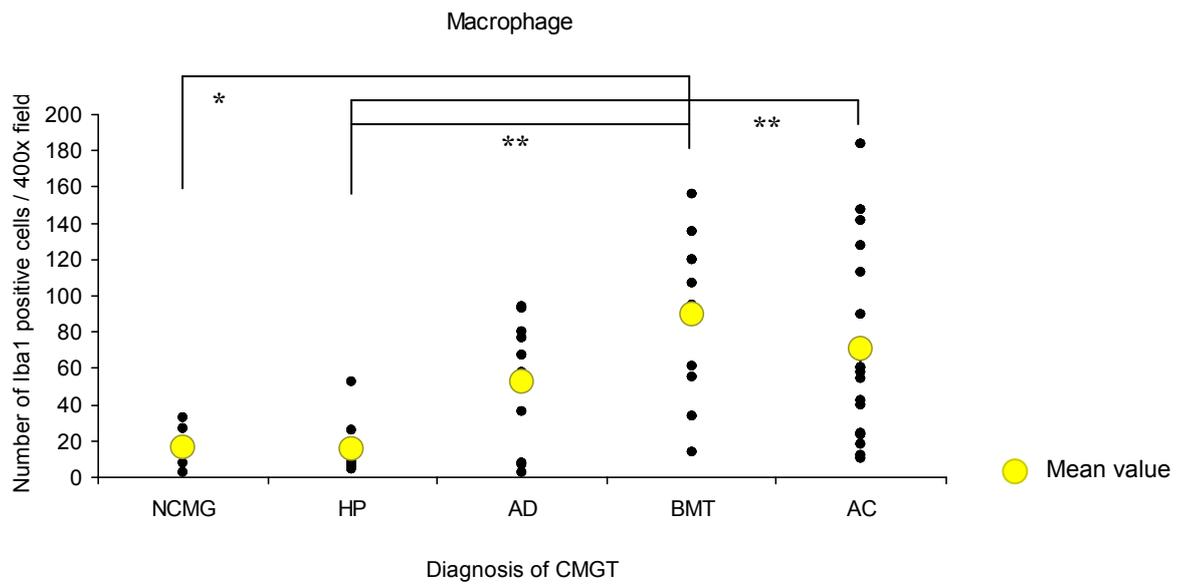
Figure 1.8. Number of Iba1 positive cells on NCMG and CMGT tissues.

*, **: Significant difference between the groups (*: *P*<0.05, **: *P*<0.01)
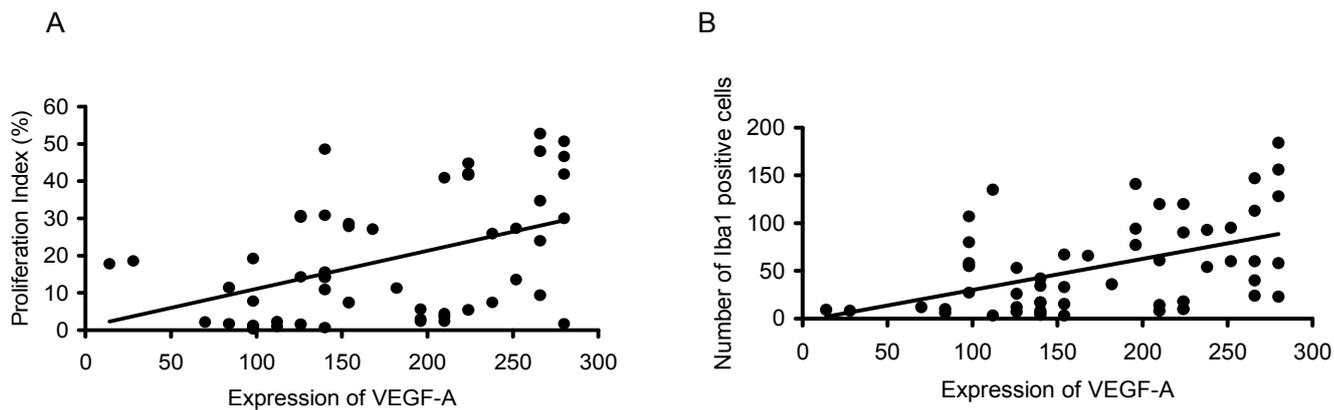
Figure 1.9. Correlation between VEGF-A expression and Ki-67 and between VEGF-A expression and Iba1 positive cells.

A: Statistical analysis demonstrated positive correlation between the expression of VEGF-A and Ki-67 positive cells (%) (correlation coefficient r=0.4419, *P*=0.0010**),

B: Statistical analysis demonstrated positive correlation between the expression of VEGF-A and Iba1 positive cells (correlation coefficient r=0.4833, *P*=0.0002**).

**: Significant difference between the groups (*P*<0.01)
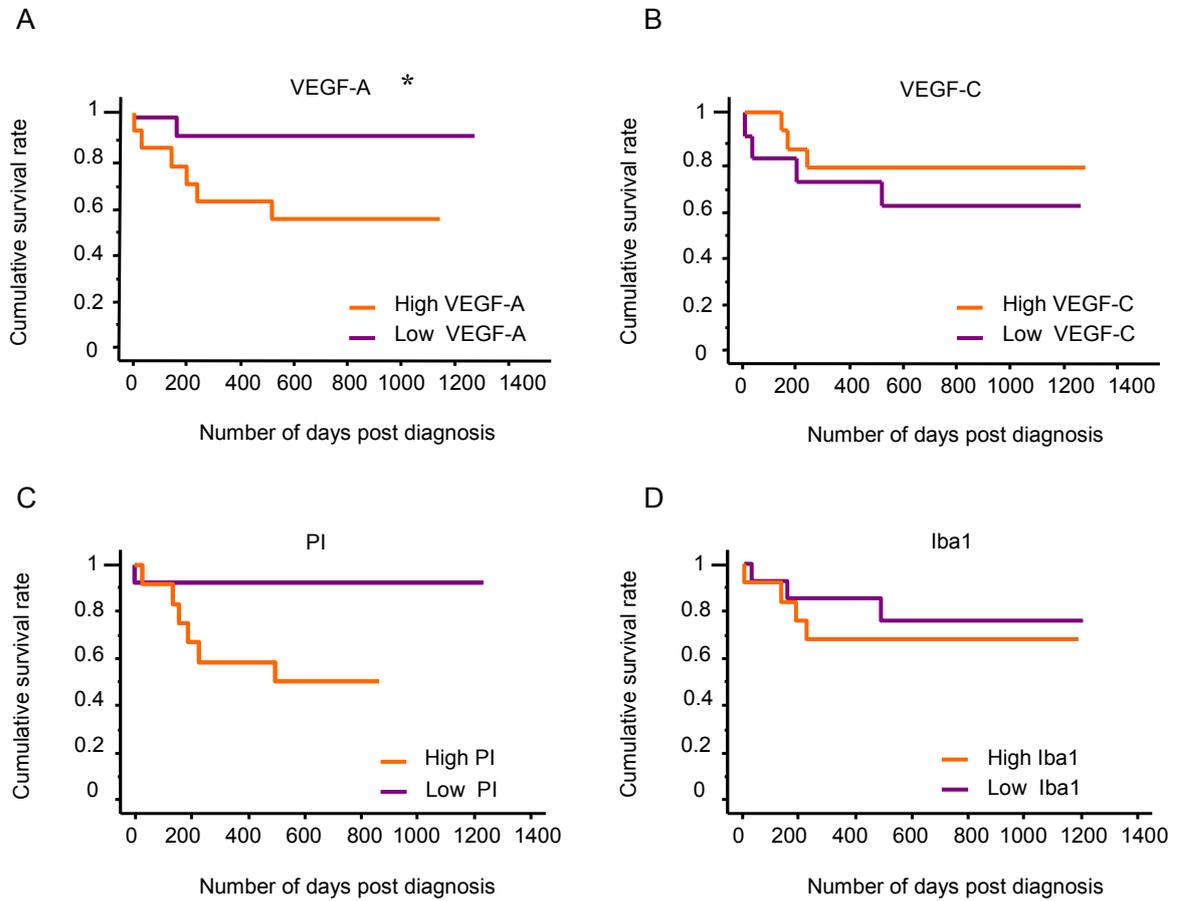
Figure 1.10. Relationship between Kaplan-Meier survival time and high or low VEGF-A and VEGF-C expressions, PI and Iba1 values in 25 dogs with MGT.

A: Low VEGF-A expression, n=12; high VEGF-A expression, n=13 (Log rank P=0.0447*).

B: Low VEGF-C expression, n=11; high VEGF-C expression, n=14 (Log rank P=0.4239).

C: Low PI, n=12; high PI, n=13 (Log rank P = 0.0563).

D: Low Iba1 value, n=12; high Iba1 value, n=13 (Log rank P=0.7257).

*: Significant difference between the low and high groups (P<0.05)

Chapter 2

Angiogenic and lymphangiogenic metastasis of canine

mammary gland tumor in a xenografted nude mouse model

Introduction

Tumor cells could spread directly from the primary tumor to distant organs via blood vessels. This process is facilitated by tumor angiogenesis. Angiogenesis is crucial for the proliferation of tumor cells, and anti-angiogenic therapy is a promising strategy aimed at inhibiting tumor growth, invasion and metastasis (Folkman, 1995). Among the many reported angiogenic factors, VEGF-A is the most effectual endothelial cell mitogen in hypoxia or hypoxic microenvironment (Ohta *et al*, 1999; Chen *et al*, 2009). Alternatively, tumor cells also could spread via lymphatic vessels from lymph nodes to distant organs and via the blood vessels which are branched from the lymph node or major lymphatic ducts by tumor lymphangiogenesis. Lymphangiogenesis can be promoted by lymphangiogenic growth factors such as VEGF-C and VEGF-D, and chemokines may contribute in attracting tumor cells toward lymphatic vessels. The rearrangement of the vessel structures and abnormal connections between the vascular and lymphatic networks may facilitate further spread to other distant lymph nodes or major organs, such as the lung, liver, brain, or bone (Achen and Stacker, 2008).

Blood microvessel density (MVD) has been confirmed as a measurement for angiogenesis and related to nodal metastases, and survival in human primary breast carcinomas (Vartanian and Weidner, 1994). These findings led several investigators to conclude that the number of vessels in tumor sections was an independent predictor of outcome in cancer patients (Ferrara and Davis-Smyth, 1997). MVD may be relevant in nodal metastases, and be a prognostic factor for survival and clinical managements for cancer patients (Fox and Harris, 2004; Mohammed *et al*, 2009). Also, lymphangiogenesis which is estimated by lymphatic vessel density (LVD) is associated with an increased incidence of lymph node metastasis, which may be essential to the metastatic process (Nathanson, 2003). There is still a considerable debate about the role of

peritumor *vs* intratumor MVD and LVD in the pathology of primary tumors (Vermeulen *et al*, 2002; Van der Auwera *et al*, 2006).

The need has arisen for reliable imaging of the vascular and lymphatic systems to determine their normal extent and pathologic changes (Baluk and McDonald, 2008). Progress in functional imaging of the vascular system and angiogenesis was earlier than imaging of lymphatics and lymphangiogenesis (Vermeulen *et al*, 1996). Nevertheless, the methodology of lymphangiogenesis quantification has recently reached to an international consensus with the abundant knowledge of molecular markers (Vermeulen *et al*, 2002; Van der Auwera *et al*, 2006). CD31, CD34, CD105, and receptors, such as VEGFR-2, von Willebrand factor, VE-cadherin, could mainly detect endothelial cells (ECs). CD31 known as PECAM-1 or endocam, is a pan-endothelial marker, being present in blood vessels and expressed at a lower level on lymphatic endothelial cells (Baluk *et al*, 2007). LYVE1, VEGFR-3, Prox1, and podoplanin (D2-40) are useful markers for microscopic imaging of lymphatic endothelial cells (LECs), depending on the histologic location (Baluk and McDonald, 2008). LYVE1 (lymphatic vessel endothelial hyaluronan receptor 1) is strongly expressed on LECs during lymphangiogenesis. Recently, these markers have enabled to explore the relationships between MVD and LVD on the peritumor and intratumor lesion and prognosis/metastasis in patients of human tumors and a xenografted mouse model of human solid tumors. In the canine tumor, there are some antibodies for detecting the blood vessels as factor Ⅷ-related antigen, CD31 and CD34, but no report on the suitable antibody for detecting only the lymphatic vessels (Graham and Myers, 1999; Tashbaeva *et al*, 2007). And also the relationship between MVD/LVD and VEGF-A/-C in canine tumors has not yet clearly elucidated.

In the previous chapter, VEGF-A and -C were expressed on CMGT tissues and it was concluded that VEGF-A may play an important role in predicting metastatic potential and

estimating prognosis in the spontaneous CMGT patients. However, the role of angiogenesis and lymphagiogenesis by VEGF-A and VEGF-C in the primary CMGT tissues and their relationship were still not clear. Further research on the tumor angiogenesis and lymphngiogenesis with assessing MVD and LVD should be needed to clarify the role of VEGF-A and VEGF-C in CMGT.

In this chapter, I first investigated the VEGF-A and VEGF-C expression on two CMGT cloned cell lines (CHMp-5b and CHMp-13a) which were previously established in our laboratory. In Section 2, clinical features such as growth pattern of primary tumor, lymph node metastasis and lung metastasis were investigated in a xenografted nude mouse model. In Section 3, expression of VEGF-A and VEGF-C was evaluated for tissues developed in the xenografted nude mice. Finally in Section 4, relationship between angiogenesis and lymphangiogenesis and VEGF-A/-C was investigated through the assessment of MVD and LVD in peri- and intra-primary lesions in the tissues developed in this nude mouse model.

Section 1

VEGF-A and VEGF-C expression on two canine mammary gland tumor cell lines

Materials and Methods

In Section 1, I evaluated the mRNA and protein expressions of VEGF-A and VEGF-C on these CMGT cloned cell lines, CHMp-5b and CHMp-13a.

Cell lines

CHMp cell line was previously established (Uyama *et al*, 2006) from the primary mass of an inflammatory CMGT patient in our laboratory, from which two cloned cell lines, CHMp-5b and CHMp-13a, were established. Cells were maintained in RPMI-1640 medium (Wako Pure Chemical Industries Ltd., Osaka, Japan) supplemented with 10% heat-inactivated (56℃, 30 minutes) fetal bovine serum (FBS) (Gibco BRL, Grand Island, NY, USA), 5mg/L gentamicin solution (Sigma-Aldrich, Inc., St.Louis, MO, USA) and 6mg/L fungizone amphotericin B (Gibco BRL), and incubated at 37℃ in a humidified atmosphere of 5% CO_2.

Quantitative real-time polymerase chain reaction

To investigate the mRNA expression of VEGF-A and VEGF-C on the cloned cells, quantitative real-time polymerase chain reaction (PCR) was performed. Total RNA was extracted from CHMp-5b and CHMp-13a cells by use of a TRIzol Reagent (Invitrogen, Carlsbad, CA, USA) according to the manufacturer's recommendation. Ten micrograms of total RNA were reverse-transcribed with the oligo dT primer and Superscript Ⅲ transcriptase (Invitrogen). Reverse-transcription products were purified with QIAquick PCR purification Kit (QIAGEN, Valencia, CA, USA). Quantitative real-time PCR was performed by real-time monitoring of the increase in florescence of SYBR-Green dye (Applied Biosystems, Foster City, CA, USA) with an ABI PRISM 7900HT Real Time PCR System (Applied Biosystems). The

PCR conditions were as follows: 1 cycle at 50℃ for 2 minutes and 95℃ for 10 minutes, and 40 cycles at 95℃ for 15 seconds and 60℃ for 1 minute. The specific primers were designed with the gene encoding VEGF-A and VEGF-C using GENETYX-MAC Ver. 8.0 (GENETYX Corp., Tokyo, Japan) (Table 2.1.1). I designed these primers from the sequences common to most of them. The expression levels of mRNA quantities across different samples were normalized to the mRNA quantity of endogenous control gene glyceraldehye-3-phospate dehydrogenase (GAPDH). Specificity of primers was confirmed using gel electrophoresis. Each experiment was performed on triplicate samples using 10 μg/ml of cDNA templates.

Western blot analysis

Sub-confluent cultured cells were harvested and washed three times in ice-cold phosphate buffer solution (PBS). Then the cells were lysed in RIPA buffer [50mM Tris-HCl, 150mM NaCl, 5mM EDTA, 1% Triton-X, 0.1% SDS, 4mM Pefabloc SC (Roche Diagnostics K.K., Basel, Switzerland), 5 μg/ml aprotinin, 5 μg/ml leupeptin, 10mM NaF, 2mM Na_3Vo_4 and 1 complete mini tablet (Roche Diagnostics)/10ml H_2O]. Lysates were centrifuged at 15,000rpm at 4℃ for 20 minutes, and protein concentrations were measured using BCA protein assay reagent (Thermo Fisher Scientific Inc., Rockford, IL, USA). Cell lysates were denatured at 98℃ for 5 minutes in 2× sample buffer. Equal amount of proteins were resolved by SDS-PAGE and blotted onto a polyvinylidene fluoride (PVDF) membrane (Bio-rad, Hercules, CA, USA). The membranes were blocked in 5% non-fat dry milk in Tris Buffered Saline-Tween20 (TBS-T) buffer for 1 hour at room temperature. The blots were incubated with appropriate primary antibodies for overnight at 4℃ with agitation. The primary antibodies used were a polyclonal rabbit anti-human VEGF-A (A-20; 1:500, Santa Cruz Biotechnology) and a polyclonal rabbit anti-human VEGF-C (H-48; 1:250, Santa Cruz Biotechnology). As an internal control, a

polyclonal rabbit anti-human pan-actin (#4968; 1:1000, Cell Signaling Technology, Inc, Danvers, MA, USA) was used. The membranes were rinsed in TBS-T, and subsequently incubated with horseradish peroxidase (HRP)-conjugated antibodies against rabbit IgG (NA934; GE Healthcare, Piscataway, NJ, USA) for one hour at room temperature with vigorous agitation. The antibody-antigen complex of proteins was visualized using the enhanced chemiluminesence (ECL) Plus detection system (GE Healthcare).

Statistical analysis

In mRNA expression analyses for CHMp-5b and CHMp-13a, the mean values of samples and standard deviation (SD) were calculated and analyzed using student t-test at a significance level of $P < 0.05$.

Results

Morphology and growth

Figure 2.1.1 shows the microscopic findings of CHMp-5b and CHMp-13a under culture condition. Morphologically, most of CHMp-5b cells were spindle-shaped, while most of CHMp-13a cells were small and round-shaped.

mRNA expression of VEGF-A and VEGF-C

Figure 2.1.2 shows mRNA expression of VEGF-A and VEGF-C on both cell lines. VEGF-A expression (range: 0.296 - 0.347) level was far higher than VEGF-C (range: 0.020 - 0.036) on both cell lines. CHMp-5b (0.321 ± 0.025) showed slightly higher VEGF-A mRNA expression than CHMp-13a (0.317 ± 0.004), but there was no significant difference between the two. CHMp-13a (0.034 ± 0.002) showed slightly higher VEGF-C mRNA expression than CHMp-5b (0.025 ± 0.005), and the difference was statistically significant ($P = 0.049$).

Expression of VEGF-A and VEGF-C proteins

Figure 2.1.3 shows the results of Western blot analysis. CHMp-5b showed higher expression of VEGF-A than CHMp-13a, while CHMp-13a showed higher expression of VEGF-C than CHMp-5b.

Summary

In Section 1, I evaluated the mRNA and protein expressions of VEGF-A and VEGF-C in two CMGT cloned cell lines. The mRNA expression level of VEGF-A was much higher than VEGF-C on both CHMp-5b and CHMp13a cell lines. This may indicate that these two cell lines had a stronger potential for angiogenesis than lymphangiogenesis. In regard to mRNA expression level of VEGF-C, CHMp-13a showed higher VEGF-C expression than CHMp-5b with a significant difference, which might suggest the difference in lymphangiogenesis potential between the two. On Western blot analysis, similar tendency to mRNA expressions was obtained. CHMp-5b showed a stronger expression of VEGF-A than CHMp-13a, while CHMp-13a showed a stronger expression of VEGF-C than CHMp-5b. These results might suggest that CHMp-5b has a stronger angiogenesis potential and CHMp-13a has a stronger lymphangiogenesis potential.

Gene	Accession No.		Primer	bp
VEGF-A	NM_001003175	sence	5`-AGAAGAGAGACATTGGTGGAGGAA-3`	208
		antisence	5`-TGGGGACAGAGGAGGGTGAA-3`	
VEGF-C	XM_540047	sence	5`-CCCAAGAAATCAACCCCTAA-3`	221
		antisence	5`-TAGTTCATCTGTGGTCTTTTCC-3`	
GAPDH	NM_001003142	sence	5`-TGACACCCACTCTTCCACCTTC-3`	105
		antisence	5`-CGGTTGCTGTAGCCAAATTCA-3`	

Table 2.1.1. Specific primers designed for canine VEGF-A, VEGF-C and GAPDH
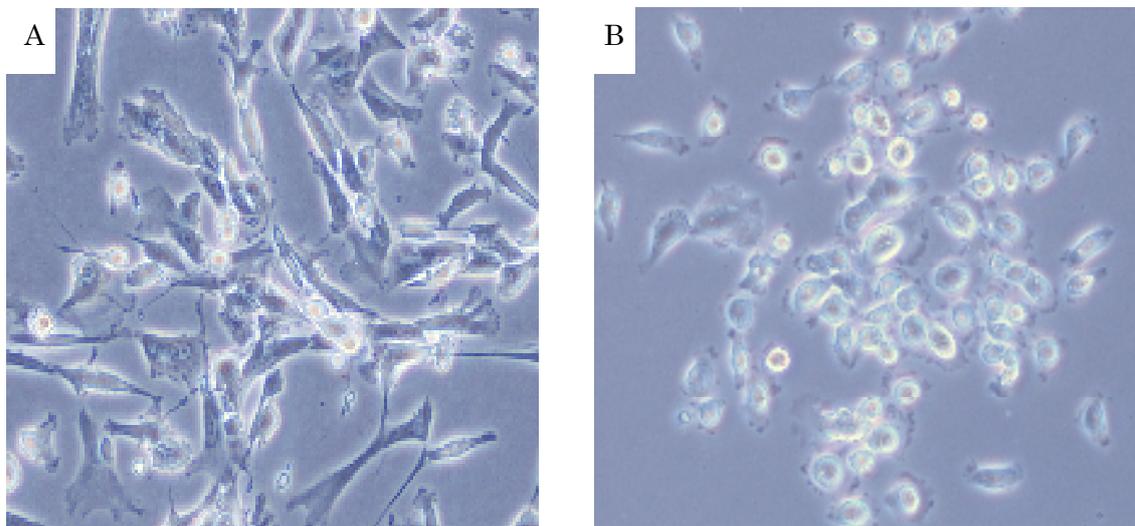
Figure 2.1.1. Phase contrast micrographs of CHMp-5b (A) and CHMp-13a (B). Morphologically, CHMp-5b showed spindle cells and CHMp-13a showed small round-shaped cells. (Magnification ×400)
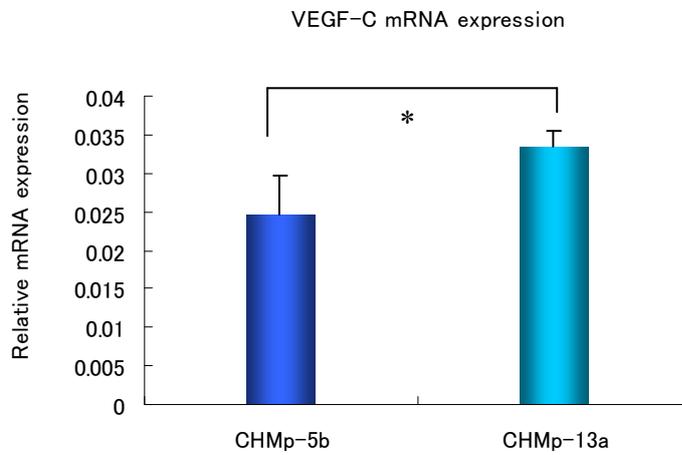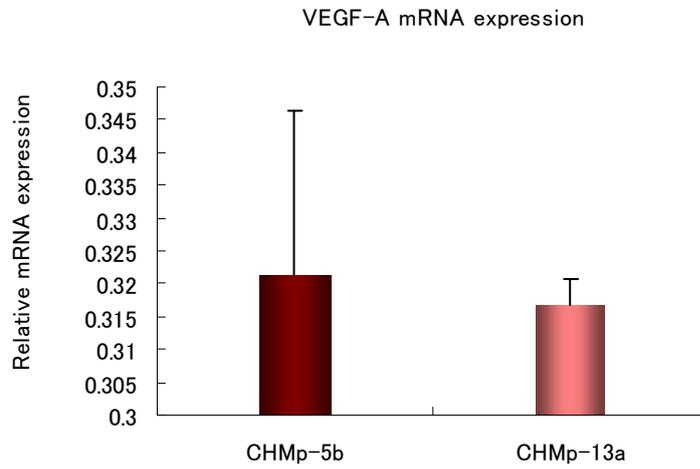
Figure 2.1.2. mRNA expressions of canine VEGF-A and VEGF-C on CHMp-5b and CHMp-13a cell lines. VEGF-A mRNA expression level was far higher than VEGF-C on both cell lines. CHMp-5b showed slightly higher VEGF-A mRNA expression than CHMp-13a, but there was no significant difference. CHMp-13a showed slightly higher VEGF-C expression than CHMp-5b, and this difference was statistically significant (*: P = 0.049).

VEGF-A   42kDa

VEGF-C   40kDa

Actin   45kDa
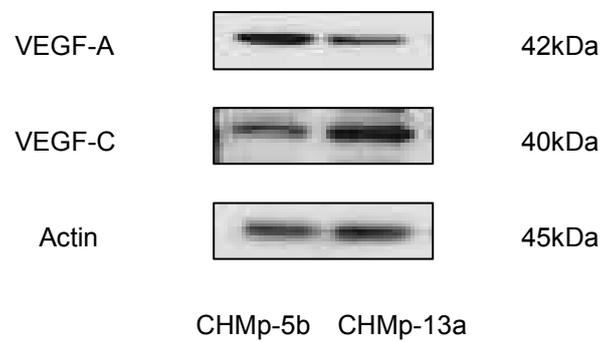
CHMp-5b   CHMp-13a

Figure 2.1.3. Western blot analysis for VEGF-A and VEGF-C proteins on CHMp-5b and CHMp-13a cell lines. CHMp-5b showed a stronger expression of VEGF-A than CHMp-13a, while CHMp-13a showed a stronger expression of VEGF-C than CHMp-5b.

Section 2

Metastatic potential of CMGT cell lines in a xenografted nude mouse model

Materials and Methods

In Section 2, I characterized the metastatic potential of these cloned cell lines, in a xenografted nude mouse model.

Mice

Six-week-old female nude mice (KSN Slc; Japan SLC, Inc., Tokyo, Japan) were used as experimental animals. The mice were maintained under the specific pathogen-free condition in a barrier facility. Three mice were put in one cage (Mouse Clean S TPX; Clea Japan, Inc., Tokyo, Japan) and fed with sterilized food (CL-2; Clea Japan) and water *ad libitum*. The mice were kept for one week in the facility before the experiment. All animal experiments were approved by the Animal Care Committee of the Graduate School of Agricultural and Life Sciences, the University of Tokyo.

Xenograft of cell lines

A total of 36 nude mice were used in this study. Three days before transplantation, the mice were irradiated with X-ray at a dose of 4 Gy. Each cell line was suspended in saline at a dose of 1 x 10^7 cells/200 $\mu\ell$ and inoculated subcutaneously into the right mammary fat pad of nude mice using a 25 gauge needle. Tumor size was measured weekly after the transplantation until the time of sacrifice. Tumor volume was calculated by the formula:

$$\text{Tumor volume (mm}^3) = 1/2 \text{ length} \times \text{width}^2.$$

Every week after the transplantation up to the week 6, mice were sacrificed and the primary and metastatic lesions of the lymph node and lung were harvested and examined grossly and histologically. The primary masses formed at the site of transplantation were

collected for formalin fixation, protein extraction and mRNA extraction. The axillary, superficial axillary and inguinal lymph nodes of right and left sides and the lung were also harvested for histopathology.

Histopathology

The primary tumor lesions, lymph nodes and the lung from the CHMp-5b- and CHMp-13a-xenografted mice were fixed in 10% neutral buffered formalin and embedded in paraffin. A series of 4 μm-thick sections were stained with H&E for histopathological examination.

Immunohistochemistry

The expression of Ki-67 on the primary lesions of CMGT developed in xenografted nude mice was analyzed by EnVision immunohistochemical procedures (DAKO EnVision+ kit/HRP). The procedures for immunohistochemistry analysis and quantification of PI were the same as described in Chapter 1.

Statistical analysis

Changes in tumor volume of the primary mass developed in nude mice xenografted with two cell lines were statistically compared using ANOVA by Bonferroni post hoc test. Lymph node and lung metastasis was compared between CHMp-5b and CHMp-13a groups by Fisher exact probability. Multiple statistical comparison of PI of primary lesions and metastatic lesions in two xenografted mouse models were made by Bonferroni correction of ANOVA. $P < 0.05$ was considered to be statistically significant.

Results

Tumor growth in xenografted nude mice

Both cell lines produced mass lesions at the xenografted site, which gradually grew over the week (Figure 2.2.1). Growth rate was much faster in nude mice xenografted with CHMp-5b than those with CHMp-13a. The tumor volume was significantly higher in CHMp-5b-xenografted nude mice than in CHMp-13a-xenografted nude mice at the fifth and sixth week of transplantation ($P < 0.01$) (Figure 2.2.2).

On histopathology, CHMp-5b developed solid carcinoma that was characterized by the arrangement of tumor cells in solid sheets, cords or nests, while CHMp-13a developed tubulopapillary carcinoma that was characterized by the formation of tubules and papillary projections (Figure 2.2.3). Compact tumor cells were predominant in the tissue of CHMp-5b-xenografted mice, compared with that in CHMp-13a-xenografted mice, in which abundant fibroblasts and stromal cells were predominant. Necrosis and cyst formation were observed within the tumor masses in some mice of both groups at the later stage.

Figure 2.2.4 shows the lymph node and lung metastasis in CHMp-5b- and CHMp-13a-xenografted mice. Metastasis was mainly observed in the right axillary and superficial axillary lymph nodes in these mice. Visible metastasis was not observed in lymph nodes of CHMp-13a-xenografted nude mice. Small foci of metastatic lesions were grossly observed on the surface of the lung in a CHMp-5b-xenografted mouse. The metastasis was confirmed by the histopathological investigation for lymph nodes and the lung (Figure 2.2.5).

Table 2.2.1 shows the incidence of lymph node and lung metastasis in nude mice xenografted with two cell lines. In CHMp-5b-xenografted mice, lymph node metastasis was observed from 3 weeks after the transplantation. On the contrary, CHMp-13a produced lymph

node metastasis in only one mouse at 6 weeks after transplantation. Fisher exact probability was 0.007 between CHMp-5b and CHMp-13a groups. In CHMp-5b-xenografted mice, lung metastasis was observed from 5 weeks after the transplantation, while CHMp-13a did not produce lung metastasis in any mice. Fisher exact probability was 0.045 between CHMp-5b groups and CHMp-13a groups.

Immunohistochemistry for Ki-67

Stronger immunostainig of Ki-67 was observed on neoplastic cells located at the border than at the necrotic centers (Figure 2.2.6). Figures 2.2.7 and 2.2.8 show the expression of Ki-67 positive cells on the tissues of primary lesions developed in nude mice xenografted with both cell lines, and changes in Ki-67 positive cell percentages (PI) in both groups. More Ki-67 positive cells were observed on tissues developed in CHMp-5b-xenografted mice than those developed in CHMp-13a-xenografted mice. PI increased in both groups according to the period after transplantation. PI of tissues in CHMp-5b-xenografted mice was significantly higher than those of CHMp-13a-xenografted mice at each period from 2 to 6 weeks after transplantation ($P < 0.01$) (Figure 2.2.9).

Figure 2.2.10 shows the expression of Ki-67 positive cells on the metastatic lesions of the lymph nodes and lung developed in nude mice xenografted with both cell lines. Figure 2.2.11 shows the difference in PI in primary and metastatic lesions at 6 weeks after transplantation in mice of both groups. PI of primary and metastatic lesions at 6 weeks after transplantation in CHMp-5b-xenografted mice was significantly higher than those of CHMp-13a-xenografted mice ($P = 0.002$ and $P = 0.019$, respectively). PI was significantly lower in the lung metastatic lesion than primary lesions and lymph node metastatic lesions in CHMp-5b-xenografted mice ($P = 0.036$ and $P = 0.018$, respectively). There was no significant difference in PI between

primary lesions and lymph node metastatic lesions in both CHMp-5b- and CHMp-13a-xenografted mice at 6 weeks after transplantation.

Summary

In Section 2, I evaluated the tumor growth in mice xenografted with two cell lines and PI of the tissues developed in these mice. Tumor growth was much faster in nude mice xenografted with CHMp-5b than those with CHMp-13a. CHMp-5b-xenografted mice showed the lymph node and lung metastasis in the earlier phase of transplantation, while no lung metastatic lesion was observed in CHMp-13a-xenografted mice.

PI of the primary and metastatic lesions in CHMp-5b-xenografted mice was significantly higher than those in CHMp-13a-xenografted mice. PI of the lung metastatic lesion in CHMp-5b-xenografted mice was significantly lower than their primary and lymph node metastatic lesions. These results may indicate the malignant character of tumors developed in CHMp-5b-xenografted mice.

	Xenografted nude mice												P
	CHMp-5b						CHMp-13a						
	1	2	3	4	5	6	1	2	3	4	5	6	
	weeks after transplantation						weeks after transplantation						
Lymph node metastasis	0/3	0/3	1/3	3/3	3/3	3/3	0/3	0/3	0/3	0/3	0/3	1/3	0.007**
Lung metastasis	0/3	0/3	0/3	0/3	2/3	3/3	0/3	0/3	0/3	0/3	0/3	0/3	0.045*

Table 2.2.1. Lymph node and lung metastasis in CHMp-5b- and CHMp-13a-xenografted nude mice. The numerator is the number of mice that had metastasis, and the denominator is the total number of mice per group. In CHMp-5b-xenografted mice, lymph node metastasis was seen from 3 weeks after transplantation. On the contrary, CHMp-13a produced lymph node metastasis in only one mouse at 6 weeks after transplantation. In CHMp-5b-xenografted mice, lung metastasis was seen from 5 weeks after transplantation. Fisher exact probability demonstrated the significant difference between the groups (*: $P < 0.05$, **: $P < 0.01$).

CHMp-5b-xenografted nude mice   CHMp-13a-xenografted nude mice

1st week

2nd week

3rd week

4th week

5th week

6th week
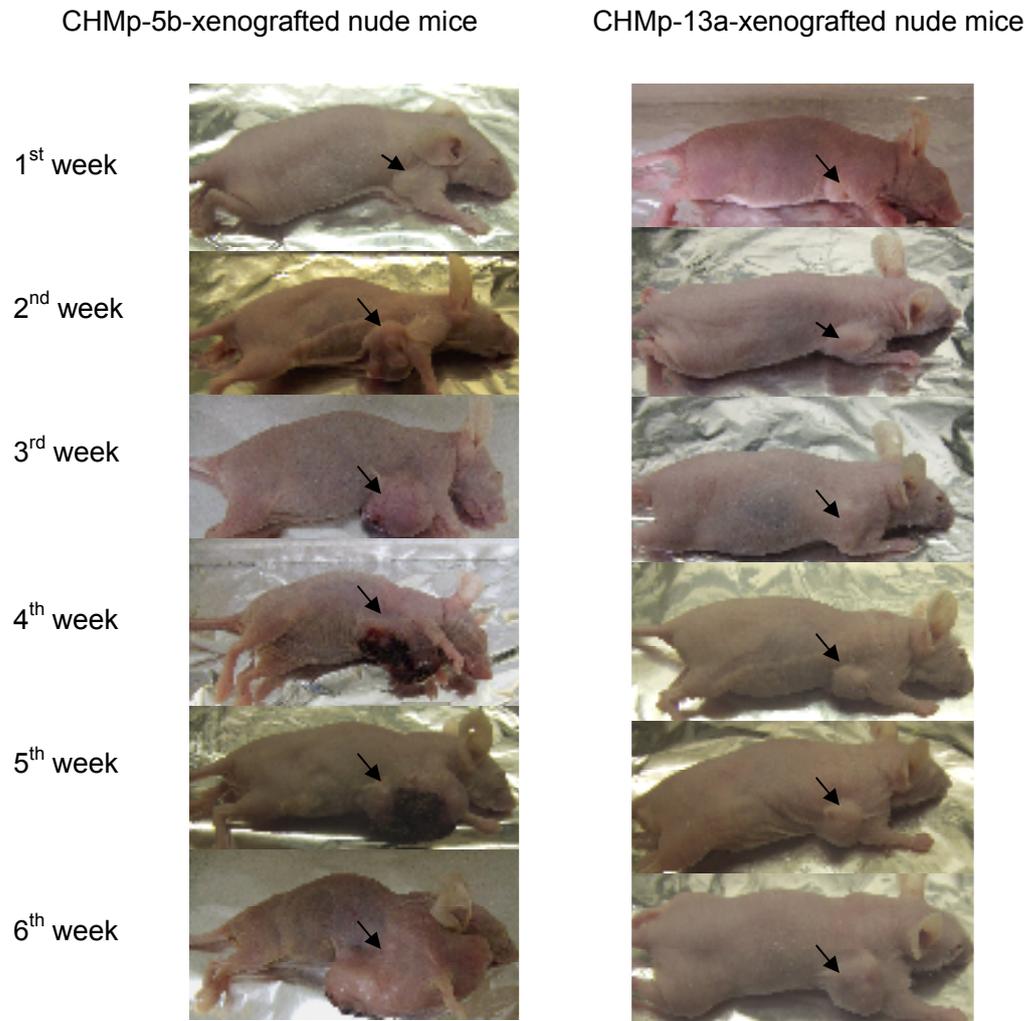
Figure 2.2.1. Gross findings of masses developed in nude mice xenografted with CHMp-5b (A) and CHMp-13a (B) cell lines. Tumor mass was formed at the right mammary fat pad of nude mice and proliferated over time. CHMp-5b produced the mass with ulceration and faster growth than CHMp-13a (arrows: primary tumors developed at the xenografted site).

Primary tumor volume
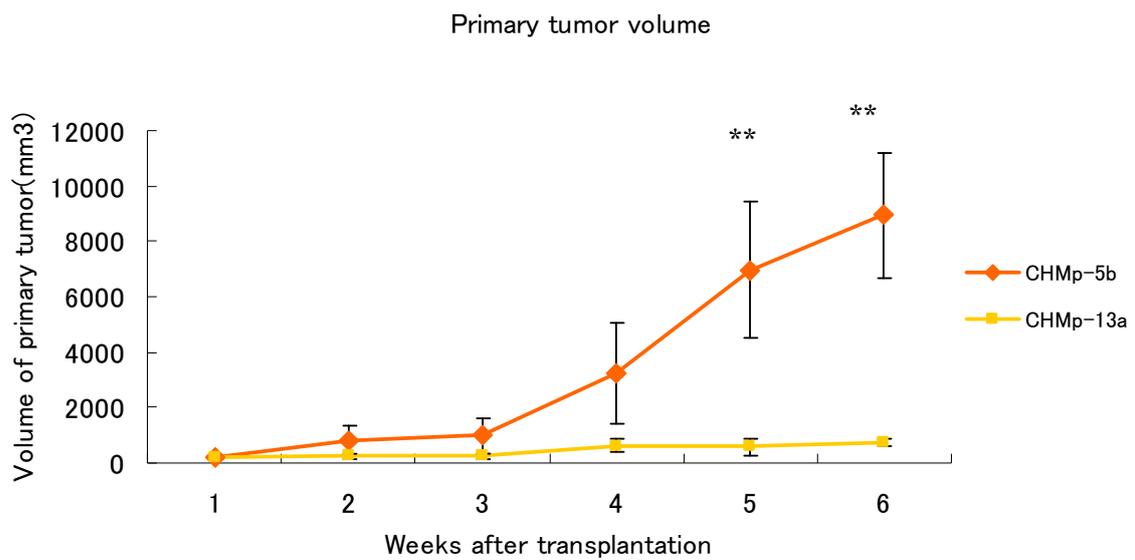
Figure 2.2.2. The changes in calculated primary tumor volume developed in xenografted nude mice. The tumor volume considerably increased in the CHMp-5b-xenografted nude mice compared to that in CHMp-13a-xenografted ones. A significant difference was detected among the two groups at the week 5 and 6 of transplantation (**: $P < 0.01$).
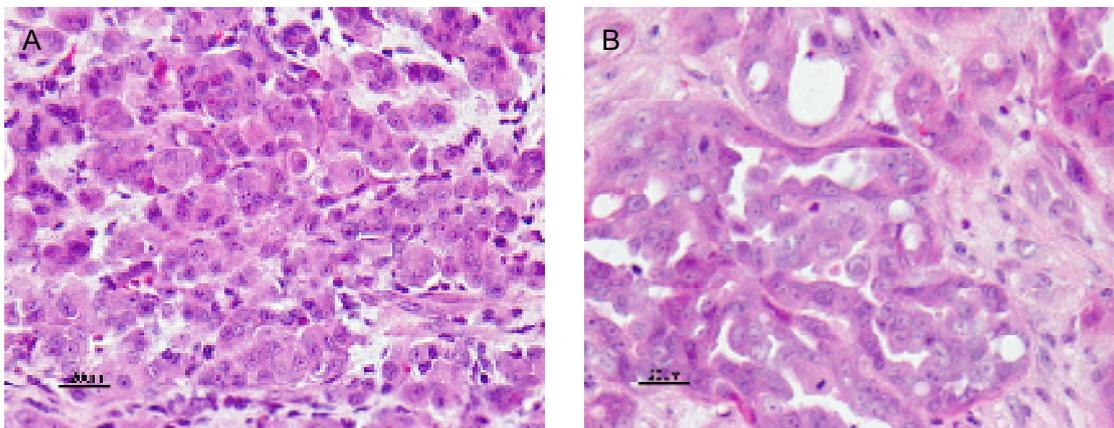
Figure 2.2.3. Histopathological findings of the masses developed at the transplanted site of nude mice. CHMp-5b developed solid carcinoma (A), while CHMp-13a developed tubulopapillary carcinoma (B).

(Magnification ×400)
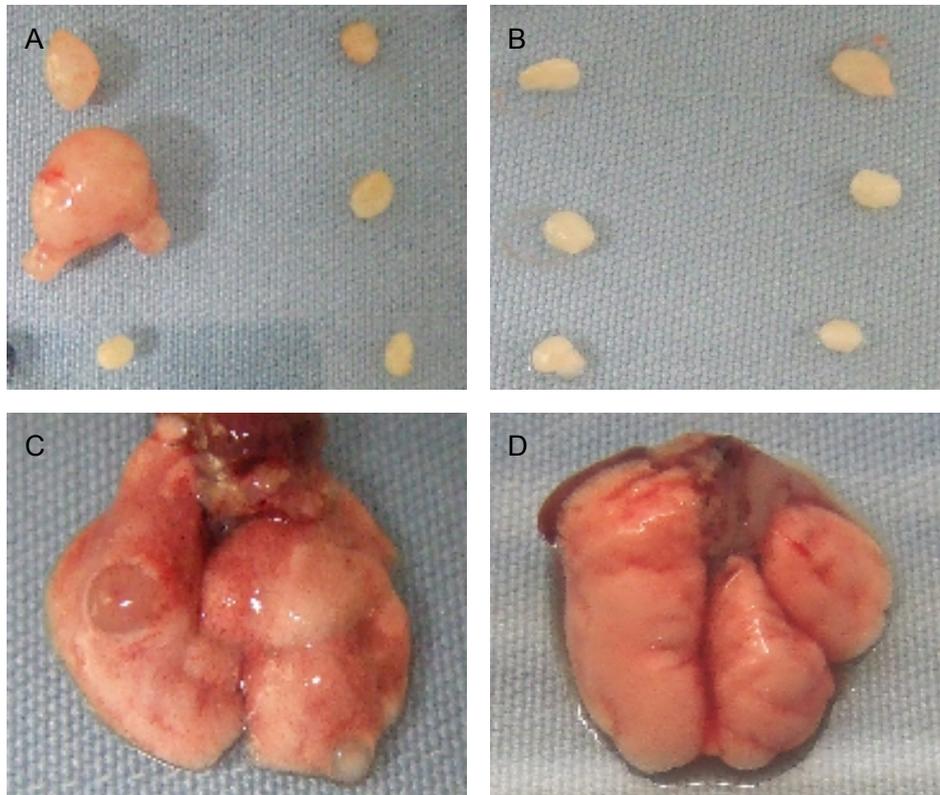
Figure 2.2.4. Gross findings of lymph nodes (LN) and the lung excised from CHMp-5b- and CHMp-13a-xenografted mice on the 6th week after transplantation.

A: Metastasis was observed in the right axillary and superficial axillary LNs of a CHMp-5b-xenografted nude mouse; upper left is the right axillary LN, middle left is right superficial axillary LN, lower left is the right inguinal LN, upper right is the left axillary LN, middle right is left superficial axillary LN and lower right is left inguinal LN.

B: Visible metastasis was not observed in LN of CHMp-13a-xenografted nude mouse

C: Small foci of metastatic lesions were observed on the surface of the lung in a CHMp-5b-xenografted mouse.

D: There was no visible metastatic lesion at the lung in nude mouse xenografted with CHMp-13a.
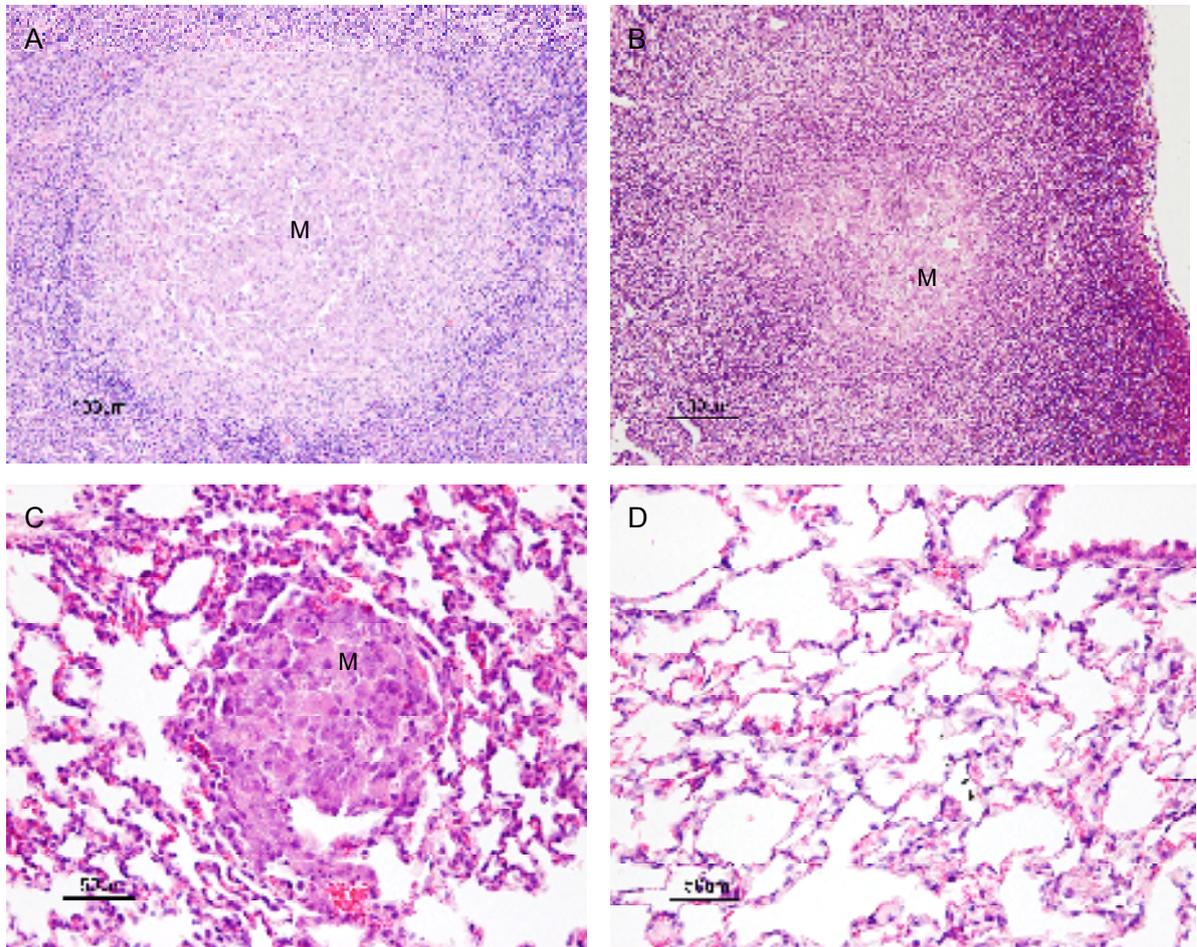
Figure 2.2.5. Histopathological findings of lymph nodes and the lung excised from CHMp-5b- and CHMp-13a-xenografted mice. (M: metastasis)

A and B: The lymph node metastatic lesions of CHMp-5b (A) - and CHMp-13a (B) -xenografted mice. (Magnification ×100)

C: The lung metastatic lesion of CHMp-5b-xenografted mouse.

D: No lung metastatic lesion of CHMp-13a-xenografted mouse.

(C and D: Magnification ×200)
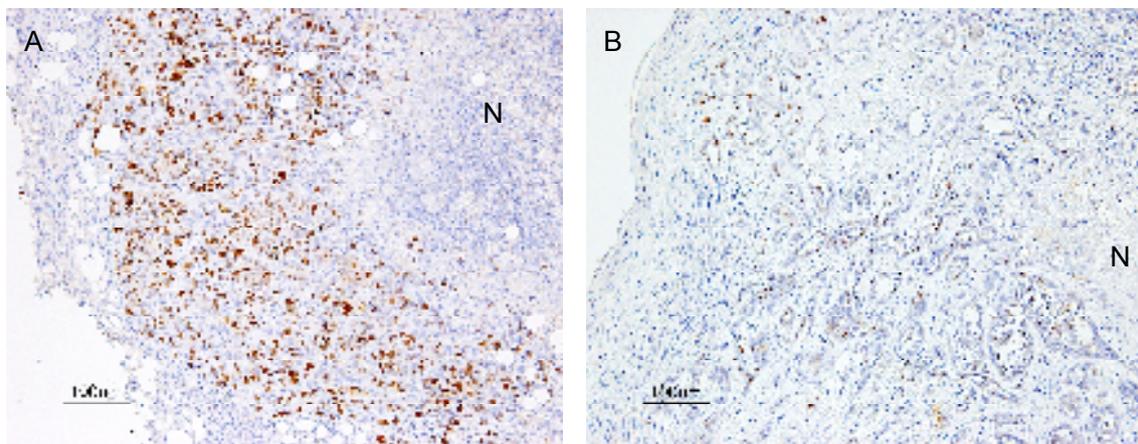
Figure 2.2.6. Photographs of immunohistochemistry for Ki-67 on primary tissues developed by transplantation of CHMp-5b (A) and CHMp-13a (B) 6 weeks after transplantation. Stronger immunostainig of Ki-67 was observed on neoplastic cells located at the border than at the necrotic centers. The more Ki-67 positive cells were observed on tissues developed in CHMp-5b-xenografted mice than those developed in CHMp-13a-xenografted mice. (N: necrosis) (Magnification ×100)

CHMp-5b-xenografted mice
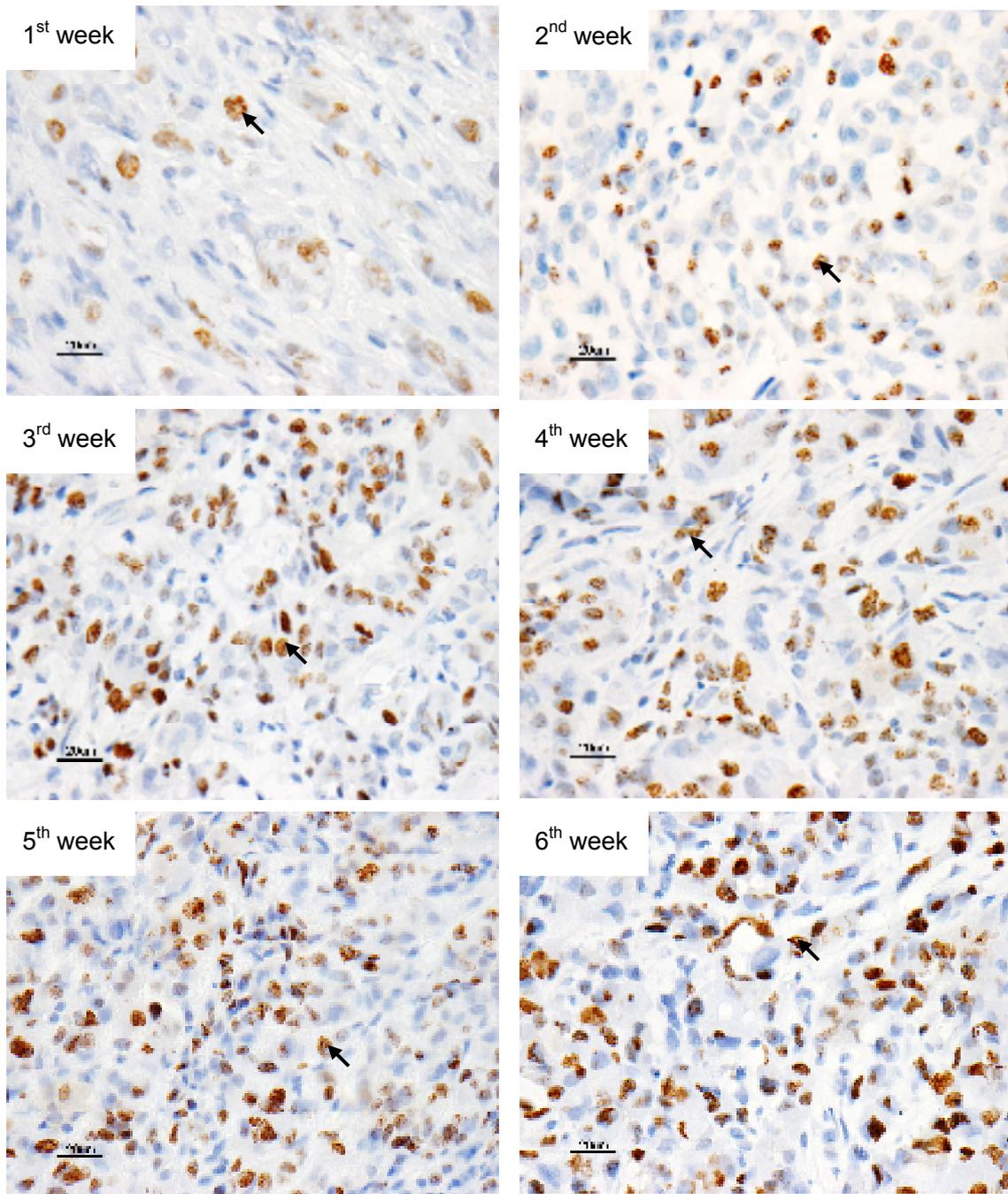
Figure 2.2.7. Ki-67 positive cells (arrows) on the tissues of primary lesions developed in CHMp-5b-xenografted mice. More Ki-67 positive cells were observed in CHMp-5b-xenografted mice according to the period after transplantation.

(Magnification ×400)

CHMp-13a-xenografted mice
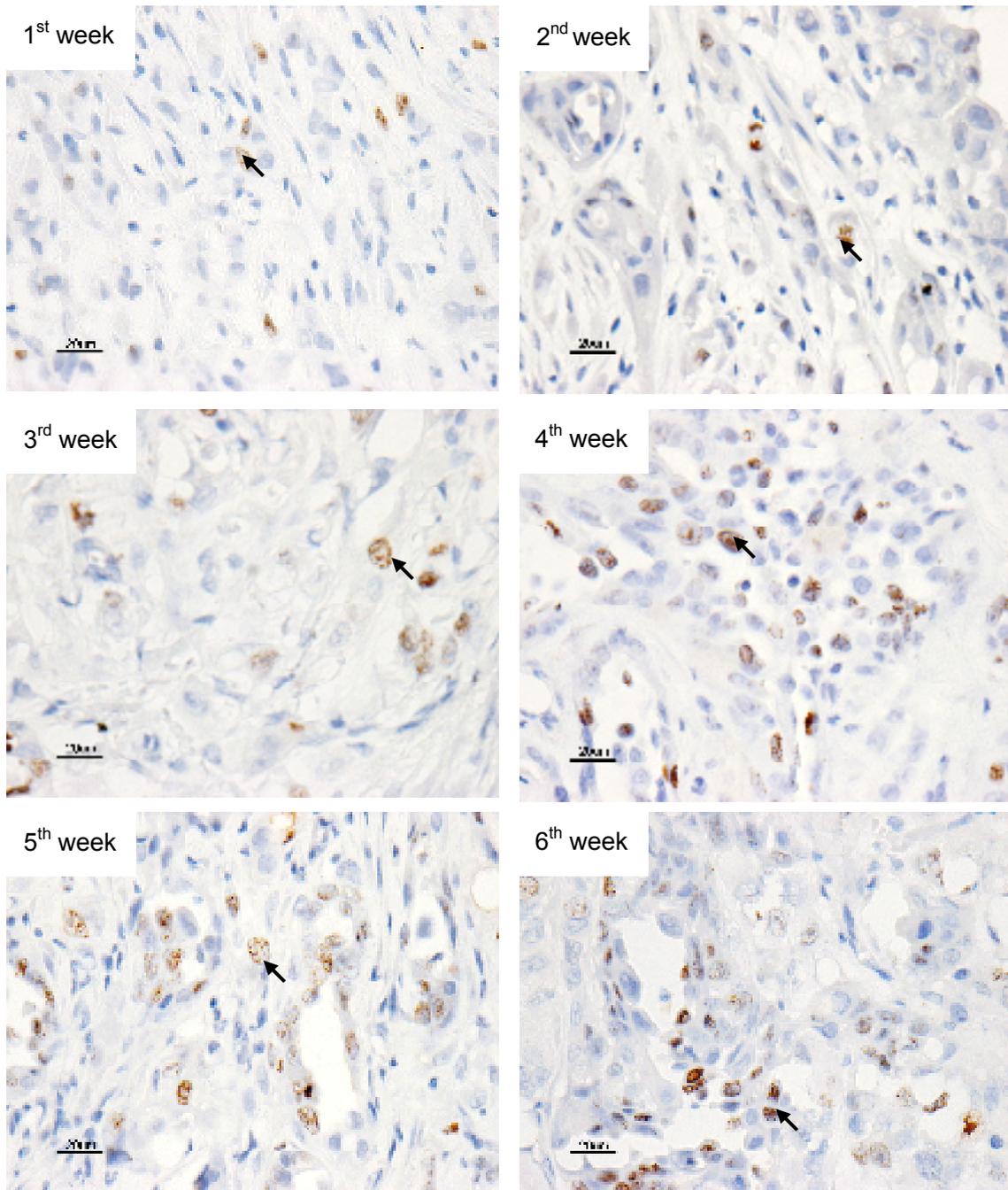
Figure 2.2.8. Ki-67 positive cells (arrows) on the tissues of primary lesions developed in CHMp-13a-xenografted mice.

(Magnification ×400)
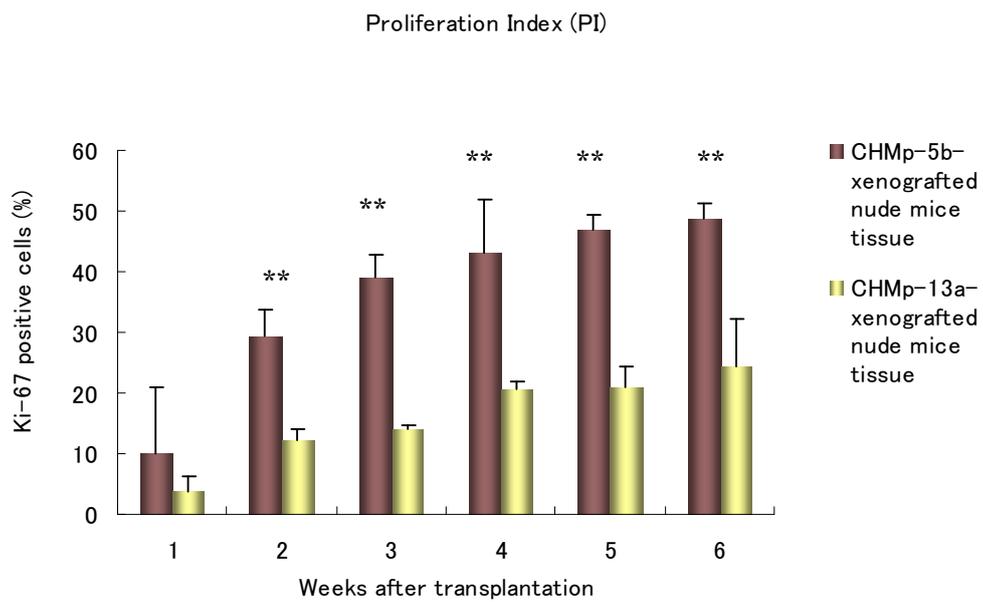
Figure 2.2.9. PI of primary lesions of CHMp-5b- and CHMp-13a-xenografted mice. PI showed higher in CHMp-5b-xenografted mice than in CHMp-13a-xenografted mice. There was a significant difference between the two from 2 weeks to 6 weeks after transplantation (**: $P < 0.01$).

	Lymph node of CHMp-5b-xenografted mice	Lymph node of CHMp-13a-xenografted mice	Lung of CHMp-5b-xenografted mice
Ki-67			
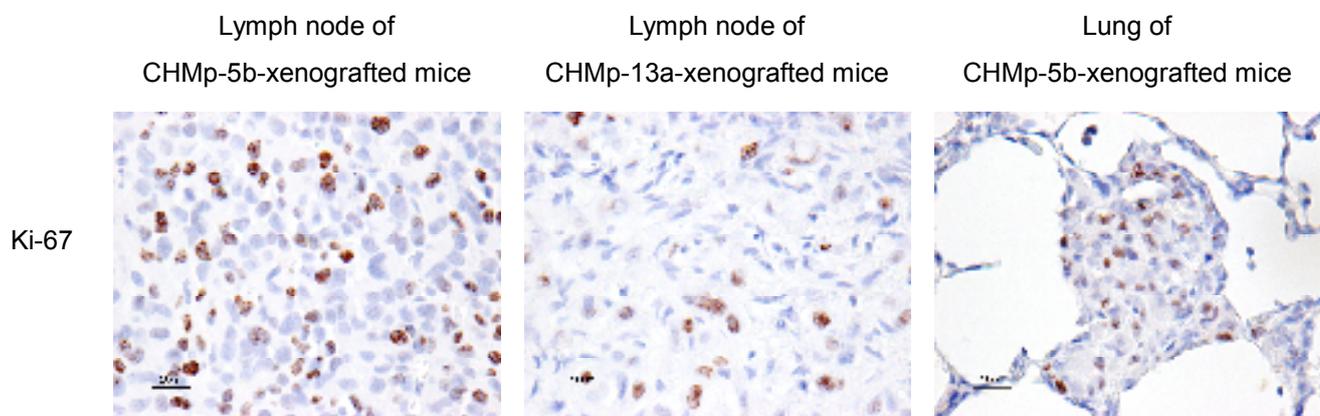
Figure 2.2.10. Photographs of immunohistochemistry for Ki-67 positive cells of metastasis lesions. The lymph node and lung metastasis developed in CHMp-5b- and CHMp-13a-xenografted mice at 6 weeks after transplantation.

(Magnification ×400)

Proliferation Index (PI)
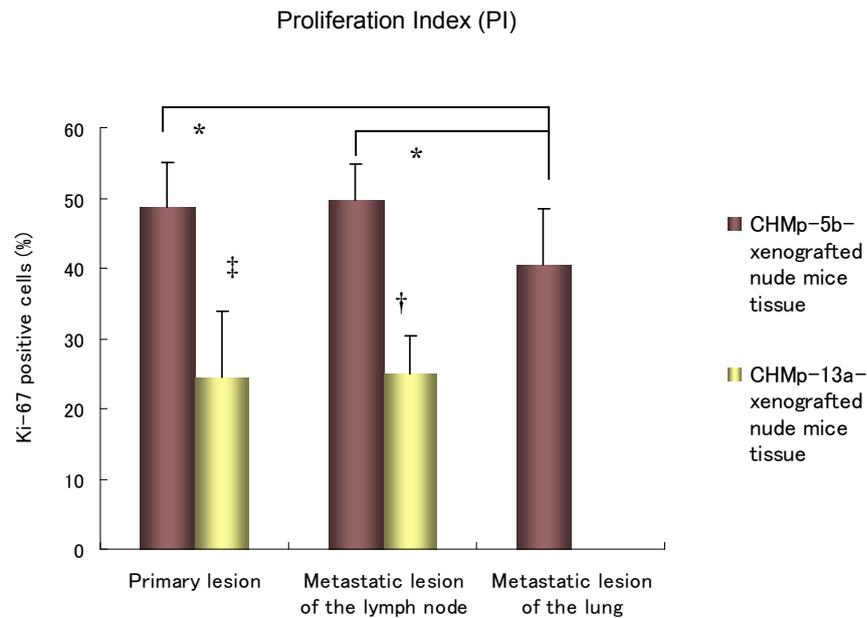
Figure 2.2.11. PI of primary and metastatic (lymph node and lung) lesions in CHMp-5b- and CHMp-13a-xenografted mice at 6 weeks after transplantation. PI was significantly higher in CHMp-5b-xenografted mice than those in CHMp-13a-xenografted mice (P = 0.002 and P = 0.019, respectively). PI in the lung metastatic lesion in CHMp-5b-xenografted mice at 6 weeks after transplantation was significantly lower than their primary and lymph node metastatic lesions (P = 0.036 and P = 0.018, respectively). There was no significant difference between the primary lesion and lymph node metastatic lesions in CHMp-5b- and CHMp-13a-xenografted mice.

†, ‡: Significant difference between CHMp-5b- and CHMp-13a-xenografted mice (†: P < 0.05, ‡: P < 0.01)

*: P < 0.05

Section 3

Expressions of VEGF-A and VEGF-C on tissues developed in nude mice xenografted with two cell lines

Materials and Methods

In this section, I investigated the expression of VEGF-A and VEGF-C on the primary tumor tissues by quantitative real-time PCR, western blot analysis and immunohistochemistry and on the lymph node and lung metastatic tissues on immunohistochemistry in CHMp-5b- and CHMp-13a-xenografted mice.

Quantitative real-time PCR

Total RNA was extracted from the primary tumor tissues developed in nude mice xenografted with the two cell lines by using the RNeasy® Mini Kit (QIAGEN) according to the manufacturer's recommendation. After the extraction of tissue RNA, quantitative real-time PCR was performed as described in Section 1 of Chapter 2.

Western blot analysis

The primary tumor tissues in nude mice were lysed in the CelLytic^{TM} MT mammalian tissue lysis/extraction reagent (Sigma-Aldrich) and complete Mini tablet (Roche diagnostics K.K). After the extraction of tissue protein, immunoblotting analysis was performed as described in Section 1 of Chapter 2.

Immunohistochemistry

The expression of VEGF-A and VEGF-C on the primary lesions, lymph nodes and lung developed in xenografted nude mice was analyzed by EnVision immunohistochemical procedures (DAKO EnVision+ kit/HRP). The primary antibodies used were a polyclonal rabbit anti-human VEGF-A (A-20; 1:500, Santa Cruz Biotechnology) and a polyclonal rabbit

anti-human VEGF-C (H-48; 1:200, Santa Cruz Biotechnology). The procedures for immunohistochemistry analysis were performed as described in Chapter 1.

Evaluation of VEGF-A/-C expressions on immunohistochemistry

Evaluation of VEGF-A and VEGF-C expressions (score) was performed by the same procedures as described in Chapter 1.

Statistical analysis

The mean and SD values of mRNA and proteins of VEGF-A and VEGF-C were calculated. Multiple statistical comparison of VEGF-A and VEGF-C mRNA expression on primary lesions in two xenografted mouse models were made by Bonferroni correction of ANOVA. For immunohistochemical analysis, comparison of variables among the groups according to the degree of VEGF-A and VEGF-C expressions was statistically evaluated using Mann-Whitney U-test with Bonferroni correction. For evaluation of correlation among the protein expressions of VEGF-A and VEGF-C and PI in two xenografted mouse models, Spearman's rank correlation was used. P values < 0.05 were considered significant.

Results

Quantitative real-time PCR

Figure 2.3.1 shows VEGF-A and VEGF-C mRNA expression levels in the tumor tissues developed in CHMp-5b- and CHMp-13a-xenografted mice. VEGF-A mRNA expression was almost 10 times higher than VEGF-C expression in all the tissue specimens of both groups during the experimental period. Primary tumor tissues in CHMp-13a-xenografted mice showed significantly higher VEGF-A mRNA expression than those in CHMp-5b-xenografted mice at 3 ($P = 0.001$), 4 ($P = 0.023$), 5 ($P = 0.0001$) and 6 ($P = 0.047$) weeks after transplantation. Primary tumor tissues in CHMp-13a-xenografted mice showed significantly higher VEGF-C mRNA expression than those in CHMp-5b-xenografted mice at 6 weeks after transplantation ($P = 0.005$).

Western blot analysis

Results of Western blot analysis were quite variable (Figure 2.3.2). VEGF-A expression on tissues of CHMp-13a-xenografted mice seemed to be stronger than those of CHMp-5b-xenografted mice. VEGF-C expression seemed to be similar in both groups without significant differences.

Immunohistochemistry

Figure 2.3.3 to Figure 2.3.6 show immunohistochemical findings of the expression of VEGF-A and VEGF-C on the tissues developed in nude mice transplanted with both cell lines. Typical granular staining of VEGF-A and VEGF-C was diffuse in the cytoplasm and membrane of mammary gland epithelial and myoepithelial cells.

Figure 2.3.7 shows scores of VEGF-A and VEGF-C expression on immunohistochemistry. Though there was no significant difference between the tissues developed by xenograft of both cell lines, scores of VEGF-A and -C expression tended to increase according to the week after transplantation in both groups. The scores of VEGF-A in tissues of CHMp-13a-xenografted mice at each week except 1 and 2 weeks after transplantation were slightly higher that those of CHMp-5b-xenografted mice, but there was no statistical significant. The scores of VEGF-C in tissues of CHMp-13a-xenografted mice at each week except 1 week after transplantation were slightly higher that those of CHMp-5b-xenografted mice, but the difference was not statistical significant.

Figures 2.3.8 and 2.3.9 show immunohistochemical findings and scores of the expression of VEGF-A and VEGF-C on the metastatic tissues developed in nude mice transplanted with CHMp-5b and CHMp-13a at 6 weeks after transplantation. On lymph node and lung metastatic tissues, VEGF-A and -C staining were significantly lower when compared to the expression in the primary mass ($P < 0.05$).

Correlations between the expression levels of VEGF-A and VEGF-C and PI values

Correlation between VEGF-A and VEGF-C expressions and PI values is shown in Table 2.3.1. There was a significant correlation between the expression of VEGF-A and VEGF-C on tissues of both CHMp-5b-xenografted mice ($r = 0.483$; $P < 0.001$) and CHMp-13a-xenografted mice ($r = 0.589$; $P < 0.001$). In the tissues of CHMp-5b-xenografted mice, the expression levels of both VEGF-A and VEGF-C were significantly correlated with PI ($r = 0.287$; $P = 0.006$ and $r = 0.543$; $P < 0.001$, respectively). In the tissues of CHMp-13a-xenografted mice, significant correlation was found between expression levels of

VEGF-A/-C and PI values ($r = 0.634$ $P < 0.001$ and $r = 0.619$; $P < 0.001$, respectively).

Summary

In Section 3, VEGF-A and VEGF-C mRNA values and VEGF-A and VEGF-C protein expressions of primary and metastatic lesions in CHMp-5b- and CHMp-13a-xenografted mice was examined and the relationship between their expressions and PI was evaluated.

VEGF-A mRNA values in the primary tissues of CHMp-13a-xenografted mice were significantly higher than those of CHMp-5b-xenografted mice after 3 weeks of transplantation. VEGF-C mRNA values were similar in both groups, though the expression levels were various, and those of CHMp-13a-xenografted mice showed significantly higher expression only at 6 weeks of transplantation. On the contrary, their protein expression on western blot analysis showed various levels in both CHMp-5b and CHMp-13a groups.

Both VEGF-A and VEGF-C scores on tissues of CHMp-5b- and CHMp-13a-xenografted mice tended to increase according to the period after transplantation, however there were no significant differences in VEGF-A and VEGF-C expressions among tissues of the different cell groups. On lymph node and lung metastatic tissues, VEGF-A and VEGF-C expressions were significantly lower when compare to those on the primary mass.

VEGF-A and VEGF-C expressions on these tissues showed significant correlation. In addition, expressions of VEGF-A and VEGF-C showed significant correlation with PI on primary tumor tissues of CHMp-5b- and CHMp-13a-xenografted mice.

	VEGF-A		VEGF-C	
	CHMp-5b	CHMp-13a	CHMp-5b	CHMp-13a
VEGF-A	.	.	.	.
VEGF-C	0.483 $P<0.001$	0.589 $P<0.001$	.	.
PI	0.287 $P=0.006$	0.634 $P<0.001$	0.543 $P<0.001$	0.619 $P<0.001$

Table 2.3.1. Spearman's rank correlations between the expressions of VEGF-A and VEGF-C and PI values on primary lesions developed in xenografted nude mice

A

VEGF-A mRNA expression

B

VEGF-C mRNA expression
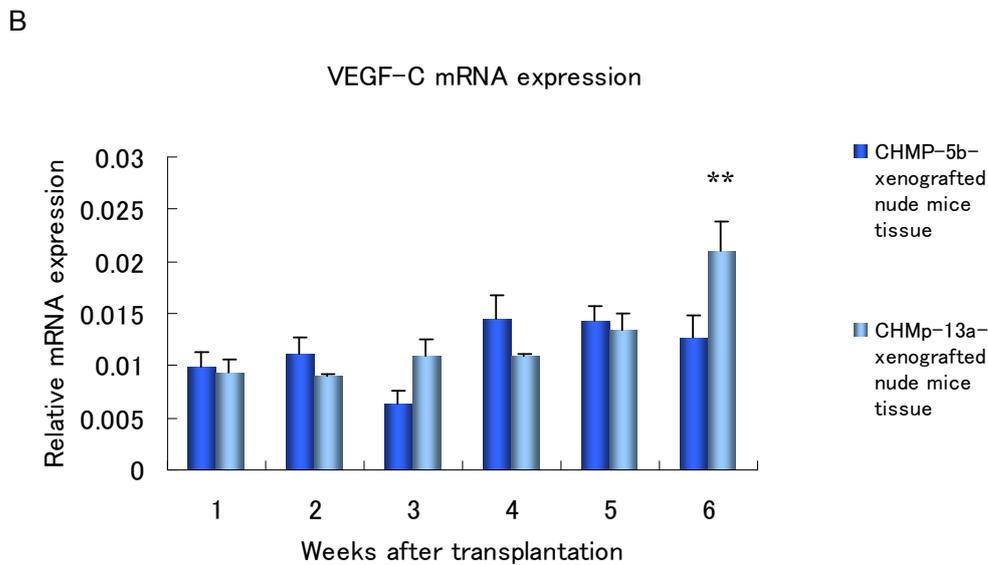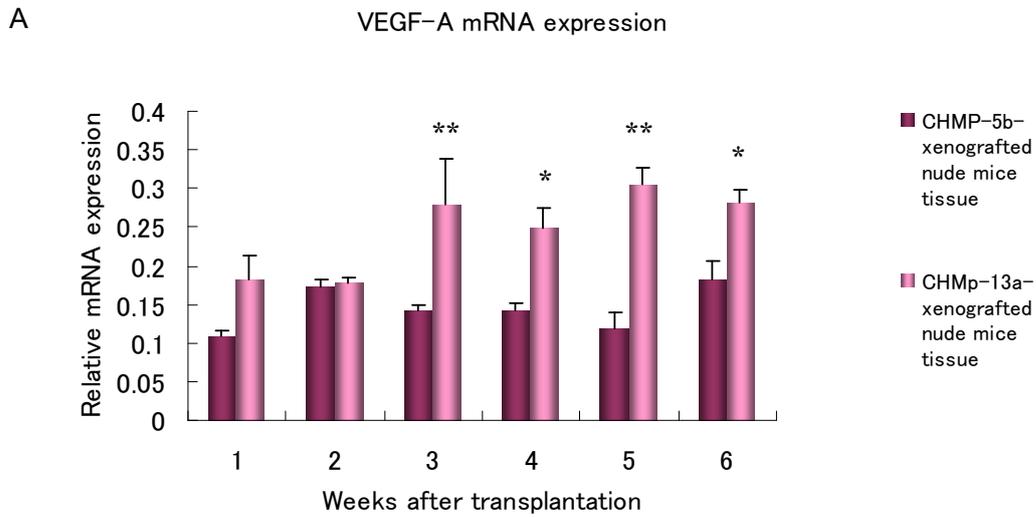
Figure 2.3.1. mRNA expression of VEGF-A and VEGF-C on the primary lesion of CHMp-5b- and CHMp-13a-xenografted mice.

A: In the expression of VEGF-A mRNA, primary tumor tissues in CHMp-13a-xenografted mice showed significantly higher than those in CHMp-5b-xenografted mice from 3 to 6 weeks after transplantation.

B: In the expression of VEGF-C mRNA, primary tumor tissues in CHMp-13a-xenografted mice showed significantly higher than those in CHMp-5b-xenografted mice in 6 weeks after transplantation.

(*: $P < 0.05$, **: $P < 0.01$)

CHM-5b primary tumor   CHMp-13a primary tumor

VEGF-A   42kDa

VEGF-C   40kDa

Actin   45kDa

      1   2   3   4   5   6   1   2   3   4   5   6

Weeks after transplantation
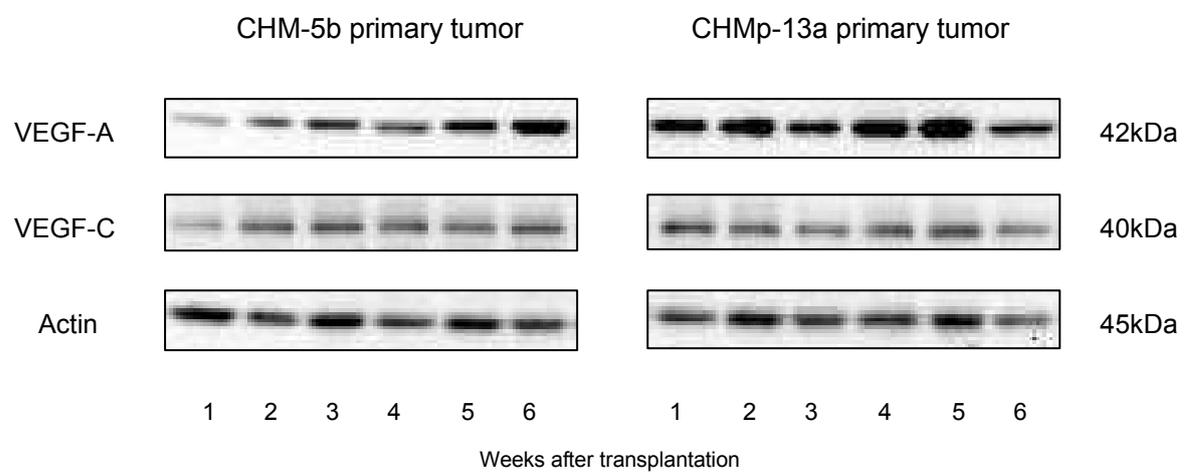
Figure 2.3.2. Western blot analysis of VEGF-A and VEGF-C on the primary tumor tissues in CHMp-5b- and CHMp-13a-xenografted mice. Their protein expression levels were various in both CHMp-5b and CHMp-13a groups.

.

Expression of VEGF-A on CHMp-5b-xenografted mice
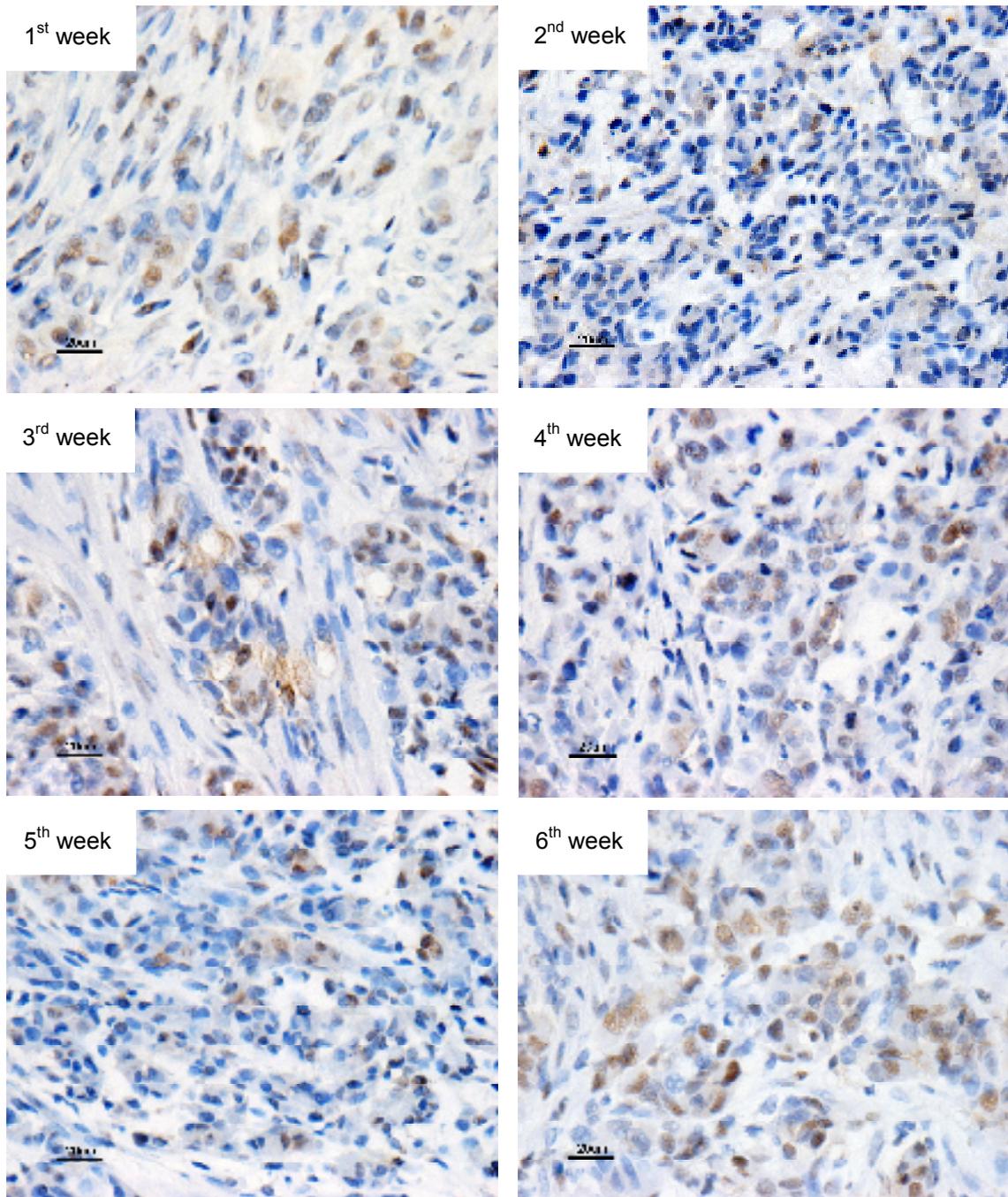
**Figure 2.3.3.** Immunohistochemistry for VEGF-A in primary tumor tissues of CHMp-5b-xenografted nude mice at 1 to 6 weeks after transplantation. Staining of VEGF-A was diffuse in the cytoplasm of tumor cells.

(Maginification ×400).

Expression of VEGF-A on CHMp-13a–xenografted mice
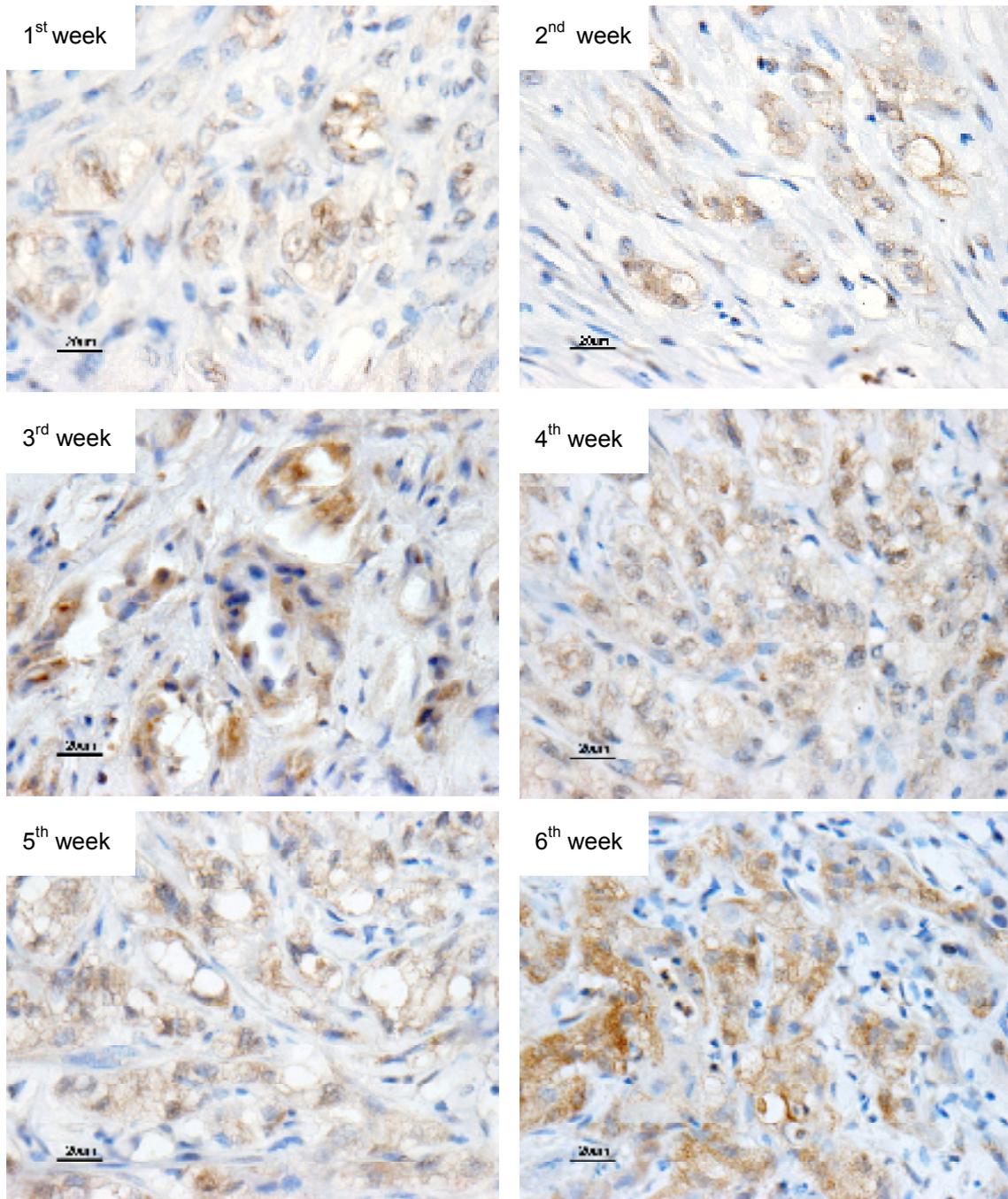
Figure 2.3.4. Immunohistochemstry for VEGF-A in primary tumor tissues of CHMp-13a-xenografted nude mice at 1 to 6 weeks after transplantation. Staining of VEGF-A was diffuse in the cytoplasm of tumor cells.

(Maginification ×400)

Expression of VEGF-C on CHMp-5b–xenografted mice
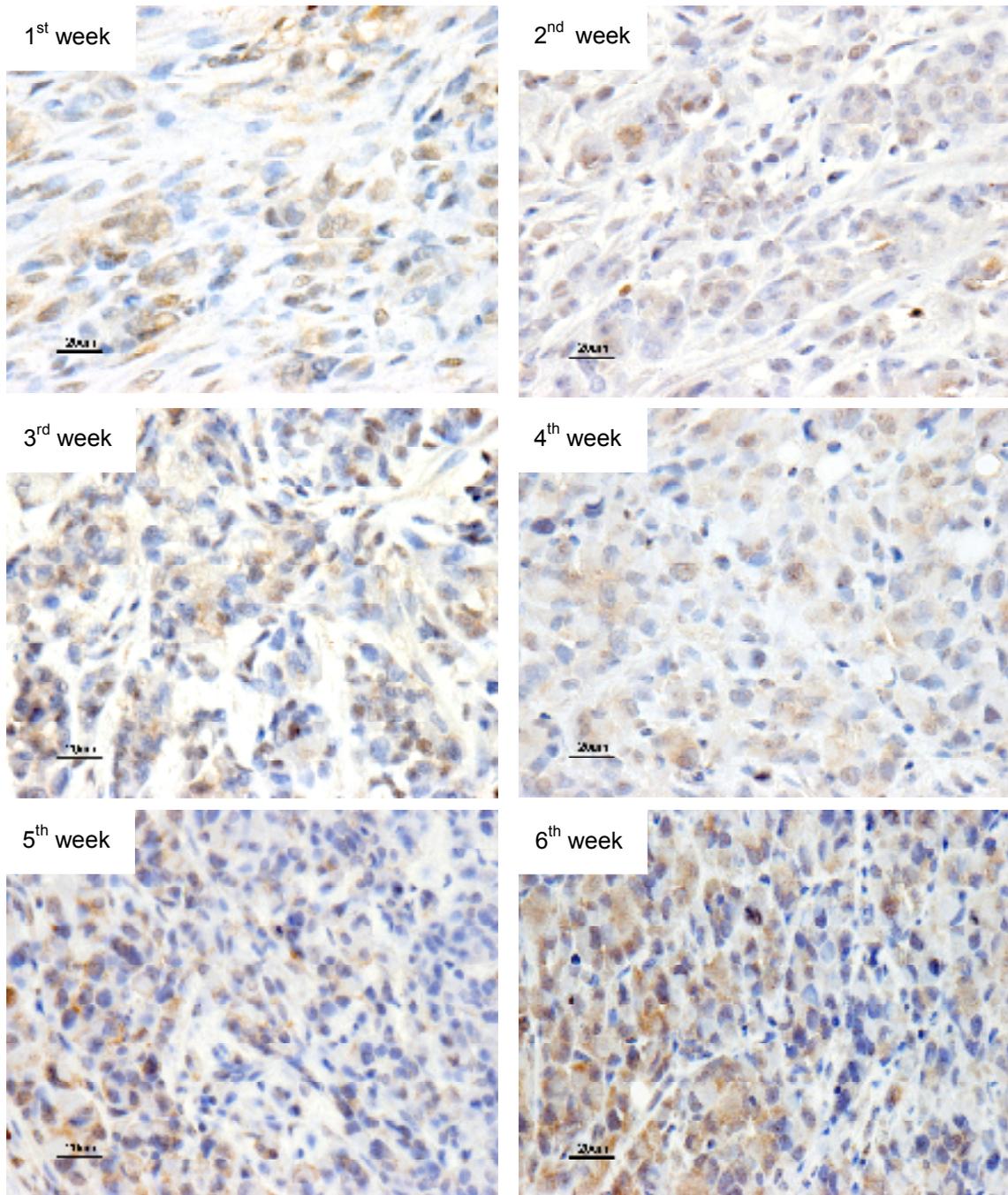
Figure 2.3.5. Immunohistochemistry for VEGF-C in primary tumor tissues of CHMp-5b-xenografted nude mice at 1 to 6 weeks after transplantation. (Maginification ×400)

Expression of VEGF-C on CHMp-13a–xenografted mice
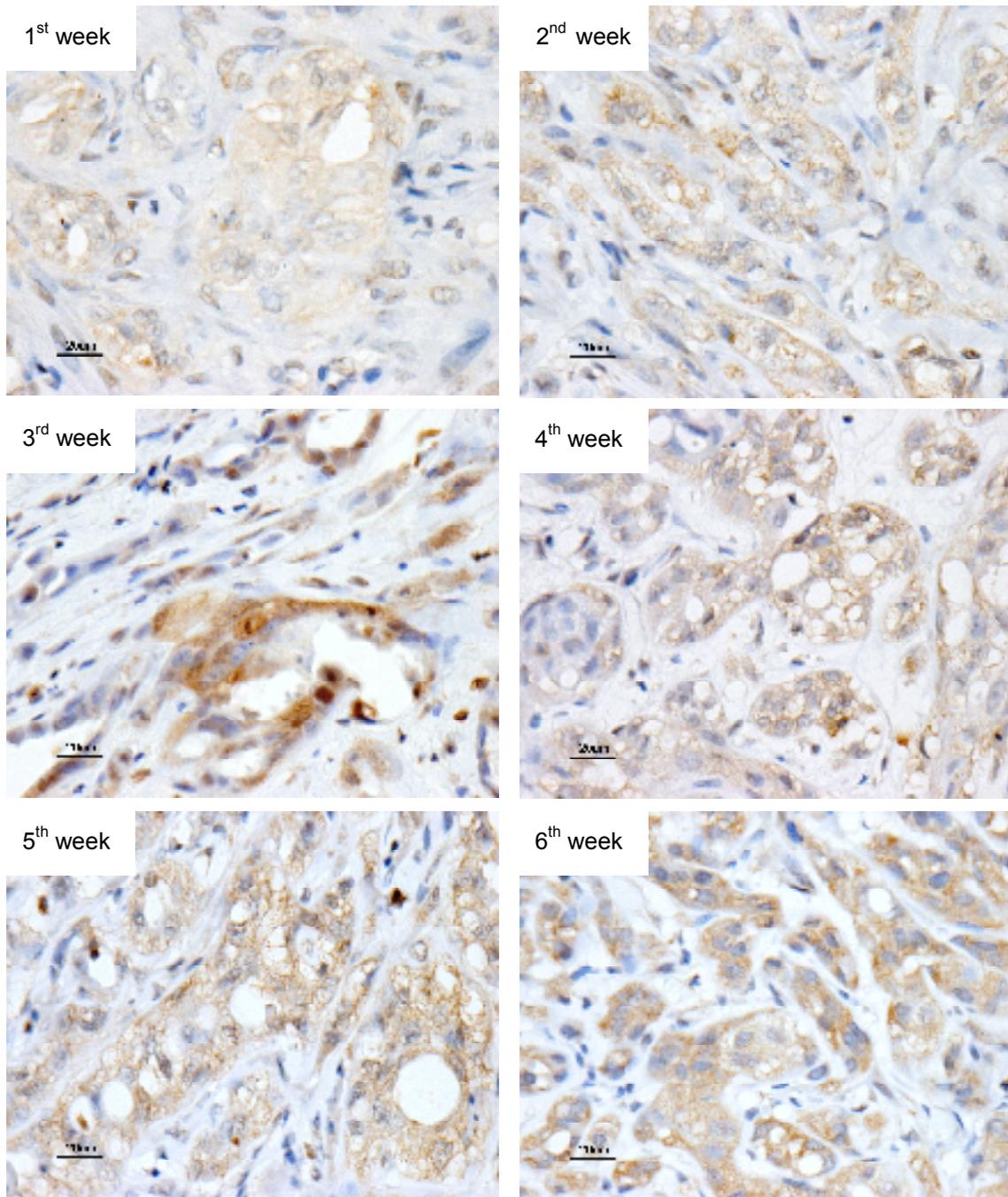
Figure 2.3.6. Immunohistochemistry for VEGF-C in primary tumor tissues of CHMp-13a-xenografted nude mice at 1 to 6 weeks after transplantation. (Maginification ×400)
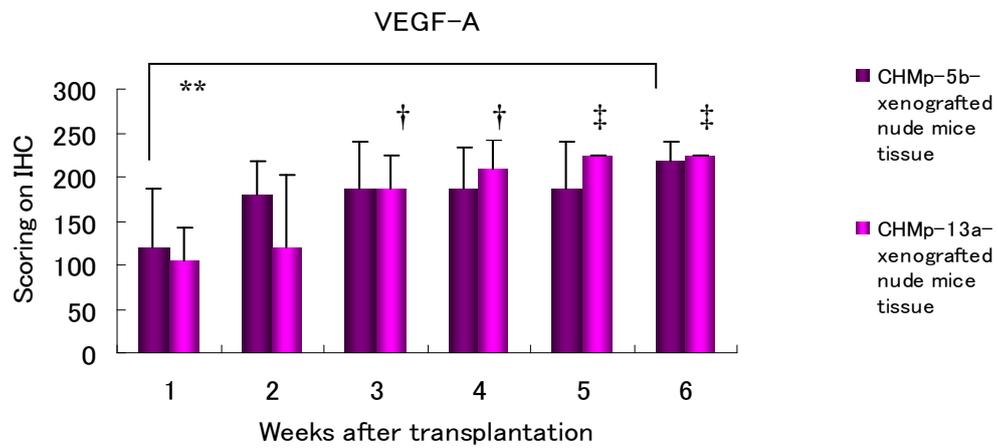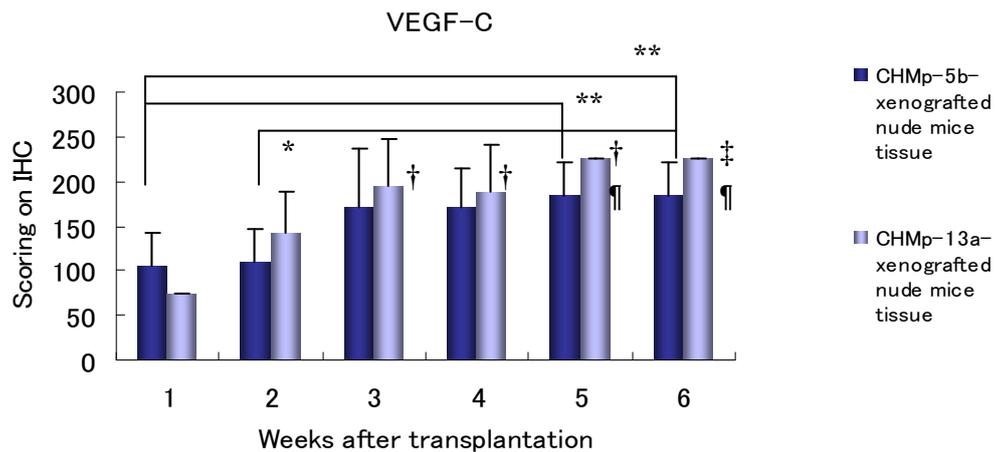
Figure 2.3.7. Scores of VEGF-A (A) and VEGF-C (B) expressions on immunohistochemistry (IHC) on the primary lesions of xenografted mice. VEGF-A and VEGF-C scores increased over time during 6 weeks. There was no significant difference between the tissues in mice xenografted with CHMp-5b and CHMp-13a at each week.

*, **: Significant difference in the score between the week after transplantation in CHMp-5b-xenografted mice (*: $P < 0.05$, **: $P < 0.01$)

†, ‡: Significant difference compared with the level of 1st week after transplantation of CHMp-13a-xenografted mice (†: $P < 0.05$, ‡: $P < 0.01$)

¶: Significant difference compared with the level of 2nd week after transplantation of CHMp-13a-xenografted mice ($P < 0.05$)

| | Lymph node of CHMp-5b-xenografted mice | Lymph node of CHMp-13a-xenografted mice | Lung of CHMp-5b-xenografted mice |
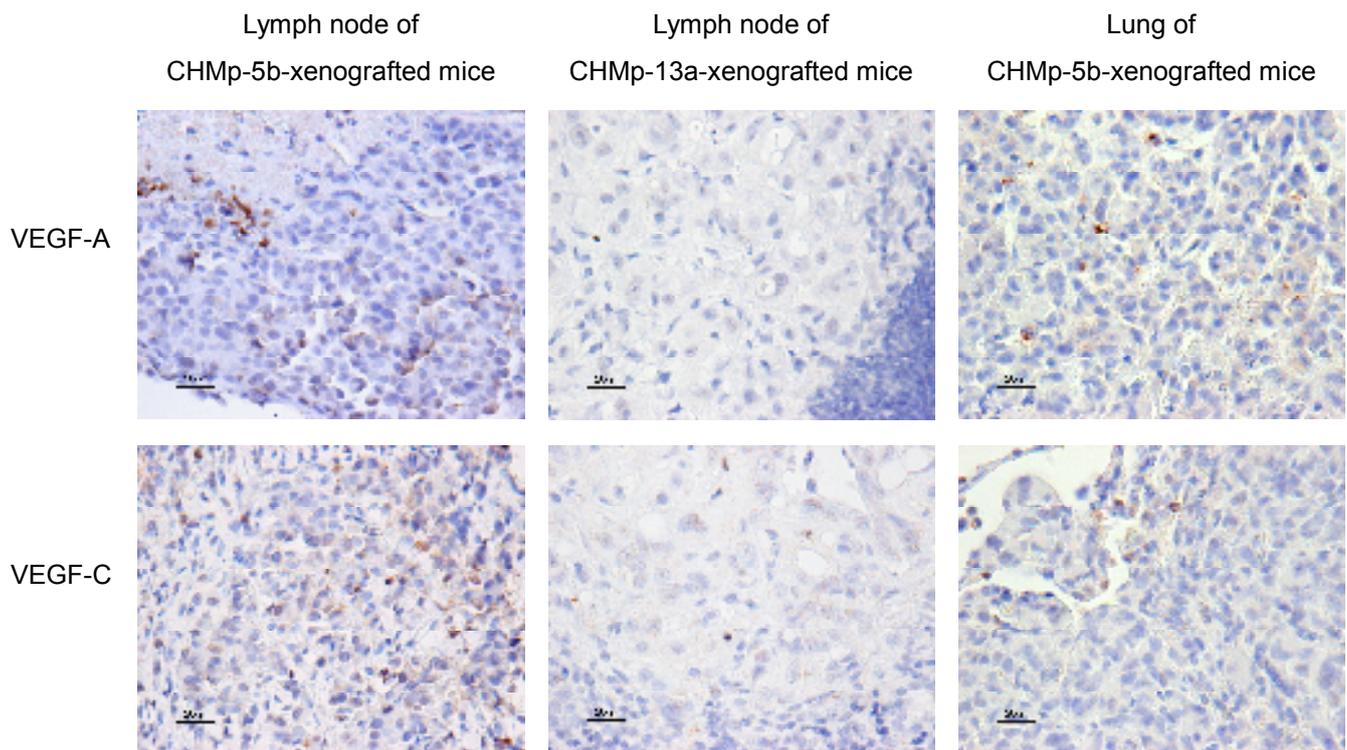
VEGF-A

VEGF-C

Figure 2.3.8. Immunohistochemistry for VEGF-A and VEGF-C in the lymph node and lung metastatic lesions at 6 weeks after transplantation in CHMp-5b- and CHMp-13a-xenografted mice. VEGF-A and -C staining on metastatic tissues were weaker than those on the primary mass in nude mice transplanted with both cell lines.

(Maginification ×400)
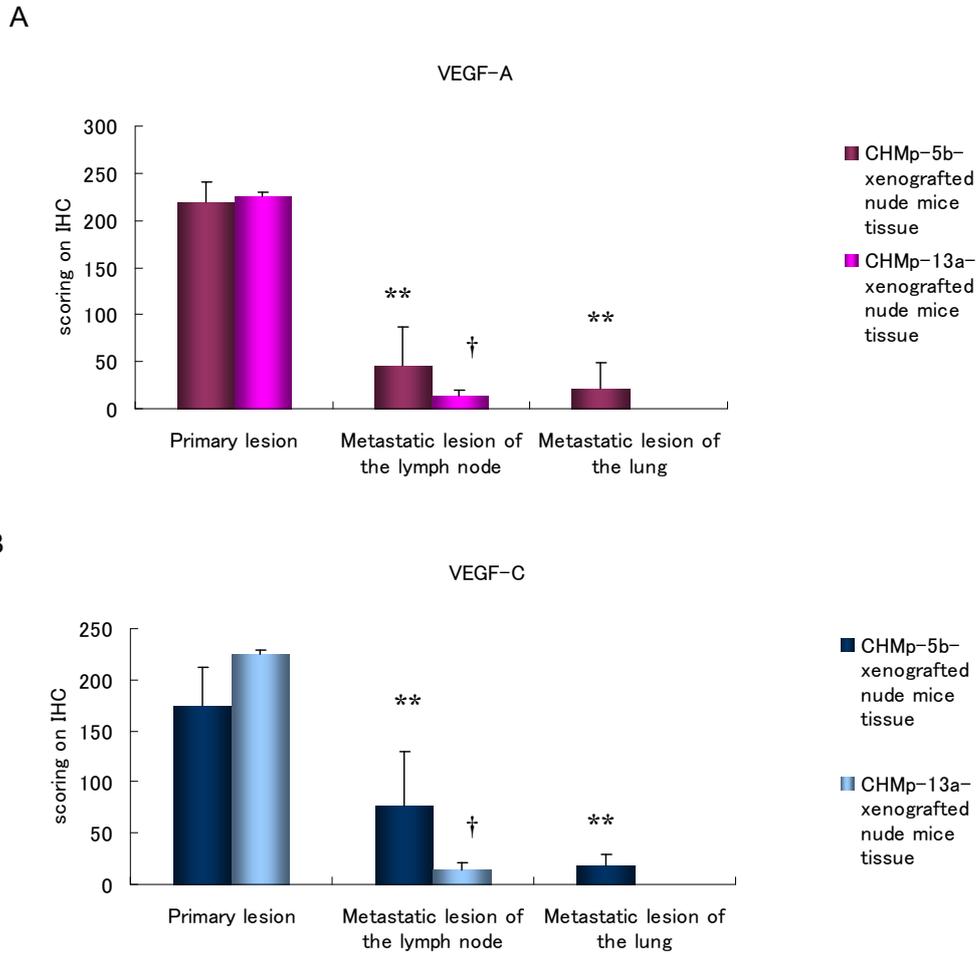
Figure 2.3.9. Scores of VEGF-A (A) and VEGF-C (B) expressions on immunohistochemistry (IHC) on primary and metastatic lesions of xenografted mice at 6 week after transplantation.

**: Significant difference between the primary and metastatic lesions in CHMp-5b group $(P < 0.01)$

†: Significant differentce between the primary and metastatic lesions of the lymph node in CHMp-13a group $(P < 0.05)$

Section 4

Angiogenesis and lymphangiogenesis of the tissues developed in xenografted nude mice

Materials and Methods

In this section, I investigated MVD and LVD in peri- and intra-primary tumor tissues and metastatic lesions of lymph nodes and the lung in CHMp-5b- and CHMp-13a-xenografted nude mice on immunohistochemistry, and the relationships between VEGF-A/-C expression and angiogenesis/lymphangiogenesis were evaluated.

Immunohistochemistry

The expression of CD31, blood vessel marker, and LYVE1, lymphatic vessel marker, in the primary lesions, lymph nodes and the lung of CMGT tissues developed in nude mice were analyzed by EnVision immunohistochemical procedures similar to Chapter 1. The antibodies used were as follows: polyclonal rabbit anti-mouse CD31 at a dilution of 1/100 (ab28364; Abcam, Inc., MA, USA) and polyclonal rabbit anti-mouse LYVE1 at a dilution of 1/200 (ab14917; Abcam, Inc.). After the incubation with these antibodies, samples were treated with polymer solution containing HRP-conjugated antibody against mouse rabbit Ig (K4003; EnVision^{TM}-HRP labeled polymer, DAKO).

Quantification of MVD and LVD on immunohistochemistry

In the field of light microscopic views using a low-power objective, microvessels or lymphatic vessels concentrated within discrete areas, termed "hot spots", were identified, then their number was counted in the same area under ×400 magnification. Each discrete and individually stained vessel structure with irrelevant of size was counted as a vessel, and the total number per each area of view was recorded. This process was repeated 5 times using the different field of view within the same section, and the mean vessel number was calculated.

MVD and LVD of primary tumor and metastatic tissues were calculated as number of vessels per the microscopic view area ($34640 \mu m^2$ field). MVD and LVD were measured at the peritumor (in the $350 \mu m$ border around the tumor) area and intratumor area of tissues developed in nude mice. Figure 2.4.1 shows the division of the peritumor area and intratumor area based on histology.

For evaluation of LVD on the lung paranchyma, hot spots were identified, then counted in the same area under ×100 magnification as number of vessels per the microscopic view area ($553944 \mu m^2$ field).

Statistical analysis

Results were expressed as mean ± SD. In each xenografted mouse, changes in MVD and LVD according to the period (for 6 weeks) were statistically evaluated using ANOVA by Fisher's least significant difference (LSD) test. For evaluation of correlation among the expressions of VEGF-A, VEGF-C, PI, MVD and LVD in two xenografted mouse models, Spearman's rank correlation was used. $P < 0.05$ was considered significant in all analyses.

Results

Immunohistochemistry for CD31 and LYVE1

Figure 2.4.2 shows the immunohistochemical findings of vascular endothelial cells and lymphatic endothelial cells stained by CD31 and LYVE1, respectively, on the normal mouse tissue. CD31 was stained on blood vessels clearly but was less stained on lymphatic endothelial cells. Vascular endothelial cells were negatively stained by LYVE1. Figure 2.4.3 shows the immunohistochemistry findings of those on the lung tissue of CHMp-5b-xenografted mice. CD31 and LYVE1 positive cells were observed in the lung tissue surrounding the metastatic lesion.

MVD

Figure 2.4.4 shows CD31-positive vessels within the primary tumor tissues developed in CHMp-5b- and CHMp-13a-xenografted mice. The microvessels of the peritumor area were shown to be enlarged and dilated cavity, while intratumoral vessels were collapsed and irregularly scattered, but numerous numbers of vessels were observed.

Figure 2.4.5 shows the MVD of primary lesions in CHMp-5b- and CHMp-13a-xenografted mice at 1 to 6 weeks after transplantation. Peritumor MVD (pMVD) in the tissues of CHMp-5b- and CHMp-13a-xenografted mice tended to increase according to the time after transplantation, except for pMVD of CHMp-5b group at 6 weeks after transplantation. Intratumor MVD (iMVD) in the tissues of the CHMp-5b- and CHMp-13a-xenografted mice also tended to increase according to the time after transplantation, except for iMVD of the CHMp-5b group at 4 and 6 weeks after transplantation and of the CHMp-13a group at 3 weeks after transplantation.

iMVD was higher in the tissues of CHMp-5b-xenografted mice than those of CHMp-13a-xenografted mice through out the experimental period. Among them, iMVD at 2 (P = 0.002), 3 (P = 0.0001), 5 (P = 0.001) and 6 (P = 0.046) weeks after transplantation in tissues of CHMp-5b-xenografted mice were significantly higher than those in CHMp-13a-xenografted mice.

There was a significant difference between pMVD and iMVD in primary tumor tissues of CHMp-5b-xenografted mice at 2 (P = 0.0009) and 3 (P = 0.012) weeks after transplantation.

pMVD of the lymph node and lung metastatic tissues could not be assessed, because CD31 was positively stained on the surface of vascular endothelial cells of postcapillary venule on the lymph node and pulmonary alveolus. iMVD of the lymph node and lung metastatic tissues could be measured, and it was significantly lower than that of the primary tumor tissue ($P < 0.05$) (Figure 2.4.6)

LVD

Figure 2.4.7 shows LYVE1-positive vessels within the primary tumor tissues developed in CHMp-5b- and CHMp-13a-xenografted mice. The peritumor lymphatic vessels (pLVD) were enlarged. Intratumor LVD (iLVD) of primary tumor tissues in nude mice transplanted with both cell lines could not be assessed because LYVE1 was shown a nonspecific reaction tumor cells.

Figure 2.4.8 shows pLVD of primary lesions in CHMp-5b- and CHMp-13a-xenografted mice from 1 to 6 weeks after transplantation. pLVD showed a gradual increase according to the period after transplantation in tissues of CHMp-5b-xenografted nude mice. There was a significant difference in pLVD between the values of 1 week and those of 5 and 6 weeks after transplantation in tissues of CHMp-5b-xenografted nude mice (P = 0.027 and P = 0.019, respectively). In tissues of CHMp-13a-xenografted mice, pLVD increased after 5 weeks of

transplantation. There was a significant difference between pLVD levels of 1, 2, 3 and 4 weeks and that of 6 weeks after transplantation in tissues of CHMp-13a-xenografted nude mice ($P =$ 0.017). pLVD of tissues in CHMp-5b-xenografted mice seemed to be higher than those of CHMp-13a-xenografted mice from 1 to 5 weeks of transplantation, among which significant difference was observed ($P = 0.0235$) at 4 weeks of transplantation.

Figures 2.4.9 and 2.4.10 show LVD of the lymph node in CHMp-5b- and CHMp-13a-xenografted mice at 1 to 6 weeks after transplantation. LYVE1-positive lymphatic vessels within the lymph node seemed to increase according to the time after transplantation.

Figures 2.4.11 and 2.4.12 show the LYVE1-positive lymphatic vessels of the lung parenchyma in CHMp-5b- and CHMp-13a-xenografted mice at 1 to 6 weeks after transplantation. Some microvessels filled with erythrocytes were positively stained by LYVE1 on the lung parenchyma in both groups. LYVE1-positive vessels within the lung parenchyma seemed to increase according to the time after transplantation. LVD of the lung parenchyma in CHMp-5b-xenografted mice at 4 to 6 weeks was significantly higher than those at 1 to 3 weeks after transplantation ($P < 0.01$) (Figure 2.4.13).

Correlations between the expression levels of VEGF-A, VEGF-C and PI and MVD and LVD values

Correlations between expressions of VEGF-A, VEGF-C and PI and MVD and LVD values of primary lesions in xenografted mice were evaluated and shown in Table 2.4.1. In the primary tumor tissues of CHMp-5b-xenografted mice, the expression level of VEGF-A was significantly correlated with pMVD ($r = 0.469$; $P < 0.001$), iMVD ($r = 0.249$; $P = 0.018$) and pLVD ($r = 0.284$; $P = 0.007$). On the contrary, VEGF-C expression did not significantly correlate with both MVD and LVD values. PI was significantly correlated with pMVD ($r =$

0.491; $P < 0.001$), iMVD ($r = 0.242$; $P = 0.028$) and pLVD ($r = 0.309$; $P = 0.003$). In primary tumor tissues of CHMp-13a-xenografted mice, the expression level of VEGF-A was significantly correlated with pMVD ($r = 0.494$; $P < 0.001$) and pLVD ($r = 0.285$; $P = 0.027$). The expression level of VEGF-C was significantly correlated with pMVD ($r = 0.510$; $P < 0.001$) and pLVD ($r = 0.315$; $P = 0.014$) and PI was significantly correlated with pMVD ($r = 0.493$; $P < 0.001$) and pLVD ($r = 0.466$; $P < 0.001$).

Table 2.4.2 shows the correlation between LVD in the lung parenchyma and VEGF-A, VEGF-C expressions and PI of the primary lesions in CHMp-5b- and CHMp-13a-xenografted mice. In the CHMp-5b-xenografted mice, the lung LVD was significantly correlated with the expression levels of VEGF-A ($r = 0.831$; $P = 0.041$) and VEGF-C ($r = 0.901$; $P = 0.014$), and PI ($r = 0.943$; $P = 0.005$) of the primary lesions. On the contrary, in the CHMp-13a-xenografted mice, the lung LVD did not significantly correlate with both VEGF-A and VEGF-C expressions and PI values of the primary lesions.

Summary

In Section 4, quantification of angiogenesis and lymphangiogenesis using CD31 and LYVE1 as the markers for vascular endothelial cells and lymphatic endothelial cells at the peritumor and intratumor sites of primary lesions in CHMp-5b- and CHMp-13a-xenografted mice was performed and relationship between their values and VEGF-A and VEGF-C expressions was evaluated.

In primary tumor tissues of CHMp-5b-xenografted mice, iMVD was significantly higher than pMVD, while there was no marked difference in their values in those of CHMp-13a-xenografted mice. iMVD in tissues of CHMp-5b-xenografted mice was significantly higher than those of CHMp-13a-xenografted mice. VEGF-A expression and PI showed a significant correlation with pMVD in primary tumor tissues of CHMp-5b- and CHMp-13a-xenografted mice and with iMVD in those tissues of CHMp-5b-xenografted mice. These results may suggest that tumor cell proliferation and intratumoral and peritumoral microvessel density may be strongly related to VEGF-A expression in CMGT. On the contrary, iMVD in the metastatic lesions was significantly lower than in primary tumor tissues.

pLVD in both tissues of CHMp-5b- and CHMp-13a-xenografted mice increased according to the time after transplantation. VEGF-A expression was correlated with LVD of peritumor lesions in CHMp-5b- and CHMp-13a-xenografted mice. In addition, VEGF-C expression was correlated with LVD of peritumor lesions in CHMp-13a-xenografted mice. These results may suggest that lymphangiogenesis of the peritumoral area might be related to VEGF-A and VEGF-C expression.

Increased numbers of LYVE1-positive vessels were found in the metastatic lung lesions of CHMp-5b-xenografted mice, as compared with CHMp-13a-xenografted mice, especially in

the later stage of development in nude mice.

	pMVD		iMVD		pLVD	
	CHMp-5b	CHMp-13a	CHMp-5b	CHMp-13a	CHMp-5b	CHMp-13a
VEGF-A	0.469 $P<0.001$	0.494 $P<0.001$	0.249 $P=0.018$	NS	0.284 $P=0.007$	0.285 $P=0.027$
VEGF-C	NS	0.510 $P<0.001$	NS	NS	NS	0.315 $P=0.014$
PI	0.491 $P<0.001$	0.493 $P<0.001$	0.294 $P=0.005$	NS	0.309 $P=0.003$	0.466 $P<0.001$

(NS: not significant)

Table 2.4.1. Spearman's rank correlations between expressions of VEGF-A, VEGF-C and PI, and MVD and LVD values of primary lesions developed in CHMp-5b- and CHMp-13a-xenografted mice.

| | Lung LVD ||
	CHMp-5b	CHMp-13a
VEGF-A	0.831 $P=0.041$	NS
VEGF-C	0.901 $P=0.014$	NS
PI	0.943 $P=0.005$	NS

(NS: not significant)

Table 2.4.2. Spearman's rank correlations between VEGF-A, VEGF-C expressions and PI of primary lesions and LVD values of the lung parenchyma developed in CHMp-5b- and CHMp-13a-xenografted mice.
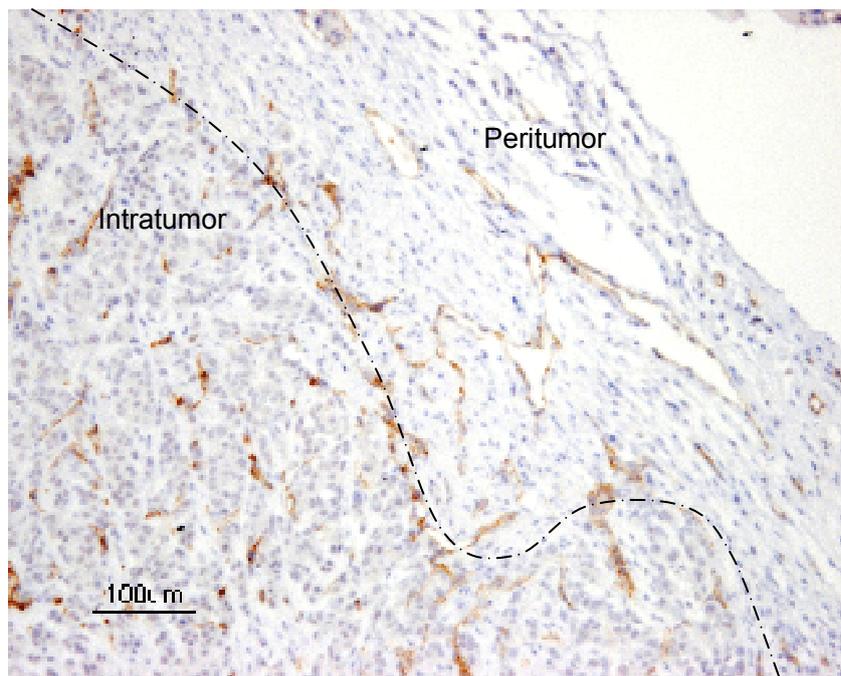
Figure 2.4.1. The tumor section with a dashed line showing two areas, intratumor and peritumor (in the 350 μm border around the tumor) areas.

(Magnification ×100, Immunohistochemistry by CD31)
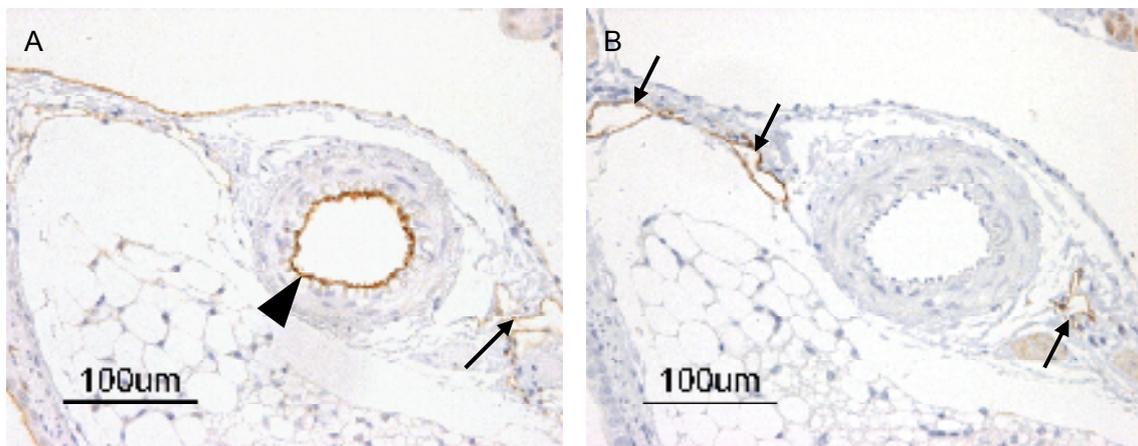
Figure 2.4.2. Discrimination of vascular endothelial cells detected by CD31 and lymphatic endothelial cells detected by LYVE1 on the normal mouse tissue.

A: CD31 was positively stained on the surface of vascular endothelial cells of an arteriole (arrowhead) and less stained on lymphatic endothelial cells (arrow)

B: LYVE1 was positively stained on the lymphatic vessels (arrows) beside an arteriole.

(Magnification ×200)
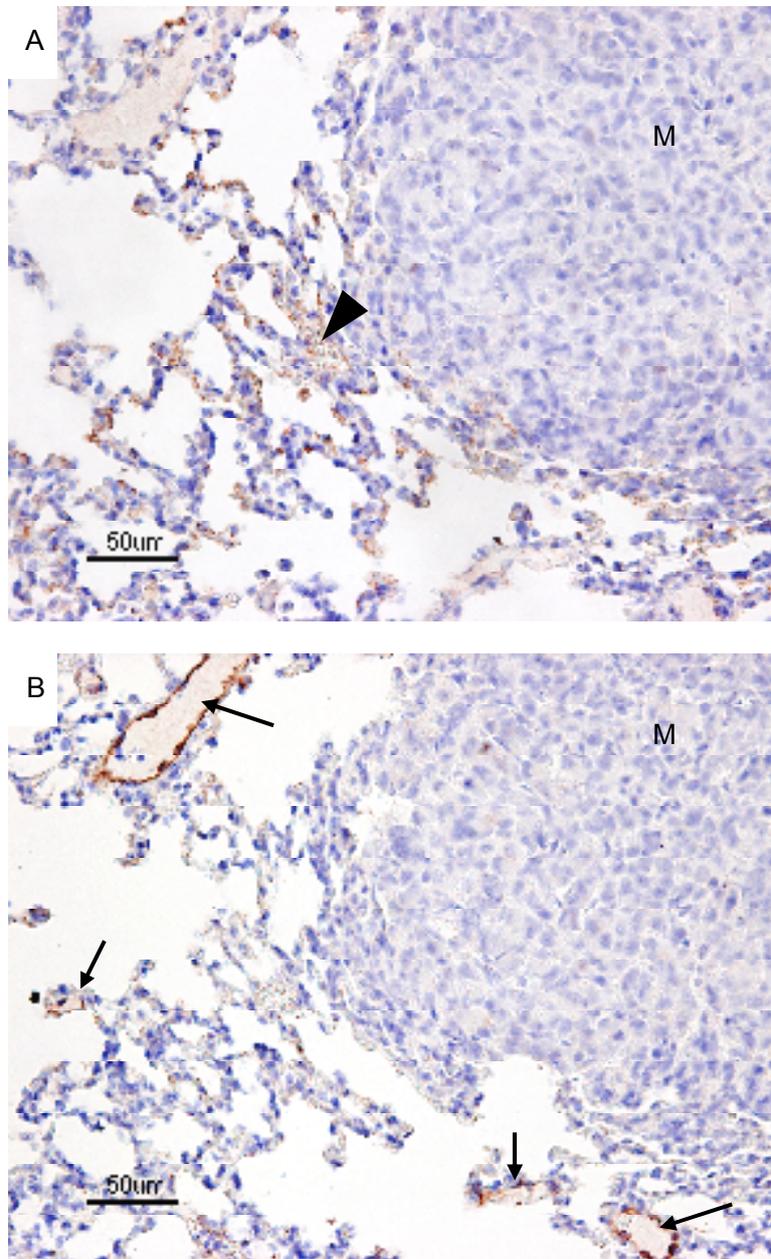
Figure 2.4.3. Vascular endothelial cells detected by CD31 and lymphatic endothelial cells detected by LYVE1 on the mouse lung. (M: metastatic lesion)

A: CD31 was positively stained on the surface of vascular endothelial cells (arrowhead) and pulmonary alveolus.

B: LYVE1 was positively stained on the lymphatic vessels (arrows).

(Magnification ×200)

Primary tumor of
CHMp-5b-xenografted mice

Primary tumor of
CHMp-13a-xenografted mice

pMVD

iMVD
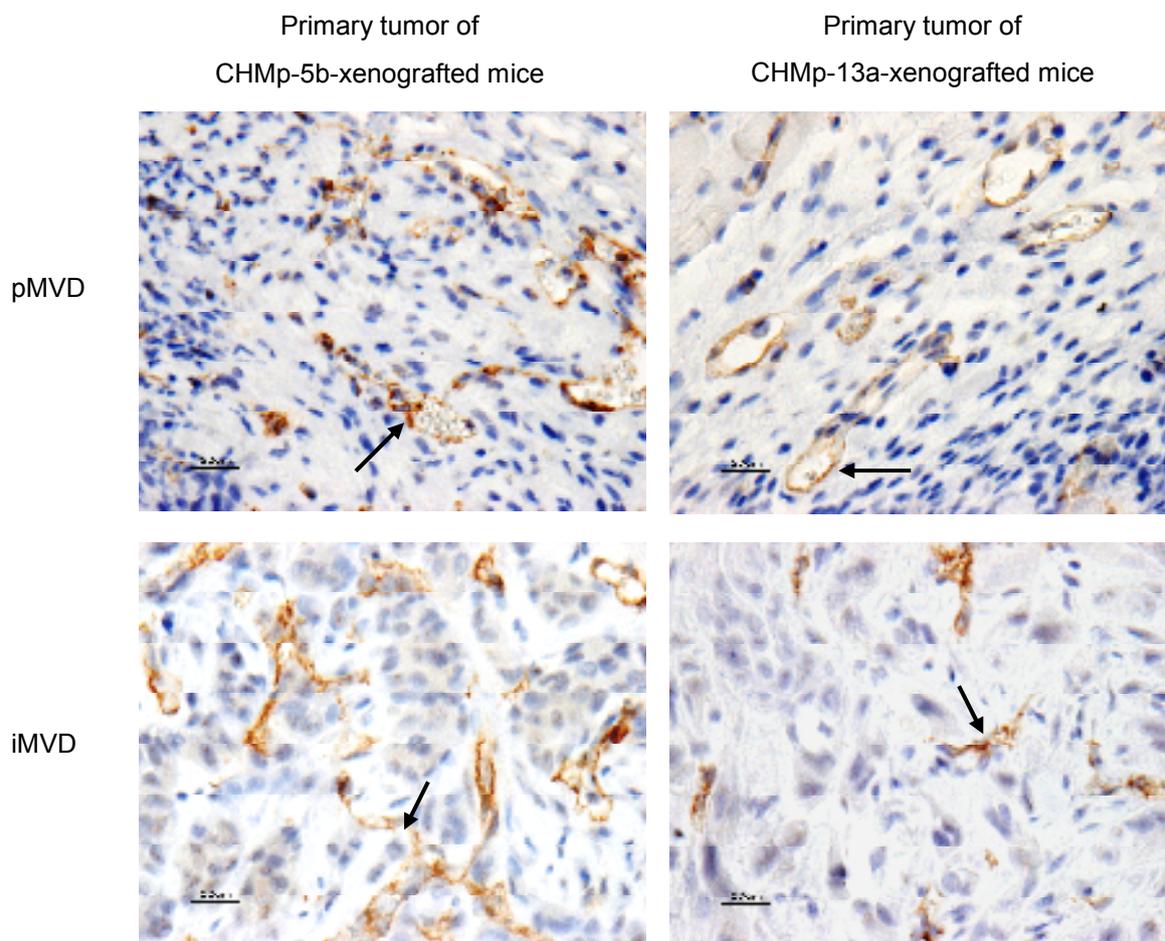
Figure 2.4.4. Immunohistochemistry to evaluate MVD by counting CD31-positive structures on the primary lesion of xenografted nude mice at 6 weeks after transplantation. Microvessels were counted within the peritumor area (pMVD) and the intratumor area (iMVD) of CHMp-5b- and CHMp-13a-xenografted mice. Arrows indicate CD31-positive structures.

(Magnification ×400)
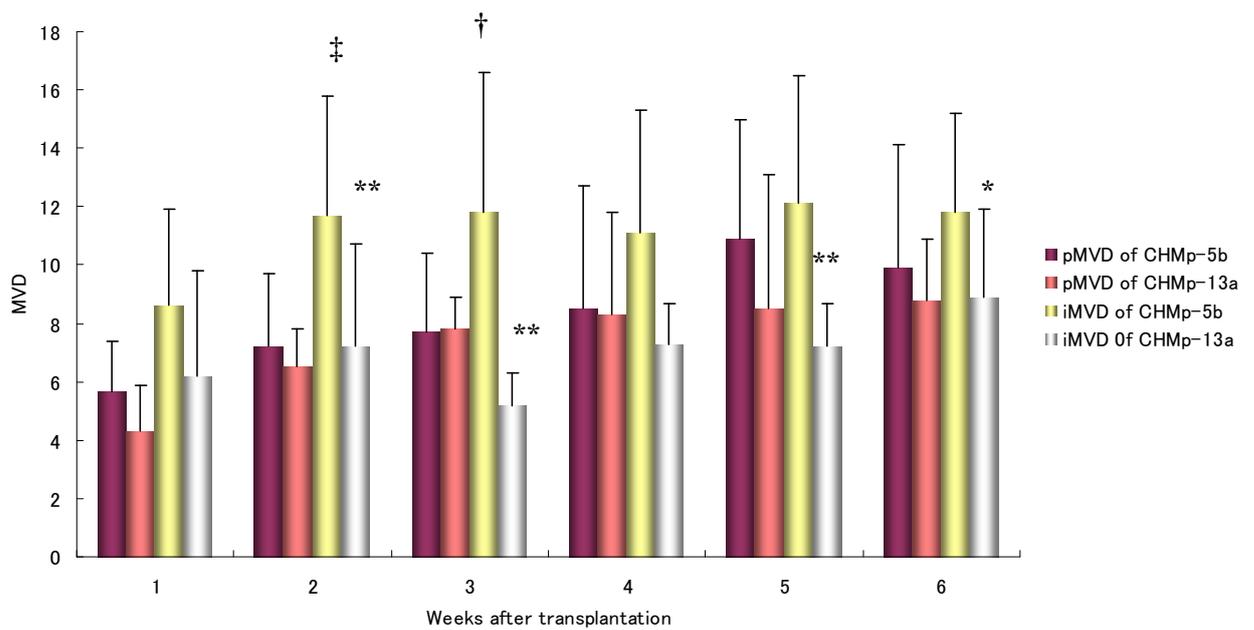
Figure 2.4.5. Peritumor (pMVD) and intratumor (iMVD) microvessel density in primary tumor tissues of CHMp-5b- and CHMp-13a-xenografted mice.

*, **: Significant difference in iMVD between the tissues of CHMp-5b and CHMp-13a groups (*: $P < 0.05$, **: $P < 0.01$)

†, ‡: Significant difference between pMVD and iMVD of tissues of CHMp-5b group (†: $P < 0.05$, ‡: $P < 0.01$)

| | Lymph node of CHMp-5b-xenografted mice | Lymph node of CHMp-13a-xenografted mice | Lung of CHMp-5b-xenografted mice |
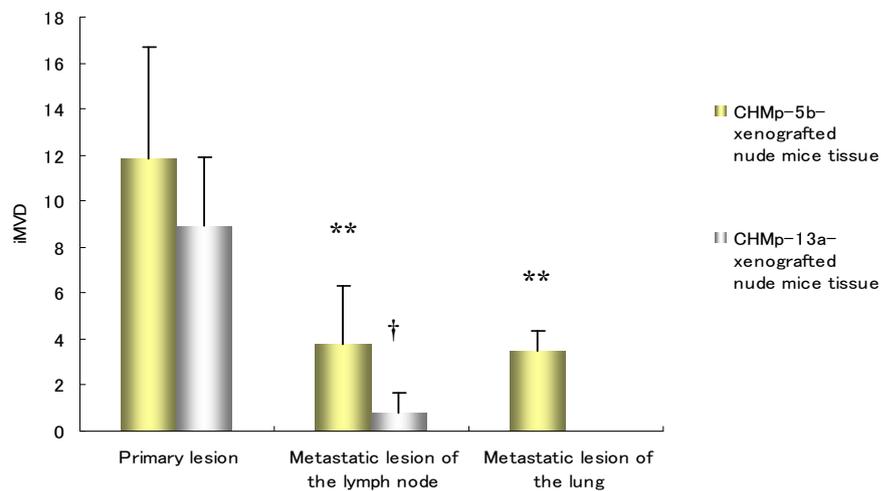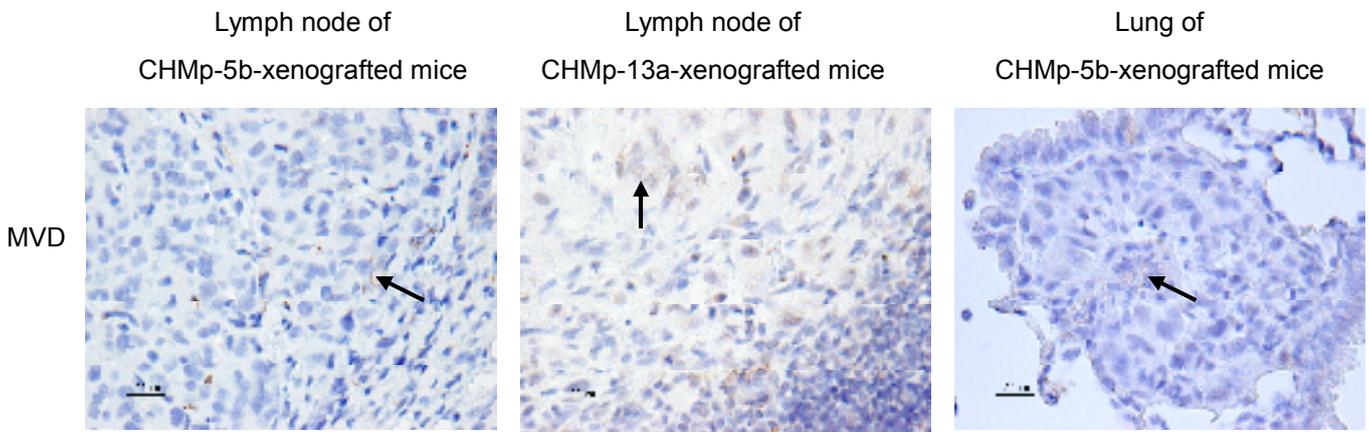
Figure 2.4.6. Immunohistochemical findings of CD31-positive structures (arrows) within the intratumor area of the lymph node and lung in CHMp-5b-xenografted mice and the lymph node in CHMp-13a-xenografted mice at 6 weeks after transplantation. The lower graph was iMVD values of the primary lesion, lymph node and lung. iMVD was significantly lower in metastatic lesions of the lymph node and lung when compare to those in the primary lesions.

(Magnification ×400)

**: Significant difference between the primary and metastatic lesions in the CHMp-5b group ($P < 0.01$)

†: Significant difference between the primary and metastatic lesions of the lymph node in the CHMp-13a group ($P < 0.05$)

Primary tumor of CHMp-5b-xenografted mice | Primary tumor of CHMp-13a-xenografted mice

pLVD

iLVD
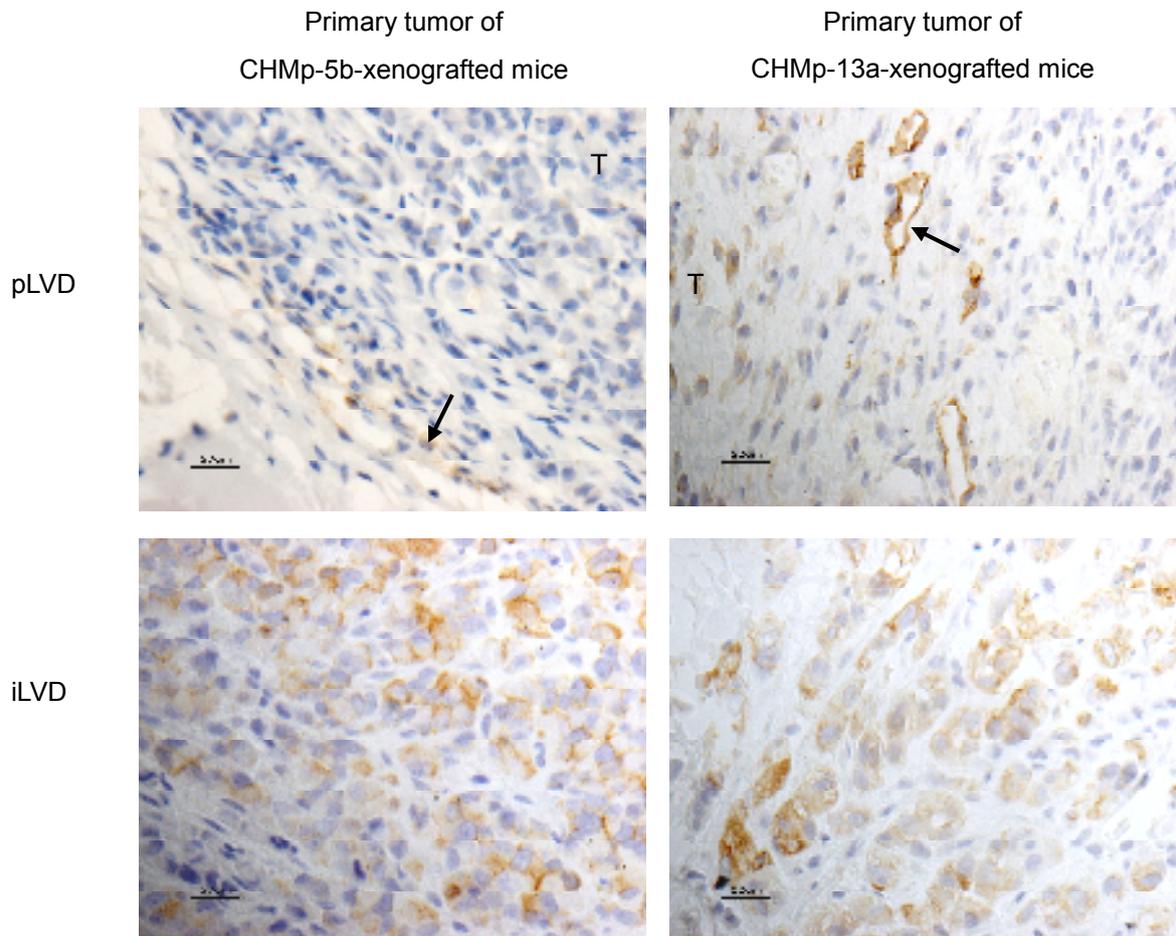
Figure 2.4.7. Immunohistochemistry to evaluate LVD by counting LYVE1-positive structures on the primary lesion of xenografted nude mice at 6 week after transplantation. Lymphatic vessles within the peritumor area (pLVD) of CHMp-5b- and CHMp-13a-xenografted mice could be counted, while the intratumor area (iLVD) of could not be assessed because LYVE1 showed a nonspecific reaction with tumor cells.

(T: tumor tissues, arrows: LYVE1-positive structure)

(Magnification ×400)
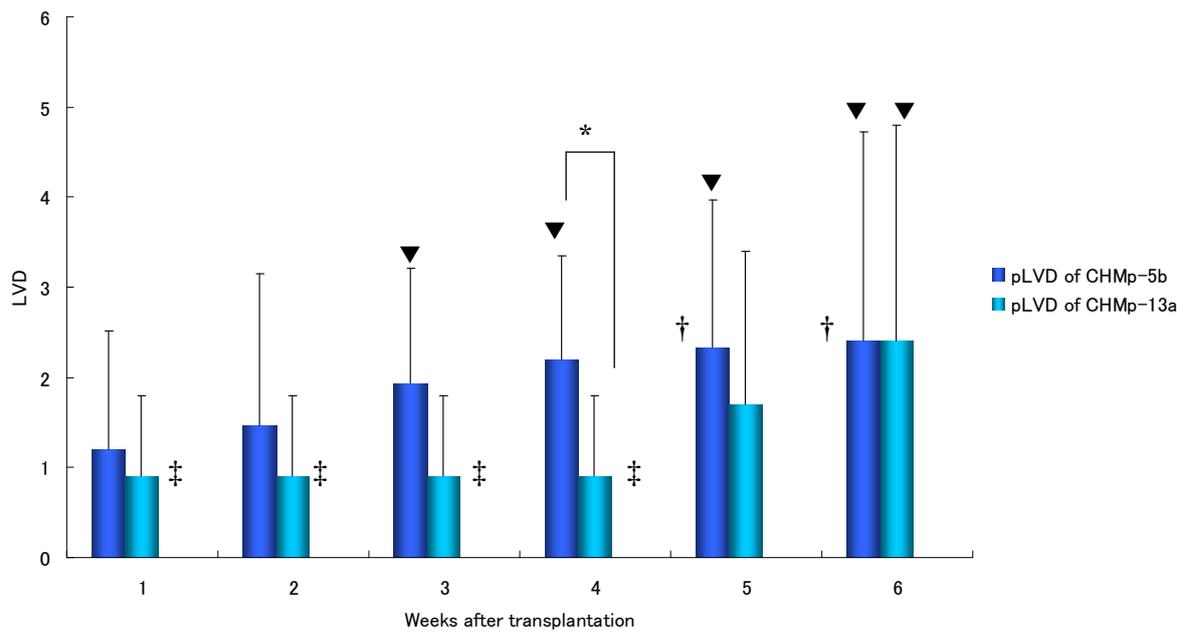
Figure 2.4.8. pLVD of primary tumor tissues in CHMp-5b- and CHMp-13a-xenografted mice

(▼: lymph node metastasis was observed in some of the nude mice)

*: Significant difference between CHMp-5b and CHMp-13a groups ($P < 0.05$)

†: Significant difference against pLVD of 1 week of CHMp-5b group ($P < 0.05$)

‡: Significant difference against pLVD of 6 weeks of CHMp-13a group ($P < 0.05$)

**Lymph node of CHMp-5b-xenografted mice**

1st week — 2nd week — 3rd week — 4th week — 5th week — 6th week — M
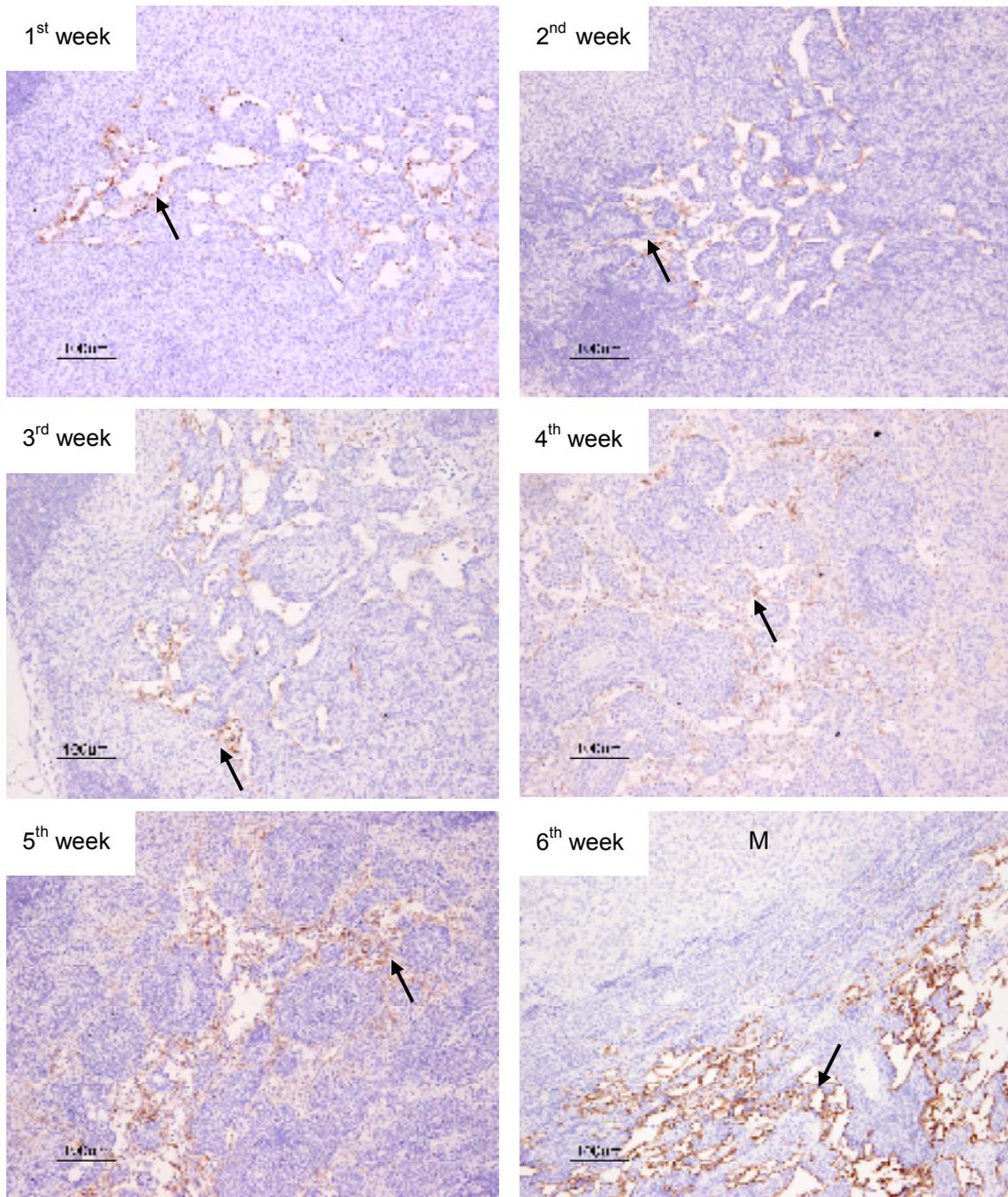
Figure 2.4.9. LYVE1-positive lymphatic vessels of the lymph node in CHMp-5b-xenografted mice at 1 to 6 weeks after transplantation. LYVE1-positive vessels (arrows) within the lymph node seemed to increase according to the time after transplantation. (M: metastatic lesion) (Magnification ×100)

Lymph node of CHMp-13a-xenografted mice
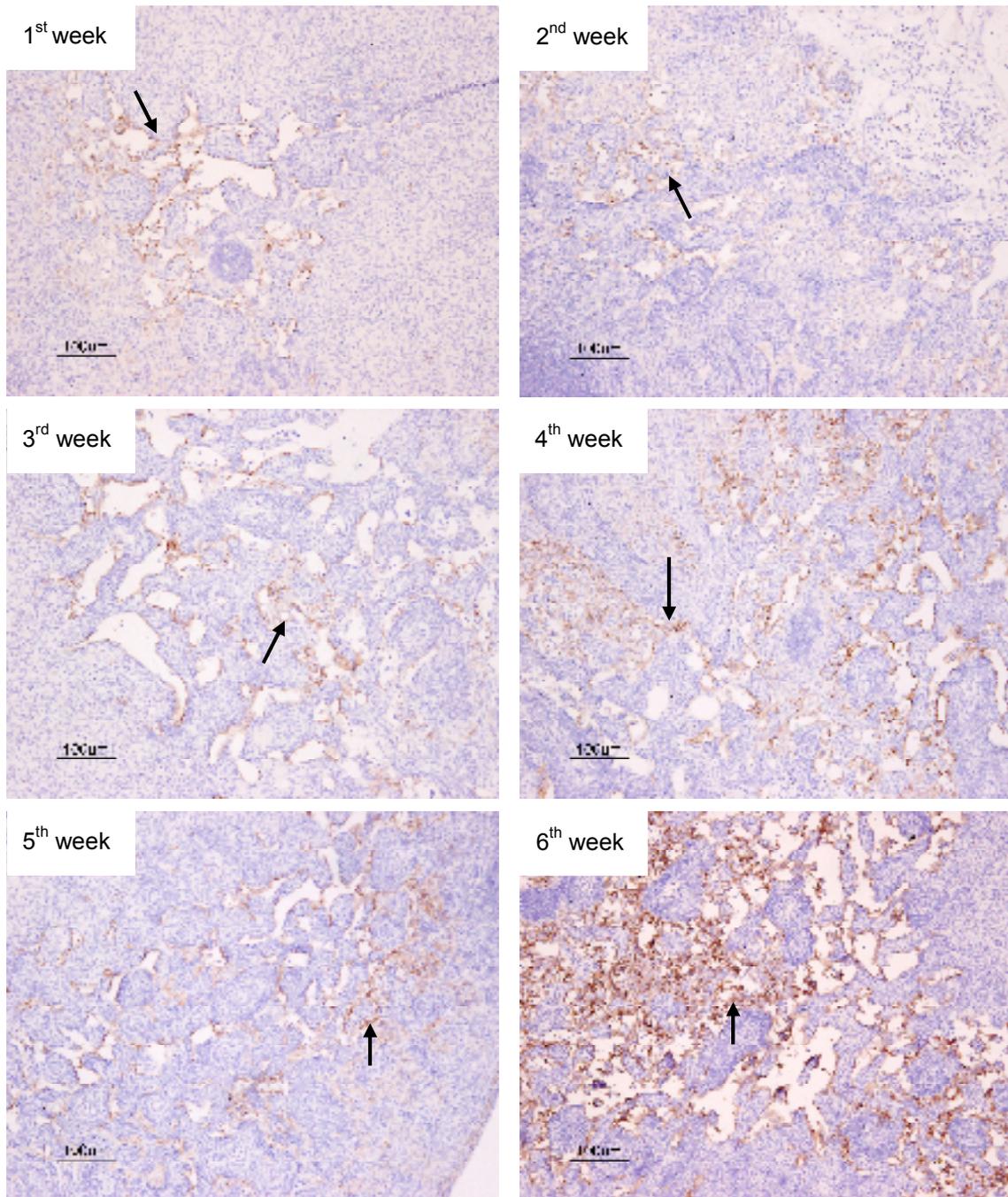
Figure 2.4.10. LYVE1-positive lymphatic vessels of the lymph node in CHMp-13a-xenografted mice at 1 to 6 weeks after transplantation. LYVE1-positive vessels (arrows) within the lymph node seemed to increase according to the time after transplantation.
(Magnification ×100)

Lung of CHMp-5b-xenografted mice
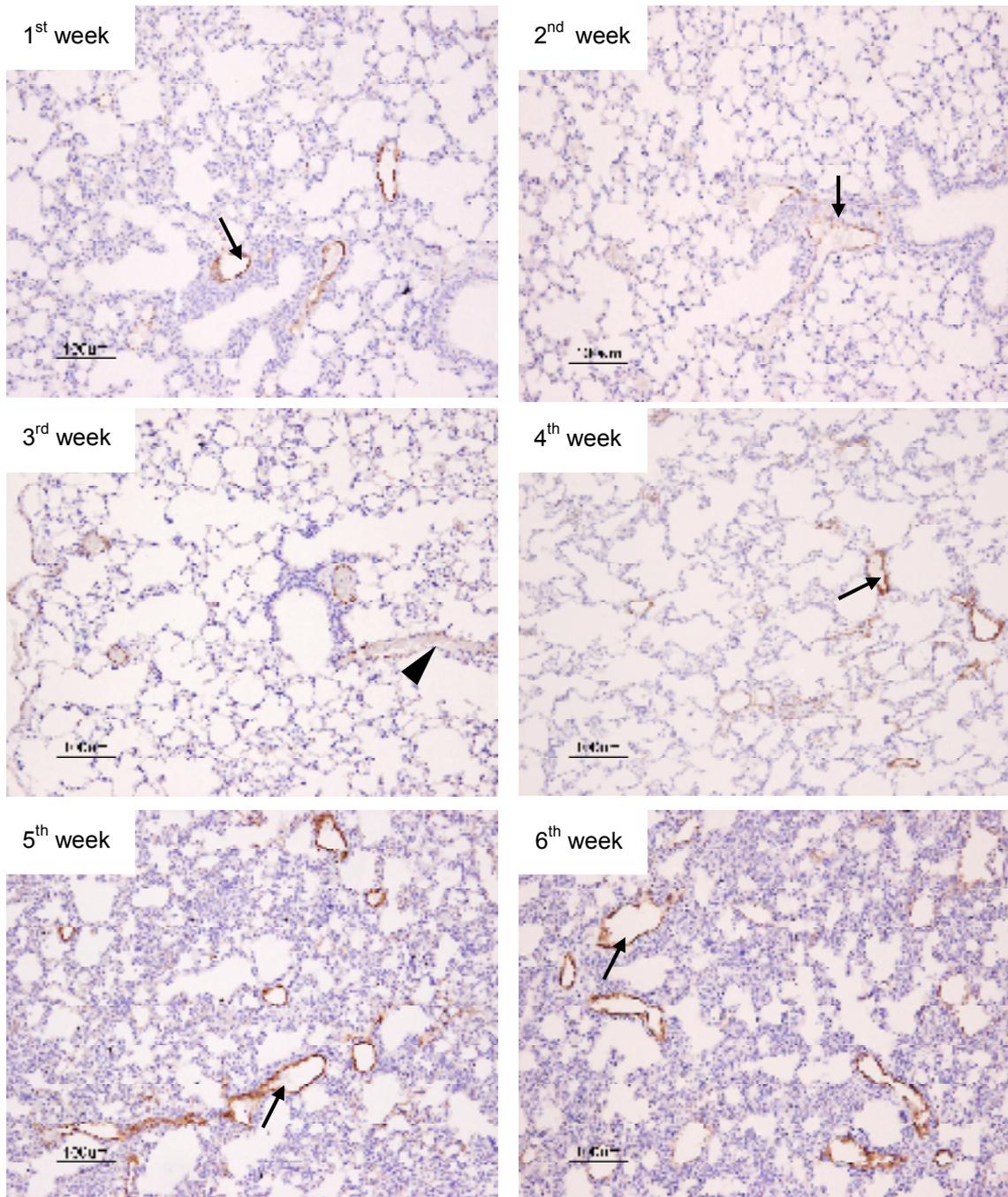
Figure 2.4.11. LYVE1-positive vessels of the lung parenchyma in CHMp-5b-xenografted mice at 1 to 6 weeks after transplantation. Some microvessels were positively stained by LYVE1 on the lung parenchyma of CHMp-5b-xenografted mice (arrowhead). LYVE1-positive vessels (arrows) within the lung parenchyma seemed to increase according to the time after transplantation. (Magnification ×100)

Lung of CHMp-13a-xenografted mice
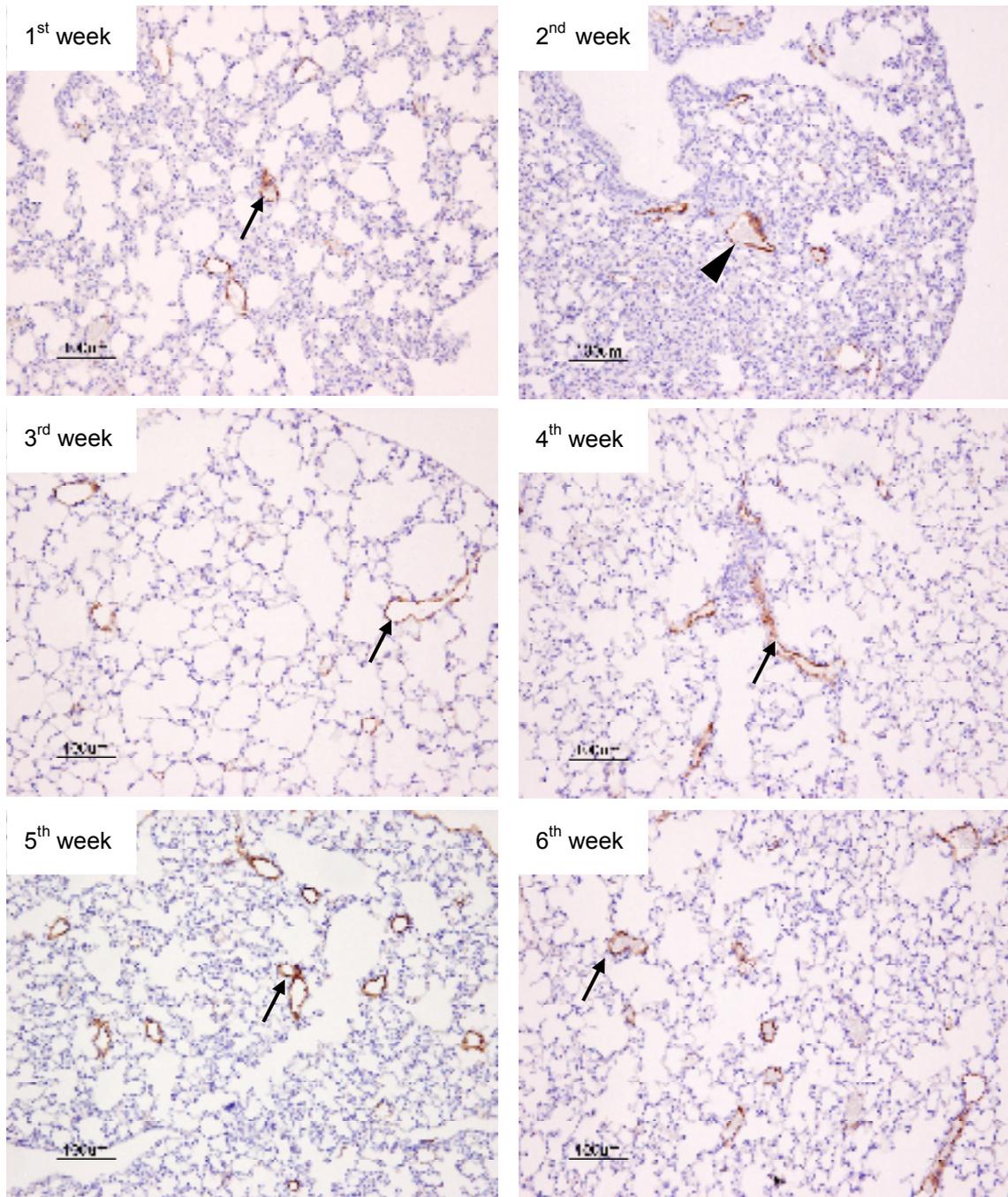
Figure 2.4.12. LYVE1-positive vessels (arrows) of the lung parenchyma in CHMp-13a-xenografted mice at 1 to 6 weeks after transplantation. Some microvessels were positively stained by LYVE1 on the lung parenchyma of CHMp-13a-xenografted mice (arrowhead).

(Magnification ×100)

LYVE1-positive vessels on the lung parenchyma
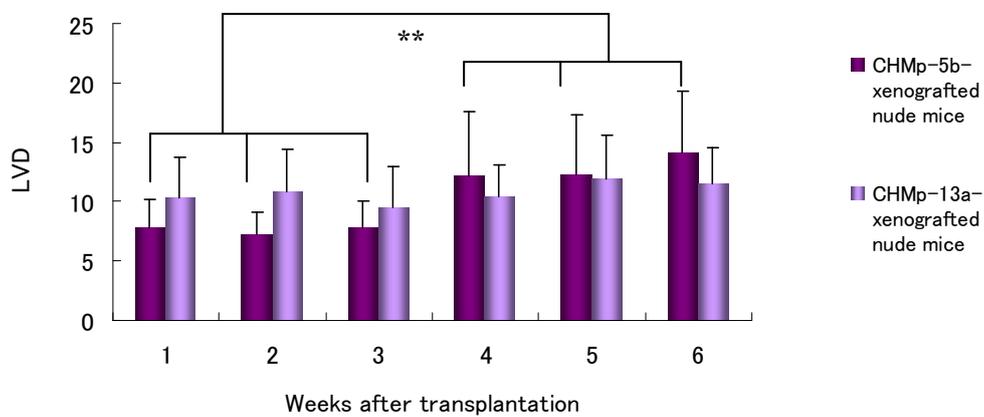
Figure 2.4.13. LYVE1-positive vessels of the lung parenchyma in CHMp-5b- and CHMp-13a-xenografted mice at 1 to 6 weeks after transplantation.

**: Significant difference between the values of 1 to 3 weeks and those of 4 to 6 weeks after transplantation in CHMp-5b-xenografted mice $(P < 0.01)$

Discussion

There are two distinct major pathways to the evolution of angiogenic and lymphangiogenic metastasis: the former is consistently related to the increased expression of VEGF-A, and the latter is usually related to the increased expression of VEGF-C (Shibuya, 2008). The objective of this study was to evaluate the role of angiogenesis and lymphagiogenesis by VEGF-A and VEGF-C in xenografted mice with CMGT cell lines.

In this *in vitro* study, the two cloned cell lines showed expression of both VEGF-A and VEGF-C, which implies that these cell lines may have similar characteristics in angiogenesis and lymphangiogenesis.

In the course of angiogenesis and lymphangiogenesis, several steps are thought to be involved and many factors are encompassed intricately in each step (Lohela *et al*, 2009; Gordon *et al*, 2010). For the molecular analysis to understand the angiogenic and lymphangiogenic metastasis mechanism, the *in vivo* experiment using animal models are quite valuable to obtain the similar situation occurred in the tumor patients (Aamdal *et al*, 1984; Price *et al*, 1984; Fidler, 1986; Fu *et al*, 1993; Nagamachi *et al*, 1998). In this study, I used an experimental animal model to evaluate the lymph node and lung metastasis for understanding of angiogenesis and lymphangiogenesis.

The two cell lines produced different types of carcinomas in xenografted nude mice. The growth potential of the primary tumor in nude mice was quite different. CHMp-5b showed rapid growth with metastasis, whereas CHMp-13a showed slower growth with less metastatic potential. Interestingly, only CHMp-5b cells metastasized to the lymph node and lung in the earlier phase of transplantation. Therefore the CHMp-5b cell line was thought to have more malignant characteristics than CHMp-13a cell line.

Ki-67 is expressed in cycling cells except for G_0 phase and disappears rapidly after mitosis (Endl and Gerdes, 2000). Expression of Ki-67, from which PI is calculated, in tumor tissues has a positive correlation with tumor size, metastasis and prognosis in human even canine (Zuccari *et al*, 2004; Kroger *et al*, 2006). In this study, PI of tumor tissues of CHMp-5b-xenografted mice was significantly higher than those of CHMp-13a-xenografted mice. These results also support that CHMp-5b has more malignant character. PI was significantly lower in the lung metastatic lesions than primary and lymph node metastatic lesions in CHMp-5b-xenografted mice, suggesting that CMGT proliferation potential in the lymph node seems to be active as in the primary lesion but that the potential may be decreased in the lung metastatic lesion.

VEGF-A mRNA expression on primary tissues of CHMp-13a-xenografted mice was significantly higher than those of CHMp-5b-xenografted mice after 3 weeks of transplantation. VEGF-C mRNA expression showed the similar pattern in both cell line groups, though the expression levels were much lower than VEGF-A mRNA. However, their protein expression levels on Western blot analysis were various in both tissues of CHMp-5b- and CHMp-13a-xenografted mice. This inconsistency on the expression of VEGF-A and VEGF-C between realtime PCR and immunoblotting was not clear. This was partly caused by inadequate tissue sampling from very small primary lesions, though I collected the several pieces from different areas. However, the mRNA expression level of VEGF-A was higher than VEGF-C in two CMGT cloned cell lines and those xenografted models. This may suggest that primary tissues with these cell lines have stronger angiogenetic than lymphangiogenetic potential.

On immunohistochemistry, the scores of VEGF-A and VEGF-C expressions increased according to the period after transplantation in both tissues of two cell line groups. The difference in VEGF-A and VEGF-C expression in tissues of CHMp-5b- and CHMp-13a-xenografted mice was not clear, though the clinical behaviors in nude mice was

considerably different between the two cell lines. However, PI values were strongly correlated with the expression of VEGF-A and VEGF-C in these tissues, suggesting the important role of VEGF-A and -C in the progression of CMGT. In this study, VEGF-A and VEGF-C staining on the lymph node and lung metastatic tissues in nude mice transplanted with both cell lines was significantly lower when compared to the expression in the primary mass. This may suggest that VEGF-A and VEGF-C in primary lesions significantly relate to the proliferation potential and malignancy through angiogenesis and lymphangiogenesis.

For the imaging of angiogenesis and lymphangiogenesis, no perfect markers have been found which work reliably in all species, tissues, vascular beds, and in all physiological and pathologic conditions (Baluk and McDonald, 2008). The heterogeneity of expression of markers in both blood and lymphatic vessels reflects underlying differences in the phenotype of endothelial cells (Groger *et al*, 2004). There have been several reports demonstrating the correlation between MVD and tumor size, grade and stage using CD31 (Choi *et al*, 2005; Saban *et al*, 2007). Bono et al. detected lymphatic vessels using LYVE1 and obtained the result that a high peritumoral lymph vessel density was associated with a poor outcome in ductal breast cancer (Bono *et al*, 2004). In this study, CD31 was stained on blood vessels clearly but was less stained on lymphatic endothelial cells, as in previous reports (Albelda *et al*, 1991; Baluk *et al*, 2007). LYVE1 was strongly expressed on the entire luminal and surface of lymphatic endothelial cells. However, while LYVE1 appears to be expressed preferentially in the lymphatic endothelium, LYVE1 was also expressed in other cell types such as some blood vessels, liver sinusoids, pulmonary capillaries, and pulmonary arteries and their branches in the lung.

iMVD values were significantly higher than pMVD values in tissues of CHMp-5b -xenografted mice at 2 and 3 weeks of transplantation. In addition, iMVD in tissues of

CHMp-5b-xenografted mice was significantly higher than those of CHMp-13a-xenografted mice. There was no significant difference between iMVD and pMVD in tissues of CHMp-13a-xenografted mice. Higher iMVD in tissues of CHMp-5b-xenografted mice was significantly correlated with expression VEGF-A. Furthermore, iMVD in both tissues of CHMp-5b- and CHMp-13a-xenografted mice had a significant correlation with PI. These results support the findings by Vartanian and Weidner, who provided evidence that the correlation between iMVD and tumor cell proliferation was consistently observed (Vartanian and Weidner, 1994), and suggested that tumor cell proliferation and intratumoral microvessel density were regulated by VEGF-A. Similar findings were also reported by de Queiroz et al. who suggested that VEGF-A participated in the intratumoral angiogenesis of soft-tissue sarcoma in dogs(de Queiroz *et al*, 2010). Canine malignant mammary tumors with metastasis to regional lymph nodes had higher microvessel counts than those without metastasis (Graham and Myers, 1999). Millanta et al. evaluated VEGF-A with VEGFR2 in CMGT and reported that iMVD could be an independent prognostic factor for canine patients, but that overall survival was not related to VEGF-A expression (Millanta *et al*, 2006).

Both pMVD and iMVD counts were stable during the 6-week experimental period. As Folkman reported, tumor cell proliferation together with angiogenesis is necessary and sufficient to generate a detectable tumor mass. Tumor cell proliferation alone, in the absence of angiogenesis, can give rise to dormant, microscopic tumors of 1 mm^3 or less, but these *in situ* cancers are harmless to the host (Folkman, 2006).

Lymphangiogenesis evaluated as LVD is associated with an increased incidence of lymph node metastasis, and it is possible that this step is essential to the metastatic process (Nathanson, 2003). In this study, pLVD showed increases in count by the time after transplantation. There is still some degree of controversy regarding the relevance of either peritumoral and/or

intratumoral lymphatic vessel in solid tumors (Rouzaut *et al*, 2007). On one hand, some findings suggest the existence of intratumoral lymphatics and their association with poor survival (Ji, 2006). On the other hand, increasing experimental evidence shows the functional lymphatics located in the tumor margin along are sufficient for lymphatic metastasis (Padera *et al*, 2002). Nevertheless, in regard to the relationship between lymphangiogenesis in tumor tissues and LVD, the majority of previous studies on cancer LVD indicated that peritumoral lymphatic vessels were predominantly responsible for promoting lymphatic cancer metastasis. Peritumoral lymphatic vessels were frequently observed with active proliferation (Padera *et al*, 2002; Bjorndahl *et al*, 2005). Lymphangiogenesis of the peritumoral area might be the most significant predictor of lymph node metastasis in CMGT xenografted mice.

VEGF-C induced formation of new lymph vessel dilatation of the dermal lymphatics when overexpressed in transgenic mice (Jeltsch *et al*, 1997). VEGF-C was known to induce the peritumoral and intratumoral lymphangiogenesis and lymphatic spread (Mattila *et al*, 2002), and increased lymphatic vessel density with lymph node metastasis in xenografted breast cancer (Skobe *et al*, 2001). In this study, correlation of VEGF-C expression was detected with lymphangiogenesis in CHMp-13a-xenografted mice, not in CHMp-5b-xenografted mice. Further elucidation of the mechanism of lymph node metastasis by lymphangiogenesis with VEGF-C is necessary in CMGT xenografted mice.

Lymph node metastasis was observed from 3 weeks of transplantation in CHMp-5b-xenografted mice and at 6 weeks of transplantation in CHMp-13a-xenografted mice. At these time points, pLVD values increased to 2.0, which might be a necessary density for lymphatic metastasis. This finding permits us to presume that a certain level of peritumoral lymphangiogenesis may be a necessary control for the lymph node metastasis

LVD of the lymph node cortex tended to increase according to the time after

transplantation in CHMp-5b- and CHMp-13a-xenografted mice. This result concurred with several previous reports. The study by Hirakawa et al. reported that overexpressed VEGF-A of skin carcinogenesis using a transgenic mice induced lymphangiogenesis within the draining lymph nodes, even before the tumor had metastasized to these tissues; this may facilitate future metastatic tumor spread within the lymphatic system (Hirakawa *et al*, 2005). Additionally, in clinical cases, lymphangiogenesis has been detected in lymph node metastases in breast cancer (Van den Eynden *et al*, 2006). The presence of tumor cells can induce lymphangiogenesis in the lymph nodes and potentially other changes in the morphology and function of various vessel types in the lymph node, providing a site for rearrangement of the vessel structures and abnormal connections between the vascular and lymphatic networks (Achen and Stacker, 2008)

Interestingly, LYVE1-positive vessels of the lung parenchyma seemed to increase according to the time after transplantation in CHMp-5b-xenografted mice, along with the primary tumor progress. Moreover, LYVE1-positive vessels of the lung showed significantly higher at 4 to 6 weeks than 1 to 3 weeks after transplantation, even before the arrival of tumor cells. In my study, lymphangiogenesis in the lung was correlated with VEGF-A and VEGF-C expression according to the tumor growth. To the best of our knowledge, this is the first report demonstrating lymphangiogenesis in the lung metastasis in an animal tumor model. These results suggest that lymphangiogenesis in the lung may facilitate metastasis, even before the arrival of tumor cells, along with lymphangiogenesis in the lymph node, simultaneously.

I found that VEGF-A had an effectual factor for malignancy and a correlation with pMVD and iMVD in a CHMp-5b xenograft model. High iMVD is important to growth of the primary tumor and expanding footprint to invasion for metastasis. Moreover, VEGF-A expression increased lymphangiogenesis, especially peritumor lesion in the xenograft model. The exact mechanism has not yet been clarified, but it is conceivable that VEGF-A may

promote lymph node and distant metastasis of cancer cells through induction of angiogenesis and lymphangiogeneis simultaneously. In concordance with the studies of Chapter 1, the results of this study reveal that up regulated VEGF-A which is accompanied with angiogenesis in canine mammary gland tumors may be prognostic for the overall survival with lymph node and lung metastasis.

Overall, these data considering the correlation with VEGF-A and VEGF-C showed that it may potentially VEGF-A is more powerful than VEGF-C on the point of both angiogenesis of intratumor and lymphangiogenesis of peritumor, but dependent on VEGF receptors quantity and affinity. However, on this study, there is a limitation that we did not detect the receptors of VEGFs which may play a role for proliferation and metastasis of CMGT, also be a matter of controversy.

Conclusion

Conclusion

The purpose of this study was to clarify the role of VEGF-A and VEGF-C for angiogenesis and lymphangiogenesis in CMGT. Therefore, I conducted two parts of experiments using canine MGT patient tissues and a nude mice xenograft model.

In Chapter 1, VEGF-A and VEGF-C expressions on the 49 spontaneous CMGT primary lesions of 25 dogs were assessed on immunohistochemistry and compared their expression with clinical features, histological types and prognostic outcome. In addition, the correlation between their expressions and PI and the number of macrophages in tumor tissues was evaluated. Adenocarcinoma tissues showed significantly higher expression of VEGF-A as compared to normal mammary gland tissues and adenoma tissues. PI and the number of macrophages, one of the important microenvironmental cells in tumor tissues and involvement of VEGF-A delivery in CMGT tissues, were distinctly correlated with the expression of VEGF-A. In addition, high expression of VEGF-A was significantly correlated with shorter patient survival. These results may suggest that VEGF-A can be a good prognostic factor in CMGT. On the other hand, expression of VEGF-C seemed no correlation with malignancy and prognosis of CMGT patients.

These correlations between VEGF-A expression, PI and macrophage number may relate to angiogenesis and/or lympahngiogenesis in CMGT tissues. However, I could not find the adequate marker for lymphatic endothelial cells of canine tissues. There have been no reports on the marker for lymphatic endothelial cells of canine tissues.

Therefore in Chapter 2, I evaluated the expression of VEGF-A and VEGF-C in mice xenografted with CMGT cell lines and microvessel density and lymphatic vessel density using antibodies for these endothelial cells of mice.

In Chapter 2, two CMGT cloned cell lines, CHMp-5b and CHMp-13a, which were previously established and cloned from a malignant mammary gland tumor patient, were used to clarify their characteristics about VEGF-A and VEGF-C. I measured the mRNA and protein levels of VEGF-A and VEGF-C in both CMGT cell lines. Both cell lines showed VEGF-A and VEGF-C expression, though the mRNA expression level of VEGF-A was significantly higher than that of VEGF-C in both cell lines. These results may indicate that these CHMp-5b and CHMp-13a had a higher angiogenic than lymphangiogenic potential.

In the orthotopic xenograft nude mouse model using these cell lines, tumor development after transplantation was significantly different between the cell lines. CHMp-5b developed far faster tumor growth and more lymph node and lung metastasis than CHMp-13a. Using the primary tumor tissues developed in nude mice xenografted these two cell lines, mRNA and protein expression levels were analyzed. In addition, quantification of angiogenesis and lymphangiogenesis were analyzed using the markers of CD31 for blood vessel endothelial cells and LVVE1 for lymphatic endothelial cells at peritumor and intratumor sites of primary lesions in xenografted mice. Then, their values were compared with VEGF-A and VEGF-C expressions as well as PI.

The gene and protein expression of VEGF-A and VEGF-C were various in the primary and metastatic tissues in xenografted mice. VEGF-A expression on the primary tumor in mice seemed to increase according to the time after transplantation and was significantly correlated with peritumor and intratumor angiogenesis, peritumor lymphangiogenesis and PI. Similarly, VEGF-C expression of the primary tumor tissues also seemed to increase according to the time after transplantation in xenografted nude mice. However, VEGF-C expression of the primary tumor tissues was significantly correlated with peritumor angiogenesis and lymphangiogenesis and PI, only in CHMp-13a-xenografted mice. VEGF-A and VEGF-C in primary lesions may

significantly related to the proliferation potential and malignancy, when compared to metastatic lesions.

Interestingly, I found a certain level of peritumoral lymphangiogenesis in primary tumor tissues of a nude mouse model. In addition, LVD within the lymph node cortex increased according to the time after transplantation in CHMp-5b- and CHMp-13a-xenografted mice. Moreover, LYVE1-positive vessels of the lung parenchyma surrounding the tumor lesion also increased according to the time after transplantation. These results may suggest that lymphangiogenesis of peritumoral tissues, lymph nodes and the lung may facilitate the growth of metastatic lesions. OrLYVE1-positive cells may increase before tumor cells have reached to the lung. It is still unclear how the LYVE1-positive cells of the lung play the role in tumor growth and metastasis, and clarification of their role should be needed.

Both *in vitro* and *in vivo* studies suggested that VEGF-A of mammary cancer may be associated with angiogenesis and lymphangiogenesis, and the clinical study using spontaneous CMGT tissues suggested that VEGF-A can be a good negative prognostic factor in CMGT. However, the role of VEGF-C on lymphangiogenesis was not clear in both spontaneous patients and xenograft mouse models.

In human medicine, expressions of both VEGF-A and VEGF-C may be an important factor to identify cancer patients with higher risk of recurrence. On the other hand, according to this study, relationships between VEGF-A/VEGF-C and angiogenesis/lymphangiogenesis were not necessarily clear in canine mammary gland tumor. In addition, the clinical significanance of pMVD, iMVD, pLVD and iLVD and the relationship with these expressions remain uncertain in CMGT. Studies on other factors and their correlations with VEGF-A and-C expression, such as bFGF which preferentially induces lymphangiogenesis over angiogenesis (Chang *et al*, 2002) or recepter tyrosine kinases (RTKs) and those ligand (London, 2009), that contribute to

angiogenic and lymphangiogenic growth, might increase our knowledge about the mechanisms of increased intratumor angiogenesis and peritumor lymphangiogenesis. Further studies on the mechanism of angiogenic and lymphangiogenic metastasis should be necessary to provide us with better understanding of metastasis mechanism.

Based on our identification of VEGF-A and VEGF-C on the primary tumor as a potent tumor angiogenesis and lymphangiogenesis factor, it will be the great interest to see whether the treatment with neutralizing monoclonal anti-VEGF-A and VEGF-C antibodies or their receptor inhibitors may approve the effectiveness for patients with CMGT, or may inhibit further metastatic spread. As shown in Figure 3, molecules of the PLCγ (phospholipaseCγ)/PKC (protein kinaseC)/MAPK (mitogen-activated protein kinase) pathway, known as a down stream of phosphorylated VEGFR2, and those of phosphatidyl inositol 3` kinase (PI3K)/Akt as well as the extracellular-signal-regulated kinases (ERKs) pathway, known as a signal transduction downstream of VEGFR3, may be correlated to further studies on the molecules to evaluate their role in the angiogenesis and lymphangiogenesis and in the prognosis of CMGT should be performed in the future (Nagy *et al*, 2007; Shibuya, 2009; Bahram and Claesson-Welsh, 2010).
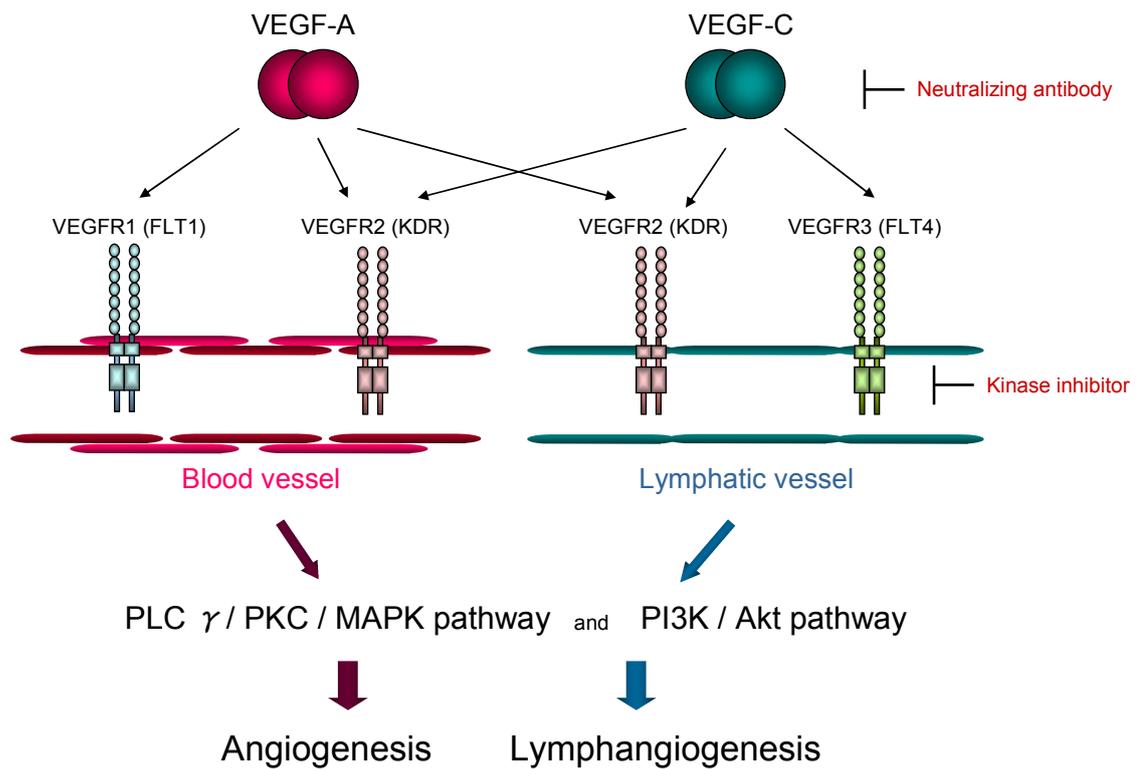
Figure 3. Suggested stream model of the future study associated with the thesis that overlapping binding patterns of VEGF-A and VEGF-C functions. VEGF-A regulates angiogenesis via binding and activation of VEGFR-1 and phosphorylated VEGFR-2 on endothelial cell membranes. In contrast, VEGF-C for lymphangiogenesis activates phosphorylation of VEGFR-2 and VEGFR-3 on the lymphatic endothelial cell membranes. Signaling by VEGFRs involves the PLCγ/PKC/MAPK and PI3K/Akt pathways, leading to downstream for angiogenesis and lymphangiogenesis.

Acknowledgements

References

Aamdal S, Fodstad O, Pihl A (1984) Human tumor xenografts transplanted under the renal capsule of conventional mice. Growth rates and host immune response. *Int J Cancer* 34(5): 725-730.

Achen MG, Mann GB, Stacker SA (2006) Targeting lymphangiogenesis to prevent tumour metastasis. *Br J Cancer* 94(10): 1355-1360.

Achen MG, Stacker SA (2008) Molecular control of lymphatic metastasis. *Ann N Y Acad Sci* 1131: 225-234.

Albelda SM, Muller WA, Buck CA, Newman PJ (1991) Molecular and cellular properties of PECAM-1 (endoCAM/CD31): a novel vascular cell-cell adhesion molecule. *J Cell Biol* 114(5): 1059-1068.

Alitalo K, Tammela T, Petrova TV (2005) Lymphangiogenesis in development and human disease. *Nature* 438(7070): 946-953.

Bahram F, Claesson-Welsh L (2010) VEGF-mediated signal transduction in lymphatic endothelial cells. *Pathophysiology* 17(4): 253-261.

Baldwin ME, Roufail S, Halford MM, Alitalo K, Stacker SA et al. (2001) Multiple forms of mouse vascular endothelial growth factor-D are generated by RNA splicing and proteolysis. *J Biol Chem* 276(47): 44307-44314.

Baluk P, Fuxe J, Hashizume H, Romano T, Lashnits E et al. (2007) Functionally specialized junctions between endothelial cells of lymphatic vessels. *J Exp Med* 204(10): 2349-2362.

Baluk P, McDonald DM (2008) Markers for microscopic imaging of lymphangiogenesis and angiogenesis. *Ann N Y Acad Sci* 1131: 1-12.

Baluk P, Tammela T, Ator E, Lyubynska N, Achen MG et al. (2005) Pathogenesis of persistent lymphatic vessel hyperplasia in chronic airway inflammation. *J Clin Invest*

115(2): 247-257.

Benjamin SA, Lee AC, Saunders WJ (1999) Classification and behavior of canine mammary epithelial neoplasms based on life-span observations in beagles. *Vet Pathol* 36(5): 423-436.

Bergers G, Hanahan D (2008) Modes of resistance to anti-angiogenic therapy. *Nat Rev Cancer* 8(8): 592-603.

Bjorndahl MA, Cao R, Burton JB, Brakenhielm E, Religa P et al. (2005) Vascular endothelial growth factor-a promotes peritumoral lymphangiogenesis and lymphatic metastasis. *Cancer Res* 65(20): 9261-9268.

Bluff JE, Menakuru SR, Cross SS, Higham SE, Balasubramanian SP et al. (2009) Angiogenesis is associated with the onset of hyperplasia in human ductal breast disease. *Br J Cancer* 101(4): 666-672.

Bono P, Wasenius VM, Heikkila P, Lundin J, Jackson DG et al. (2004) High LYVE-1-positive lymphatic vessel numbers are associated with poor outcome in breast cancer. *Clin Cancer Res* 10(21): 7144-7149.

Carmeliet P, Ferreira V, Breier G, Pollefeyt S, Kieckens L et al. (1996) Abnormal blood vessel development and lethality in embryos lacking a single VEGF allele. *Nature* 380(6573): 435-439.

Chang L, Kaipainen A, Folkman J (2002) Lymphangiogenesis new mechanisms. *Ann N Y Acad Sci* 979: 111-119.

Chen L, Endler A, Shibasaki F (2009) Hypoxia and angiogenesis: regulation of hypoxia-inducible factors via novel binding factors. *Exp Mol Med* 41(12): 849-857.

Choi WW, Lewis MM, Lawson D, Yin-Goen Q, Birdsong GG et al. (2005) Angiogenic and lymphangiogenic microvessel density in breast carcinoma: correlation with clinicopathologic parameters and VEGF-family gene expression. *Mod Pathol* 18(1): 143-152.

Cuevas I, Boudreau N (2009) Managing tumor angiogenesis: lessons

from VEGF-resistant tumors and wounds. *Adv Cancer Res* 103: 25-42.

Cursiefen C, Chen L, Borges LP, Jackson D, Cao J et al. (2004) VEGF-A stimulates lymphangiogenesis and hemangiogenesis in inflammatory neovascularization via macrophage recruitment. *J Clin Invest* 113(7): 1040-1050.

de Queiroz GF, Dagli ML, Fukumasu H, Zavala AA, Matera JM (2010) Vascular endothelial growth factor expression and microvascular density in soft tissue sarcomas in dogs. *J Vet Diagn Invest* 22(1): 105-108.

Dore M, Lanthier I, Sirois J (2003) Cyclooxygenase-2 expression in canine mammary tumors. *Vet Pathol* 40(2): 207-212.

Dumont DJ, Jussila L, Taipale J, Lymboussaki A, Mustonen T et al. (1998) Cardiovascular failure in mouse embryos deficient in VEGF receptor-3. *Science* 282(5390): 946-949.

Dvorak HF, Harvey VS, Estrella P, Brown LF, McDonagh J et al. (1987) Fibrin containing gels induce angiogenesis. Implications for tumor stroma generation and wound healing. *Lab Invest* 57(6): 673-686.

Egeblad M, Werb Z (2002) New functions for the matrix metalloproteinases in cancer progression. *Nat Rev Cancer* 2(3): 161-174.

Endl E, Gerdes J (2000) The Ki-67 protein: fascinating forms and an unknown function. *Exp Cell Res* 257(2): 231-237.

Ferrara N (1996) Vascular endothelial growth factor. *Eur J Cancer* 32A(14): 2413-2422.

Ferrara N (2002) VEGF and the quest for tumour angiogenesis factors. *Nat Rev Cancer* 2(10): 795-803.

Ferrara N (2004) Vascular endothelial growth factor: basic science and clinical progress. *Endocr Rev* 25(4): 581-611.

Ferrara N, Davis-Smyth T (1997) The biology of vascular endothelial growth factor. *Endocr Rev* 18(1): 4-25.

Fidler IJ (1986) Rationale and methods for the use of nude mice to study the biology and therapy of human cancer metastasis. *Cancer Metastasis Rev* 5(1): 29-49.

Folkman J (1971) Tumor angiogenesis: therapeutic implications. *N Engl J Med* 285(21): 1182-1186.

Folkman J (1995) Angiogenesis in cancer, vascular, rheumatoid and other disease. *Nat Med* 1(1): 27-31.

Folkman J (2006) Angiogenesis. *Annu Rev Med* 57: 1-18.

Fox SB, Harris AL (2004) Histological quantitation of tumour angiogenesis. *APMIS* 112(7-8): 413-430.

Fu X, Le P, Hoffman RM (1993) A metastatic orthotopic-transplant nude-mouse model of human patient breast cancer. *Anticancer Res* 13(4): 901-904.

Furudoi A, Tanaka S, Haruma K, Kitadai Y, Yoshihara M et al. (2002) Clinical significance of vascular endothelial growth factor C expression and angiogenesis at the deepest invasive site of advanced colorectal carcinoma. *Oncology* 62(2): 157-166.

Gannon G, Mandriota SJ, Cui L, Baetens D, Pepper MS et al. (2002) Overexpression of vascular endothelial growth factor-A165 enhances tumor angiogenesis but not metastasis during beta-cell carcinogenesis. *Cancer Res* 62(2): 603-608.

Goldfarb SB, Traina TA, Dickler MN (2010) Bevacizumab for advanced breast cancer. *Womens Health (Lond Engl)* 6(1): 17-25.

Gordon MS, Mendelson DS, Kato G (2010) Tumor angiogenesis and novel antiangiogenic strategies. *Int J Cancer* 126(8): 1777-1787.

Graham JC, Myers RK (1999) The prognostic significance of angiogenesis in canine mammary tumors. *J Vet Intern Med* 13(5): 416-418.

Groger M, Loewe R, Holnthoner W, Embacher R, Pillinger M et al. (2004) IL-3 induces

expression of lymphatic markers Prox-1 and podoplanin in human endothelial cells. *J Immunol* 173(12): 7161-7169.

Gu Y, Qi X, Guo S (2008) Lymphangiogenesis induced by VEGF-C and VEGF-D promotes metastasis and a poor outcome in breast carcinoma: a retrospective study of 61 cases. *Clin Exp Metastasis* 25(7): 717-725.

Harrell MI, Iritani BM, Ruddell A (2007) Tumor-induced sentinel lymph node lymphangiogenesis and increased lymph flow precede melanoma metastasis. *Am J Pathol* 170(2): 774-786.

Hattori K, Miyachi S, Kobayashi N, Kojima T, Negoro M et al. (2005) Contralateral meningeal artery supply of paramedian meningiomas. *Surg Neurol* 64(3): 242-248.

Heckman CA, Holopainen T, Wirzenius M, Keskitalo S, Jeltsch M et al. (2008) The tyrosine kinase inhibitor cediranib blocks ligand-induced vascular endothelial growth factor receptor-3 activity and lymphangiogenesis. *Cancer Res* 68(12): 4754-4762.

Hirakawa S, Kodama S, Kunstfeld R, Kajiya K, Brown LF et al. (2005) VEGF-A induces tumor and sentinel lymph node lymphangiogenesis and promotes lymphatic metastasis. *J Exp Med* 201(7): 1089-1099.

Hiratsuka S, Nakao K, Nakamura K, Katsuki M, Maru Y et al. (2005) Membrane fixation of vascular endothelial growth factor receptor 1 ligand-binding domain is important for vasculogenesis and angiogenesis in mice. *Mol Cell Biol* 25(1): 346-354.

Hurwitz H, Fehrenbacher L, Novotny W, Cartwright T, Hainsworth J et al. (2004) Bevacizumab plus irinotecan, fluorouracil, and leucovorin for metastatic colorectal cancer. *N Engl J Med* 350(23): 2335-2342.

Ishikawa K, Sakai H, Hosoi M, Yanai T, Masegi T (2006) Evaluation of cell proliferation in canine tumors by the bromodeoxyuridine labeling method, immunostaining of Ki-67 antigen and proliferating cell nuclear antigen. *Journal of Toxicologic Pathology* 19 (3): 123-127.

Jain RK (2005) Normalization of tumor vasculature: an emerging concept in antiangiogenic therapy. *Science* 307(5706): 58-62.

Jeltsch M, Kaipainen A, Joukov V, Meng X, Lakso M et al. (1997) Hyperplasia of lymphatic vessels in VEGF-C transgenic mice. *Science* 276(5317): 1423-1425.

Ji RC (2006) Lymphatic endothelial cells, tumor lymphangiogenesis and metastasis: New insights into intratumoral and peritumoral lymphatics. *Cancer Metastasis Rev* 25(4): 677-694.

Jinnin M, Medici D, Park L, Limaye N, Liu Y et al. (2008) Suppressed NFAT-dependent VEGFR1 expression and constitutive VEGFR2 signaling in infantile hemangioma. *Nat Med* 14(11): 1236-1246.

Joukov V, Sorsa T, Kumar V, Jeltsch M, Claesson-Welsh L et al. (1997) Proteolytic processing regulates receptor specificity and activity of VEGF-C. *EMBO J* 16(13): 3898-3911.

Kaipainen A, Korhonen J, Mustonen T, van Hinsbergh VW, Fang GH et al. (1995) Expression of the fms-like tyrosine kinase 4 gene becomes restricted to lymphatic endothelium during development. *Proc Natl Acad Sci U S A* 92(8): 3566-3570.

Kamath A, Helie M, Bifulco CB, Li WW, Concato J et al. (2009) Lack of immunohistochemical detection of VEGF in prostate carcinoma. *Appl Immunohistochem Mol Morphol* 17(3): 227-232.

Karamysheva AF (2008) Mechanisms of angiogenesis. *Biochemistry (Moscow)* 73(7): 751-762.

Karkkainen MJ, Haiko P, Sainio K, Partanen J, Taipale J et al. (2004) Vascular endothelial growth factor C is required for sprouting of the first lymphatic vessels from embryonic veins. *Nat Immunol* 5(1): 74-80.

Kato Y, Asano K, Mogi T, Kutara K, Teshima K et al. (2007) Clinical significance of circulating vascular endothelial growth factor in dogs with mammary gland tumors. *J Vet Med Sci* 69(1): 77-80.

Kerjaschki D (2005) The crucial role of macrophages in lymphangiogenesis. *J Clin Invest* 115(9): 2316-2319.

Kinoshita J, Kitamura K, Kabashima A, Saeki H, Tanaka S et al. (2001) Clinical significance of vascular endothelial growth factor-C (VEGF-C) in breast cancer. *Breast Cancer Res Treat* 66(2): 159-164.

Kondo K, Kaneko T, Baba M, Konno H (2007) VEGF-C and VEGF-A synergistically enhance lymph node metastasis of gastric cancer. *Biol Pharm Bull* 30(4): 633-637.

Kroger N, Milde-Langosch K, Riethdorf S, Schmoor C, Schumacher M et al. (2006) Prognostic and predictive effects of immunohistochemical factors in high-risk primary breast cancer patients. *Clin Cancer Res* 12(1): 159-168.

Leek RD, Hunt NC, Landers RJ, Lewis CE, Royds JA et al. (2000) Macrophage infiltration is associated with VEGF and EGFR expression in breast cancer. *J Pathol* 190(4): 430-436.

Lohela M, Bry M, Tammela T, Alitalo K (2009) VEGFs and receptors involved in angiogenesis versus lymphangiogenesis. *Curr Opin Cell Biol* 21(2): 154-165.

London CA (2009) Tyrosine kinase inhibitors in veterinary medicine. *Top Companion Anim Med* 24(3): 106-112.

London CA, Malpas PB, Wood-Follis SL, Boucher JF, Rusk AW et al. (2009) Multi-center, placebo-controlled, double-blind, randomized study of oral toceranib phosphate (SU11654), a receptor tyrosine kinase inhibitor, for the treatment of dogs with recurrent (either local or distant) mast cell tumor following surgical excision. *Clin Cancer Res* 15(11): 3856-3865.

Matsui J, Funahashi Y, Uenaka T, Watanabe T, Tsuruoka A et al. (2008) Multi-kinase inhibitor E7080 suppresses lymph node and lung metastases of human mammary breast tumor MDA-MB-231 via inhibition of vascular endothelial growth factor-receptor (VEGF-R) 2 and VEGF-R3 kinase. *Clin Cancer Res* 14(17): 5459-5465.

Mattila MM, Ruohola JK, Karpanen T, Jackson DG, Alitalo K et al. (2002) VEGF-C induced lymphangiogenesis is associated with lymph node metastasis in orthotopic MCF-7 tumors. *Int J Cancer* 98(6): 946-951.

Millanta F, Caneschi V, Ressel L, Citi S, Poli A (2010) Expression of vascular endothelial

growth factor in canine inflammatory and non-inflammatory mammary carcinoma. *J Comp Pathol* 142(1): 36-42.

Millanta F, Silvestri G, Vaselli C, Citi S, Pisani G et al. (2006) The role of vascular endothelial growth factor and its receptor Flk-1/KDR in promoting tumour angiogenesis in feline and canine mammary carcinomas: a preliminary study of autocrine and paracrine loops. *Res Vet Sci* 81(3): 350-357.

Misdorp W, Else RW, Hellmen E, Lipscomb TP (1999). Histological Classification of Mammary Tumors of the Dog and the Cat. 2nd series Ⅶ ed. Washinton, D.C., World Health Organization.

Mohammed RA, Ellis IO, Elsheikh S, Paish EC, Martin SG (2009) Lymphatic and angiogenic characteristics in breast cancer: morphometric analysis and prognostic implications. *Breast Cancer Res Treat* 113(2): 261-273.

Mohammed RA, Green A, El-Shikh S, Paish EC, Ellis IO et al. (2007) Prognostic significance of vascular endothelial cell growth factors -A, -C and -D in breast cancer and their relationship with angio- and lymphangiogenesis. *Br J Cancer* 96(7): 1092-1100.

Mylona E, Alexandrou P, Mpakali A, Giannopoulou I, Liapis G et al. (2007) Clinicopathological and prognostic significance of vascular endothelial growth factors (VEGF)-C and -D and VEGF receptor 3 in invasive breast carcinoma. *Eur J Surg Oncol* 33(3): 294-300.

Nagamachi Y, Tani M, Shimizu K, Tsuda H, Niitsu Y et al. (1998) Orthotopic growth and metastasis of human non-small cell lung carcinoma cell injected into the pleural cavity of nude mice. *Cancer Lett* 127(1-2): 203-209.

Nagy JA, Dvorak AM, Dvorak HF (2007) VEGF-A and the induction of pathological angiogenesis. *Annu Rev Pathol* 2: 251-275.

Nakamura Y, Yasuoka H, Tsujimoto M, Yang Q, Tsukiyama A et al. (2003) Clinicopathological significance of vascular endothelial growth factor-C in breast carcinoma with long-term follow-up. *Mod Pathol* 16(4): 309-314.

Nathanson SD (2003) Insights into the mechanisms of lymph node metastasis. *Cancer* 98(2): 413-423.

Nishimura R, Osako T, Okumura Y, Hayashi M, Arima N (2010) Clinical significance of Ki-67 in neoadjuvant chemotherapy for primary breast cancer as a predictor for chemosensitivity and for prognosis. *Breast Cancer* 17(4): 269-275.

O-charoenrat P, Rhys-Evans P, Eccles SA (2001) Expression of vascular endothelial growth factor family members in head and neck squamous cell carcinoma correlates with lymph node metastasis. *Cancer* 92(3): 556-568.

Obermair A, Kucera E, Mayerhofer K, Speiser P, Seifert M et al. (1997) Vascular endothelial growth factor (VEGF) in human breast cancer: correlation with disease-free survival. *Int J Cancer* 74(4): 455-458.

Ohsawa K, Imai Y, Sasaki Y, Kohsaka S (2004) Microglia/macrophage-specific protein Iba1 binds to fimbrin and enhances its actin-bundling activity. *J Neurochem* 88(4): 844-856.

Ohta Y, Shridhar V, Bright RK, Kalemkerian GP, Du W et al. (1999) VEGF and VEGF type C play an important role in angiogenesis and lymphangiogenesis in human malignant mesothelioma tumours. *Br J Cancer* 81(1): 54-61.

Padera TP, Kadambi A, di Tomaso E, Carreira CM, Brown EB et al. (2002) Lymphatic metastasis in the absence of functional intratumor lymphatics. *Science* 296(5574): 1883-1886.

Partanen TA, Arola J, Saaristo A, Jussila L, Ora A et al. (2000) VEGF-C and VEGF-D expression in neuroendocrine cells and their receptor, VEGFR-3, in fenestrated blood vessels in human tissues. *FASEB J* 14(13): 2087-2096.

Pasquier E, Kavallaris M, Andre N (2010) Metronomic chemotherapy: new rationale for new directions. *Nat Rev Clin Oncol* 7(8): 455-465.

Pavlakis K, Messini I, Vrekoussis T, Yiannou P, Keramopoullos D et al. (2008) The assessment of angiogenesis and fibroblastic stromagenesis in hyperplastic and pre-invasive breast lesions. BMC Cancer 8, 88

Pollard JW (2008) Macrophages define the invasive microenvironment in breast cancer. *J Leukoc Biol* 84(3): 623-630.

Price JE, Barth RF, Johnson CW, Staubus AE (1984) Injection of cells and monoclonal antibodies into mice: comparison of tail vein and retroorbital routes. *Proc Soc Exp Biol Med* 177(2): 347-353.

Pugh CW, Ratcliffe PJ (2003) Regulation of angiogenesis by hypoxia: role of the HIF system. *Nat Med* 9(6): 677-684.

Qiu C, Lin DD, Wang HH, Qiao CH, Wang J et al. (2008) Quantification of VEGF-C expression in canine mammary tumours. *Aust Vet J* 86(7): 279-282.

Qiu CW, Lin DG, Wang JQ, Li CY, Deng GZ (2008) Expression and significance of PTEN and VEGF in canine mammary gland tumours. *Vet Res Commun* 32(6): 463-472.

Raica M, Cimpean AM, Ribatti D (2009) Angiogenesis in pre-malignant conditions. *Eur J Cancer* 45(11): 1924-1934.

Roberts N, Kloos B, Cassella M, Podgrabinska S, Persaud K et al. (2006) Inhibition of VEGFR-3 activation with the antagonistic antibody more potently suppresses lymph node and distant metastases than inactivation of VEGFR-2. *Cancer Res* 66(5): 2650-2657.

Rouzaut A, Irigoyen M, Montuenga LM (2007) Lymphangiogenesis and lung cancer. *J Thorac Oncol* 2(5): 384-386.

Saban MR, Towner R, Smith N, Abbott A, Neeman M et al. (2007) Lymphatic vessel density and function in experimental bladder cancer. BMC Cancer 7, 219

Santos AA, Oliveira JT, Lopes CC, Amorim IF, Vicente CM et al. (2010) Immunohistochemical expression of vascular endothelial growth factor in canine mammary tumours. *J Comp Pathol* 143(4): 268-275.

Sarli G, Preziosi R, De Tolla L, Brunetti B, Benazzi C (2004) E-cadherin immunoreactivity in canine mammary tumors. *J Vet Diagn Invest* 16(6): 542-547.

Sasaki Y, Ohsawa K, Kanazawa H, Kohsaka S, Imai Y (2001) Iba1 is an actin-cross-linking protein in macrophages/microglia. *Biochem Biophys Res Commun* 286(2): 292-297.

Scholzen T, Gerdes J (2000) The Ki-67 protein: from the known and the unknown. *J Cell Physiol* 182(3): 311-322.

Schoppmann SF, Birner P, Stockl J, Kalt R, Ullrich R et al. (2002) Tumor-associated macrophages express lymphatic endothelial growth factors and are related to peritumoral lymphangiogenesis. *Am J Pathol* 161(3): 947-956.

Shibuya M (2008) Vascular endothelial growth factor-dependent and -independent regulation of angiogenesis. *BMB Rep* 41(4): 278-286.

Shibuya M (2009) Unique signal transduction of the VEGF family members VEGF-A and VEGF-E. *Biochem Soc Trans* 37(Pt 6): 1161-1166.

Shibuya M, Claesson-Welsh L (2006) Signal transduction by VEGF receptors in regulation of angiogenesis and lymphangiogenesis. *Exp Cell Res* 312(5): 549-560.

Shweiki D, Itin A, Soffer D, Keshet E (1992) Vascular endothelial growth factor induced by hypoxia may mediate hypoxia-initiated angiogenesis. *Nature* 359(6398): 843-845.

Skobe M, Hawighorst T, Jackson DG, Prevo R, Janes L et al. (2001) Induction of tumor lymphangiogenesis by VEGF-C promotes breast cancer metastasis. *Nat Med* 7(2): 192-198.

Solinas G, Germano G, Mantovani A, Allavena P (2009) Tumor-associated macrophages (TAM) as major players of the cancer-related inflammation. *J Leukoc Biol* 86(5): 1065-1073.

Sorenmo K (2003) Canine mammary gland tumors. *Vet Clin North Am Small Anim Pract* 33: 573-596.

Stacker SA, Williams RA, Achen MG (2004) Lymphangiogenic growth factors as markers of tumor metastasis. *APMIS* 112(7-8): 539-549.

Straume O, Jackson DG, Akslen LA (2003) Independent prognostic impact of lymphatic

vessel density and presence of low-grade lymphangiogenesis in cutaneous melanoma. *Clin Cancer Res* 9(1): 250-256.

Su JL, Yen CJ, Chen PS, Chuang SE, Hong CC et al. (2007) The role of the VEGF-C/VEGFR-3 axis in cancer progression. *Br J Cancer* 96(4): 541-545.

Tang DG, Honn KV (1994) Adhesion molecules and tumor metastasis: an update. *Invasion Metastasis* 14(1-6): 109-122.

Tashbaeva RE, Hwang DN, Song GS, Choi NH, Lee JH et al. (2007) Cellular characterization of multidrug resistance P-glycoprotein, alpha fetoprotein, and neovascular endothelium-associated antigens in canine hepatocellular carcinoma and cirrhotic liver. *Vet Pathol* 44(5): 600-606.

Tobler NE, Detmar M (2006) Tumor and lymph node lymphangiogenesis--impact on cancer metastasis. *J Leukoc Biol* 80(4): 691-696.

Toi M, Inada K, Suzuki H, Tominaga T (1995) Tumor angiogenesis in breast cancer: its importance as a prognostic indicator and the association with vascular endothelial growth factor expression. *Breast Cancer Res Treat* 36(2): 193-204.

Tsutsui S, Yasuda K, Suzuki K, Tahara K, Higashi H et al. (2005) Macrophage infiltration and its prognostic implications in breast cancer: the relationship with VEGF expression and microvessel density. *Oncol Rep* 14(2): 425-431.

Uchida N, Nagai K, Sakurada Y, Shirota K (2008) Distribution of VEGF and flt-1 in the normal dog tissues. *J Vet Med Sci* 70(11): 1273-1276.

Uyama R, Nakagawa T, Hong SH, Mochizuki M, Nishimura R et al. (2006) Establishment of four pairs of canine mammary tumour cell lines derived from primary and metastatic origin and their E-cadherin expression. *Vet Comp Oncol* 4(2): 104-113.

Van den Eynden GG, Van der Auwera I, Van Laere SJ, Huygelen V, Colpaert CG et al. (2006) Induction of lymphangiogenesis in and around axillary lymph node metastases of patients with breast cancer. *Br J Cancer* 95(10): 1362-1366.

Van der Auwera I, Cao Y, Tille JC, Pepper MS, Jackson DG et al. (2006) First international consensus on the methodology of lymphangiogenesis quantification in solid human tumours. *Br J Cancer* 95(12): 1611-1625.

Van der Auwera I, Van Laere SJ, Van den Eynden GG, Benoy I, van Dam P et al. (2004) Increased angiogenesis and lymphangiogenesis in inflammatory versus noninflammatory breast cancer by real-time reverse transcriptase-PCR gene expression quantification. *Clin Cancer Res* 10(23): 7965-7971.

van Rijn SJ, Grinwis GC, Penning LC, Meij BP (2010) Expression of Ki-67, PCNA, and p27kip1 in canine pituitary corticotroph adenomas. *Domest Anim Endocrinol* 38(4): 244-252.

Vartanian RK, Weidner N (1994) Correlation of intratumoral endothelial cell proliferation with microvessel density (tumor angiogenesis) and tumor cell proliferation in breast carcinoma. *Am J Pathol* 144(6): 1188-1194.

Vermeulen PB, Gasparini G, Fox SB, Colpaert C, Marson LP et al. (2002) Second international consensus on the methodology and criteria of evaluation of angiogenesis quantification in solid human tumours. *Eur J Cancer* 38(12): 1564-1579.

Vermeulen PB, Gasparini G, Fox SB, Toi M, Martin L et al. (1996) Quantification of angiogenesis in solid human tumours: an international consensus on the methodology and criteria of evaluation. *Eur J Cancer* 32A(14): 2474-2484.

Weigand M, Hantel P, Kreienberg R, Waltenberger J (2005) Autocrine vascular endothelial growth factor signalling in breast cancer. Evidence from cell lines and primary breast cancer cultures in vitro. *Angiogenesis* 8(3): 197-204.

Wirzenius M, Tammela T, Uutela M, He Y, Odorisio T et al. (2007) Distinct vascular endothelial growth factor signals for lymphatic vessel enlargement and sprouting. *J Exp Med* 204(6): 1431-1440.

Withrow SJ, Vail DM (2007). Small Animal Clinical Oncology. 4th ed. Philadelphia, SAUNDERS.

Yamashita A, Maruo K, Suzuki K, Shirota K, Kobayashi K et al. (2001) Experimental

chemotherapy against canine mammary cancer xenograft in SCID mice and its prediction of clinical effect. *J Vet Med Sci* 63(8): 831-836.

Yang W, Klos K, Yang Y, Smith TL, Shi D et al. (2002) ErbB2 overexpression correlates with increased expression of vascular endothelial growth factors A, C, and D in human breast carcinoma. *Cancer* 94(11): 2855-2861.

Zhang BC, Gao J, Wang J, Rao ZG, Wang BC et al. (2010) Tumor-associated macrophages infiltration is associated with peritumoral lymphangiogenesis and poor prognosis in lung adenocarcinoma. *Med Oncol*: Epub ahead of print.

Zuccari DA, Santana AE, Cury PM, Cordeiro JA (2004) Immunocytochemical study of Ki-67 as a prognostic marker in canine mammary neoplasia. *Vet Clin Pathol* 33(1): 23-28.